PARTICULATE MATTER (PM) EXPOSURE FOR COMMUTERS IN LOS ANGELES: CHEMICAL CHARACTERIZATION AND IMPLICATIONS TO PUBLIC HEALTH

by

Winnie Kam

A dissertation presented to the

FACULTY OF THE USC GRADUATE SCHOOL

In partial fulfillment of the requirements for the degree of

Doctor of Philosophy

in

Environmental Engineering

May 2013

Dedication

To my parents, Kay and Paul,

for their unconditional love and support.

Acknowledgements

The last four years have been an amazing journey for me both personally and professionally. Since joining the aerosol lab at University of Southern California in 2009, first as a master's student then as a PhD student, I have grown immensely as an academic scientist. This thesis would not have been possible without the help of many people for whom I would like to pay my sincerest gratitude.

First and foremost, I would like to thank my advisor Professor Constantinos Sioutas for his confidence in me and for his guidance in my doctoral research work. His deep knowledge of aerosol research and scientific intuition has been invaluable towards my progress as a PhD student. I am forever indebted to him for providing this priceless opportunity for me to be a part of his premiere research group that continues to be at the forefront of aerosol research.

I would also like to thank all members of my guidance committee, Professor Ronald C Henry, Professor Jiu-Chiuan Chen, Professor Scott Fruin, and Professor James Moffett for their thoughtful suggestions and continual support of my research work. Special thanks to Professor James J Schauer and Dr. Martin M Shafer of University of Wisconsin-Madison for their insightful comments, which have been a substantive contribution to the development of my dissertation.

Since research in the aerosol lab is largely a collective effort, my thesis would not be possible without the help of a number of former and current colleagues at USC: Dr. Zhi Ning, Dr. Kalam Cheung, Dr. Payam Pakbin, Dr. Vishal Verma, Dr. Neelakshi Hudda, Nancy Daher, James Liacos, Dongbin Wang, Niloofar Hajibeiklou, and Shruthi Balasubramanian. I would like to especially acknowledge Dr. Zhi Ning, Assistant Professor at City University of Hong Kong,

for his mentorship during the early stages of my study and for his patience and friendship. It has been a great pleasure to work with everyone that has been a part of the aerosol lab. In addition, I would also like to thank Dr. Evangelia Kostenidou, Genevieve McSpaden, Ivy Zheng, and Xu Zhen. Although their stay with the aerosol lab was brief, their involvement and commitment to various research projects will be remembered.

Lastly, I would like to thank my fiancé, Kenneth C Leung, for his unending support and trust in me during the course of my study.

Table of Contents

List of Figures

List of Tables

Abstract

According to the U.S. Census Bureau, 570,000+ commuters in Los Angeles travel for over 60 minutes to work. Studies have shown that a substantial portion of particulate matter (PM) exposure can occur during this commute depending on the mode of transport. This thesis focuses on the PM exposure for commuters of four microenvironments in Los Angeles including subway, light-rail, freeways, and surface streets.

The first part of the thesis focuses on the subway and light-rail commute environments. Elevated concentrations of PM have been found in a number of worldwide underground transit systems, with major implications regarding exposure of commuters to PM and its associated health effects. An extensive sampling campaign was to measure PM concentrations in two lines of the Los Angeles Metro system – an underground subway line (Metro red line) and a ground-level light-rail line (Metro gold line). Considering that a commuter typically spent 75% of time inside the train and 25% of time waiting at a station, subway commuters were exposed on average to PM_{10} and $PM_{2.5}$ concentrations that were 1.9 and 1.8 times greater than the light-rail commuters. The average PM_{10} concentrations for the subway at station platforms and inside the train were 78.0 $\mu g/m^3$ and 31.5 $\mu g/m^3$, respectively; for the light-rail line, corresponding PM_{10} concentrations were 38.2 $\mu g/m^3$ and 16.2 $\mu g/m^3$. Regression analysis demonstrated that personal exposure concentrations for the light-rail line are strongly associated with ambient PM levels (R^2=0.61), while PM concentrations for the subway line are less influenced by ambient conditions (R^2=0.38) and have a relatively stable background level of about 21 $\mu g/m^3$. Mass balance showed that in coarse PM ($PM_{10-2.5}$), iron makes up 27%, 6%, and 2% of gravimetric mass for red line, gold line, and USC, respectively; in fine PM, iron makes up 32%, 3%, and 1%. Non-crustal metals, particularly Cr, Mn, Co, Ni, Mo, Cd, and Eu were elevated for the red line

and, to a lesser degree, the gold line. Bivariate analysis showed that reactive oxygen species (ROS) activity is strongly correlated with water-soluble Fe (R^2=0.77), Ni (R^2=0.95), and OC (R^2=0.92). A multiple linear regression model (R^2=0.94, $p<0.001$) using water-soluble Fe and OC as predictor variables was developed to explain the variance in ROS.

The second part of the thesis focuses on PM exposure for private commuters of freeways and surface streets. An on-road sampling campaign was conducted to assess on-road PM composition for three size fractions ($PM_{10-2.5}$,$PM_{2.5-0.25}$, and $PM_{0.25}$) on three representative roadways in Los Angeles: 1) the I-110, a high-traffic freeway composed mostly of light-duty vehicles (LDVs), 2) the I-710, a major freeway for heavy-duty vehicles (HDVs) travelling to and from the Ports of Los Angeles and Long Beach, and 3) Wilshire/Sunset Blvd, two major surface streets. Results showed that the $PM_{0.25}$ fraction is heavily influenced by vehicular emissions, as indicated by average roadway PM concentrations that were 48.0±9.4% higher than those observed at USC ($p<0.05$), while the $PM_{10-2.5}$ fraction is mostly influenced by resuspension of road dust and the $PM_{2.5-0.25}$ fraction is mainly composed of secondary species. With very low EC levels in $PM_{10-2.5}$, the most notable difference among the three roadway environments was the $PM_{2.5}$ EC levels observed on the I-710, which are 2.0±0.2 μg/m^3 and 4.1 times greater than USC.

Next, fuel-based emission factors (mass of pollutant per kg of fuel) were calculated to assess the emissions profile of a light-duty vehicle (LDV) traffic fleet characterized by stop-and-go driving conditions that are reflective of urban street driving. Emission factors for metals and trace elements were highest in $PM_{10-2.5}$ while emission factors for polycyclic aromatic hydrocarbons (PAHs) and hopanes and steranes were highest in $PM_{0.25}$. $PM_{2.5}$ emission factors were also compared to previous freeway, roadway tunnel, and dynamometer studies based on an LDV fleet to determine how various environments and driving conditions may influence

concentrations of PM components. The on-road sampling methodology deployed in the current study captured substantially higher levels of metals and trace elements associated with vehicular abrasion (Fe, Ca, Cu, and Ba) and crustal origins (Mg and Al) than previous LDV studies. The semi-volatile nature of PAHs resulted in higher levels of PAHs in the particulate phase for LDV tunnel studies (Phuleria et al. 2006) and lower levels of PAHs in the particulate phase for freeway studies (Ning et al. 2008). With the exception of a few high molecular weight PAHs, the current study's emission factors were in between the LDV tunnel and LDV freeway studies. In contrast, hopane and sterane emission factors were generally comparable between the current study, the LDV tunnel, and LDV freeway, as expected given the greater atmospheric stability of these organic compounds.

Lastly, PM exposures for all commute environments were compared using mass per volume of air as the metric of comparison. Metals associated with stainless steel, notably Fe, Cr, and Mn, were elevated for the red line (subway), most likely from abrasion processes between the rail and brakes; elements associated with tire and brake wear and oil additives (Ca, Ti, Sn, Sb, and Pb) were elevated on roadways. Elemental concentrations on the gold line (light-rail) were the lowest. Overall, the 710 exhibited high levels of PAHs (3.0 ng/m^3), most likely due to its high volume of HDVs, while the red and gold lines exhibited low PAH concentrations (0.6 and 0.8 ng/m^3 for red and gold lines, respectively). Lastly, lung cancer risk due to inhalation of PAHs was calculated based on a commuter lifetime (45 years for 2 hours per workday). Results showed that lung cancer risk for the 710 is 3.8 and 4.5 times higher than the light-rail (gold line) and subway (red line), respectively. With low levels of both metals and PAH pollutants, our results indicate that commuting on the light-rail (gold line) may have potential health benefits when compared to driving on freeways and busy roadways.

Chapter 1 Introduction

1.1 Background

An aerosol is defined as a solid or liquid suspended in a gas medium. It is a two-phase system and describes various forms of microscopic particles that remain in the air such as resuspended soil dust, particles generated from vehicular combustion, photochemically formed particles, and sea salt from the ocean. Particulate matter (PM) refers to the particles or liquid droplets in the aerosol and is responsible for environmental effects such as visibility and climate as well as numerous adverse health effects. In addition, PM is a major component of photochemical smog and influences surface albedo by decreasing the amount of heat reaching the surface (Seinfeld and Pandis 2006). The composition of PM is highly complex and varies depending on local sources, source strength, and atmospheric processes such regional transport and gas-to-particle partitioning. Therefore, investigating the physico-chemical and toxicological characteristics of PM is crucial in understanding its environmental and health effects for both policymakers and for the general public.

Particulate matter is made up of a number of chemical constituents including inorganic ions (nitrate and sulfate), crustal metals and trace elements, elemental carbon (EC), and organic species. The chemical components are derived from both natural and anthropogenic sources. Natural sources include resuspended crustal elements, sea spray, and windborne biological materials; anthropogenic sources include vehicular emissions, burning of fossil fuels and biomass, and emissions from industrial activity. Particles that are emitted directly into the atmosphere are known as primary pollutants, while particles formed in the atmosphere are known as secondary pollutants, i.e. photochemical reactions with gaseous precursors (i.e.

nitrogen oxides). Once emitted, particles may undergo various physical and chemical processes that may alter particle size and chemical composition.

1.2 Characteristics of airborne particles

In the context of PM, the most important parameter is particle size, which is usually expressed as aerodynamic diameter or dp. Because particles exist in various shapes, aerodynamic diameter is defined as the diameter of a unit density sphere that has the same settling velocity as the particle. Airborne particles can range from the submicron (<1um) mode to tens of microns in size. There are three major PM size fractions: coarse mode (or $PM_{10-2.5}$) contains particles in the range of 2.5 to 10μm, accumulation mode contains particles in the range of 100nm to 2.5μm, and ultrafine PM are particles less than 100nm. Fine PM (or $PM_{2.5}$) refers to particles less than 2.5μm and PM_{10} refers to particles less than 10μm. Particles greater than 10μm are typically of less interest because these particles are characterized by low atmospheric residence times and respiratory deposition in the nasal region, while PM_{10} can enter the thoracic region and is of great interest to air pollution studies and for regulatory purposes.

The PM size ranges exhibit differences in respiratory deposition, atmospheric formation and deposition mechanisms, particle composition, and optical properties. The coarse fraction is formed mainly from mechanical processes such as grinding, erosion, and wind resuspension, and due to its relatively high settling velocity, its primary deposition mechanism is gravitational settling (Hinds 1999). The accumulation mode is formed mainly through physical atmospheric aging processes such as coagulation of smaller particles and growth of existing particles by condensation. This mode tends to remain in the atmosphere for longer because its removal mechanism is neither dominated by gravitational settling or coagulation processes. Ultrafine particles are formed through incomplete combustion and gas-to-particle nucleation processes and

are primarily removed through coagulation with other particles into a larger size mode. Although they have negligible mass, they dominate in particle number concentration and are efficiently deposited by diffusional mechanisms into all regions of the respiratory tract, including the alveolar region. In addition, its greater surface area per mass compared with larger particles renders ultrafine particles to be more biologically active (Brown et al. 2001; Oberdorster et al. 2005).

Currently, PM_{10} and $PM_{2.5}$ are regulated in the National Ambient Air Quality Standards (NAAQS) under the Environmental Protection Agency (EPA), which uses mass concentration ($\mu g/m^3$) as the metric for regulation. The law sets two standards: the primary standard is designed to protect public health (i.e. sensitive populations such as children, elderly, and those with respiratory illnesses) and the secondary standard is designed to protect public welfare (i.e. visibility, damage to buildings and crops).

1.3 Health effects associated with PM

Adverse health effects associated with PM remains the one of the main motivations for current aerosol research. Numerous studies have found a link between respiratory, pulmonary, cardiovascular effects and long-term exposure to atmospheric PM (Samet et al. 2000; Schwartz et al. 2002; Pope and Dockery 2006; Li et al. 2009). Recent in-vivo and in-vitro studies have shown that ultrafine particles may trigger a proinflammatory response in the mouse brain that can contribute to neurodegenerative diseases (Campbell et al. 2005; Morgan et al. 2011). Although the biological mechanisms responsible for toxicity of PM are still uncertain, numerous studies have found a positive correlation with PM toxicity and its chemical components, including organic carbon (OC) and elemental carbon (EC) (Mar et al. 2000; Metzger et al. 2004),

trace metals (Saldiva et al. 2002), and quinones and polycyclic aromatic hydrocarbons (PAHs) (Xia et al. 2004).

It is also postulated that PM components have oxidative properties and the potential to generate reactive oxygen species (ROS) which contribute to oxidative stress in the human body. While ROS is a natural byproduct of aerobic metabolism, an imbalance in ROS levels may affect tissue oxygen homeostasis. An increase in ROS concentrations has been shown to play a direct role in pulmonary inflammation (Tao et al. 2003), which may lead to decreased lung function and exacerbation of respiratory diseases such as asthma and chronic obstructive pulmonary disease (COPD). The magnitude of ROS generation has also been hypothesized to be driven by redox reactions of soluble PM constituents such as transition metals (Verma et al. 2010) and organic compounds (Cho et al. 2005) as well as the PM size fraction (Hu et al. 2008). Because of the complex chemical nature of PM and the spatial and temporal variation of local PM sources, further research is needed to understand the physical processes and the chemical components that contribute to ambient PM.

1.4 Rationale for research

In major metropolitan areas, vehicular emissions are the primary source of ambient PM (Schauer et al. 1996), and are of particular importance to populations in the vicinity of trafficked areas or downwind of major freeways. Studies conducted near freeways and major roadways have found that PM levels were substantially elevated relative to areas that are farther from the traffic source (Zhu et al. 2002; Ning et al. 2010). Populations in the proximity of trafficked roadways are most susceptible to PM health effects (Tonne et al. 2007). However, the most sensitive demographics are developing children near roadways (Brunekreef et al. 1997; Dales et al. 2009) and the elderly (Liao et al. 1999; Creason et al. 2001).

Although the U.S. EPA estimates people spend an average of approximately 90% of their time indoors (U.S. EPA "The Inside Story: A Guide to Indoor Air Quality"), a large portion of their total daily PM exposure may be due to time spent outdoors or during their commute on roadways. The U.S. Census Bureau estimates a total of 4.5M workers that are age 16 and over in Los Angeles, who have a mean travel time to work of 30.7 minutes, resulting in a round trip commute of approximately 1 hour. However, Figure 1.1 shows that the travel time to work is not normally distributed and approximately 13.8% travel for 60 minutes or more each way to work (2011 American Community Survey), accounting for over 621,000 people in Los Angeles.

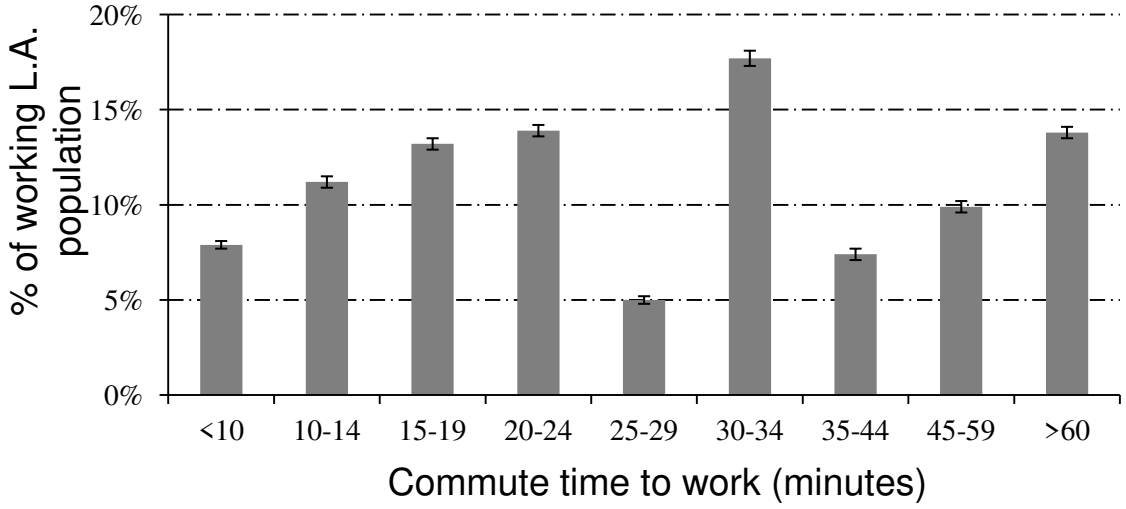

Figure 1.1 Time spent traveling to work for the L.A. population (%).

Source: 2011 American Community Survey (ACS)

As one of the largest and most populated cities in the world, a number of transport modes are available for the residents of L.A. including the subway, light-rail, train, bus, and private vehicles. Due to the sprawled urban nature of L.A., private vehicles dominates as the major mode of transportation and accounts for over 80% of the working population (2011 ACS), contributing to the notorious traffic congestion of its major highway systems. Depending on the

mode of commute, the passenger may be exposed to PM of various species and concentration levels. Thus, understanding the chemical composition of PM for different commute microenvironments is essential in assessing passenger exposure and potential health endpoints associated with PM inhalation. In particular, my current research will focus on the exposure assessment for public and private commuters in five different commute environments: light-rail, subway, freeways, and surface streets.

1.4.1 Exposure assessment for passengers on the L.A. Metro subway and light-rail

Metro systems are an important transportation mode in megacities across the world that commuters take on a daily basis. However, recent measurements in cities across the world indicate that subway systems may present a unique microenvironment with particulate matter (PM) concentrations subject to different influences than ground-level sources. Earlier studies have documented elevated PM levels in major subway systems across the world. Mean exposure levels in the London Underground rail system were 3-8 times higher than street-level transportation modes (Adams et al. 2001); average daytime $PM_{2.5}$ and PM_{10} levels in a Paris railway station were approximately 5-30 times higher than levels on Paris streets (Raut et al. 2009). In addition, elevated concentrations of elements especially Fe, Mn, Cu, Ni, Cr have been observed in numerous subway systems relative to ambient urban concentrations. A personal exposure assessment of a passenger on the Helsinki subway system determined an increase of 3% for total fine PM exposure levels, but nearly 200% increase for Fe, 60% increase for Mn, and 40% increase for Cu (Aarnio et al. 2005). Another study estimated that commuters in London spending 2h in the subway per day would increase their personal daily exposure by 17 $\mu g/m^3$ (Seaton et al. 2005). High Mn, Cr and Fe concentrations of 160-350 times greater than the

median for outdoors residential areas were observed for teenage commuters in the New York City subway system (Chillrud et al. 2004).

Although passengers spend a relatively short amount of time in subway systems, exposures to high concentrations of PM with enriched levels of certain elements may have significant health implications. Few toxicological studies, primarily in-vitro, have been conducted on the health impacts of subway particles. Stockholm subway particles were found to be 8 times more genotoxic than ambient particles and up to 4 times more like to cause oxidative stress to cells (Karlsson et al. 2005). Furthermore, the Stockholm subway particles caused more DNA damage than particles produced from wood combustion (Karlsson et al. 2006). On the other hand, studies have reported PM levels to be lower for the Hong Kong (Chan et al. 2002) and Guangzhou (Chan et al. 2002) subway systems than compared to other transport modes. Therefore, differences between subway ventilation methods, braking systems, wheel type, air conditioning, system age, and train motive source make it impossible to directly extrapolate results from previous studies to other subway systems.

1.4.2 Exposure assessment for passengers in private vehicles in L.A.

In major metropolitan areas, the major source of PM is from vehicular combustion (Schauer et al. 1996; Querol et al. 2001), and populations in the proximity of trafficked roadways are most susceptible to PM health effects (Tonne et al. 2007). However, the most sensitive demographics are developing children near roadways (Brunekreef et al. 1997; Dales et al. 2009) and the elderly (Liao et al. 1999; Creason et al. 2001). Although the underlying physiological pathways for PM toxicity are uncertain, several studies have postulated that certain PM components may play a role, including elemental carbon (EC), organic carbon (EC), and trace metals (Metzger et al. 2004; Ostro et al. 2008; Verma et al. 2010).

As a result, it is important to characterize PM at major roadway environments, where elevated levels of PM have been observed (Zhu et al. 2002). Various methodologies have been used to assess the impact of vehicular emissions on ambient air. Chassis dynamometer studies can measure the emissions of a target vehicle in a controlled environment (Schauer et al. 1999; Yanowitz et al. 1999), but cannot account for particle aging and atmospheric dilution effects. Another method is roadside sampling, where continuous and time-integrated instruments are used to measure both physical and chemical components of PM at designated sites downwind of roadways (Kuhn et al. 2005b; Ning et al. 2010). Several recent studies have conducted on-road sampling, in which a mobile laboratory (typically a hybrid or electric vehicle) equipped with various continuous instruments have been used to measure black carbon (BC) (Fruin et al. 2004), particle size distribution (Gouriou et al. 2004; Westerdahl et al. 2005; Weimer et al. 2009), $PM_{2.5}$, particle-bound PAH, and gaseous pollutants including NOx, CO, ozone, and hydrocarbons (Bukowiecki et al. 2002; Ning and Chan 2007; Weiss et al. 2011). However, there are no previous on-road studies that have reported time-integrated chemical speciation data, which would substantially enhance the current knowledge base of on-roadway PM as well as provide a more comprehensive exposure assessment for commuters.

1.5 Major research questions

The objective of my thesis is to investigate a major research problem and address a number of relevant research questions. The overarching theme of my proposal is the PM exposure of commuters using different transport modes and how the different microenvironments contribute to chemical composition of the PM. Although the results presented will mostly focus on the mass concentrations and chemical composition of PM samples collected in the various commute microenvironments, toxicity results will also be

discussed with implications to public health assessment. The major research questions I am proposing to investigate in my thesis are:

1) In terms of PM composition, what are passengers exposed to on the L.A. Metro subway and light-rail lines and to what degree is it elevated or not elevated relative to urban ambient air?
2) How does the PM exposure in the two aforementioned L.A. Metro environments compare to passengers commuting in private vehicles on major roadways and surface streets in L.A.?
3) Of the 5 commute microenvironments (subway, light-rail, freeway with mostly light-duty vehicles, freeway with a higher percentage of heavy-duty vehicles, and major arterial roads) presented, which type of passengers are exposed to the greatest PM toxicity and what are the main factors contributing to this health effect?

As air pollution is a regional problem, the results from my current work and my future investigation will be specific to the areas of Los Angeles. Chapter 1 has provided an introduction to air pollution and the major health problems associated with particulate matter in the context of major metropolitan areas. It has also provided the rationale as to why assessing PM exposure for various commute microenvironments is essential in understanding how differences in PM composition can contribute to adverse health effects. Chapter 2 and 3 discusses the results based on a METRO study in Los Angeles investigating a light-rail (METRO gold line) and a subway (METRO red line). Major results for PM mass and chemical speciation data and toxicity results are presented. Chapters 4 and 5 will present the results based on a major on-road study for three differential private commute environments including an HDV freeway (710), an LDV freeway

(110), and major surface streets. Chapter 4 focuses on a mass balance analysis and comparison of major PM components, while chapter 5 focuses on LDV emission factors based on measurements at the surface street environment. Chapter 6 integrates the METRO and on-road campaign and focuses comparing PM components and species that are associated with adverse health effects between the five commute microenvironments. At the end, estimates of lung cancer risk are computed for all environments and are compared. Chapter 7 provides a conclusion of the thesis and recommendations for future work and regulation.

Chapter 2 Particulate matter (PM) concentrations in underground and ground-level rail systems of the Los Angeles Metro

2.1 Sampling methodology for L.A. Metro subway and light-rail study

Two lines of the L.A. Metro system were sampled in this study – the red and gold lines. The red line is a subway line that spans approximately 17 km connecting downtown L.A. to North Hollywood. Weekly ridership for the red line is estimated to be 150,000, which is the highest of the Metro rail lines and accounts for almost 50% of system wide ridership. The gold line, which began operation in 2003, is a ground-level light-rail line that connects Pasadena to downtown L.A. Weekly ridership for the gold line is estimated to be 35,000 as of August 2010. For both lines, trains pass every 8-10 minutes during rush hours and 10-12 minutes during normal hours. A one-way trip to and from Union Station is approximately 30 minutes (www.metro.net). Figure 2.1 shows a map of where the Metro red and gold lines run, two nearby air quality monitoring sites (Downtown L.A. and Burbank), and the University of Southern

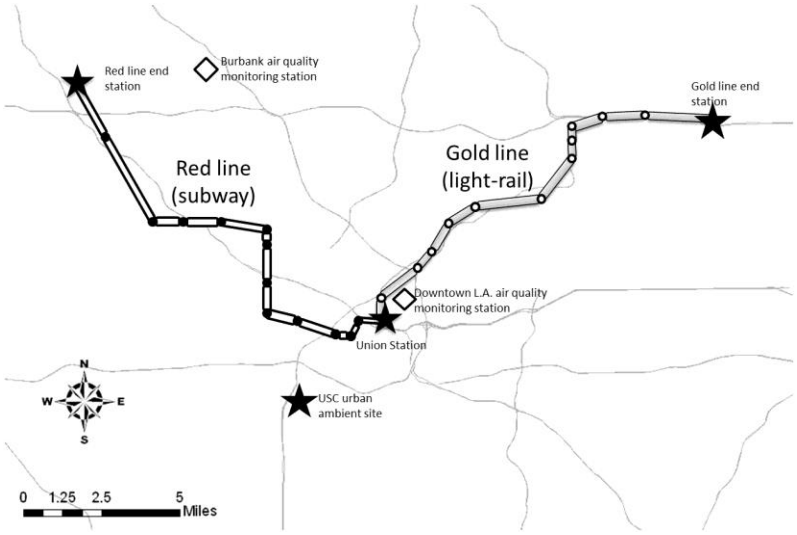

Figure 2.1 Map of sampling routes, the Metro red line (subway) and gold line (light-rail), two nearest air quality monitoring stations, and the University of Southern California (USC) urban ambient site

California (USC) urban ambient site, which was used to represent urban background concentrations.

2.1.1 Monitoring instruments and sampling campaigns

The Q-Trak Indoor Air Quality Monitor Model 7565 (TSI Inc., Shoreview, MN) was used to determine CO_2 concentrations, temperature, and relative humidity at a logging interval of 15 seconds. The DustTrak Aerosol Monitor Model 8520 (TSI Inc., Shoreview, MN) was used to measure continuous $PM_{2.5}$ and PM_{10} concentrations at a logging interval of 30 seconds. Previous studies have shown that light-scattering aerosol measuring devices are subject to error when relative humidity is greater than 60% (Lowenthal et al. 1995; Sioutas et al. 2000; Chakrabarti et al. 2004). Q-Trak reported relative humidity levels that are within the operating range of the DustTrak. Airborne PM was collected with the Sioutas™ Personal Cascade Impactor Sampler (SKC Inc., Eighty-Four, PA), also referred to as PCIS (Misra et al. 2002; Singh et al. 2003), which was operated with a Leland Legacy Pump (SKC Inc., Eighty-Four, PA) at a flow rate of 9 liters per minute (lpm) (Brinkman et al. 2008). The pumps were calibrated with Gilian Gilibrator-2 Air Flow Calibrator (Sensidyne Inc., Clearwater, FL) before and after sampling. During the sampling, the pump flows were checked regularly with flow meters. The PCIS was prepared using one impaction stage with a cutpoint of 2.5 μm and an after filter stage, collecting coarse and fine PM, respectively. For the purpose of chemical analysis, the PCIS were loaded with two types of filters. One was loaded with PTFE (Teflon) filters, with a 25mm Zefluor supported PTFE filter (Pall Life Sciences, Ann Arbor, MI) as the impaction substrate and a 37mm PTFE membrane filter with PMP ring (Pall Life Sciences, Ann Arbor, MI) as the after filter. The other unit was loaded with quartz microfiber filters (Whatman International Ltd, Maidstone, England). The Teflon filters were gravimetrically analyzed using a MT5

Microbalance (Mettler-Toledo Inc., Columbus OH), which has a detection limit of 10μg. A total of 9 PCIS were deployed in this study, with 3 PCIS for each line and 3 PCIS at the fixed site. Figure 2.2b shows the setup of the PCIS inside the carry-on suitcases that were used for PM collection on the subway.

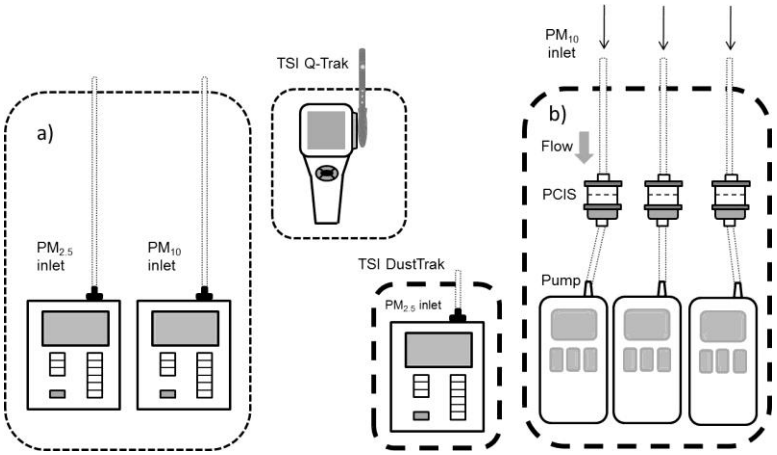

Figure 2.2 (a) Carry-on suitcase setup for station/train intensive campaign, two DustTraks with $PM_{2.5}$ and PM_{10} inlet and TSI Q-Trak. (b) Setup for the personal exposure campaign, three personal cascade impactor samplers (PCIS) with battery-powered pumps and DustTrak

The sampling campaign took place from May 3 – August 13, 2010. Two sub-campaigns were undertaken during this period: 1) the station/train intensive campaign, which focuses on measuring real-time $PM_{2.5}$, PM_{10}, and CO_2 concentrations simultaneously at each station and inside the train, and 2) the personal exposure campaign, focusing on airborne PM exposures for Metro commuters by sampling concurrently on the red line, gold line, and at the USC ambient fixed site. The station/train intensive sampling occurred on a weekly basis and alternated between the two lines each week (i.e. each line is sampled every other week), accruing 7 days of sampling for each line. The subject carried a suitcase equipped with two DustTraks, one with a $PM_{2.5}$ inlet and one with a PM_{10} inlet, and a Q-Trak (Figure 2.2a). For the personal exposure campaign, the red line, gold line, and USC fixed ambient site were sampled concurrently for 3.5

hours (9:30 am to 1:00 pm) for 4 out of the 5 weekdays. The campaign was designed to determine the personal PM exposure of riders on both lines and compare with each other and with an urban ambient site (USC). The two subjects were directed to spend approximately 75% of time in the train and 25% of time at stations, which represents a typical commute of a passenger. The two subjects each carried a suitcase with 3 PCIS (two with PTFE filters and one with quartz filters) and 3 pumps inside and one DustTrak with a $PM_{2.5}$ inlet (Figure 2.2b). The PCIS are attached with pre-tested PM_{10} inlets (Arhami et al. 2009) so that the impaction substrates are only collecting coarse particles ($PM_{10-2.5}$). The USC urban ambient site was also equipped with an identical suitcase and inlets with 3 PCIS (2 Teflon, 1 quartz) inside. For each site, two samples were collected.

2.1.2 Quality assurance

To determine the comparability of the two DustTraks deployed for the sampling campaign, the DustTraks were tested by collocated sampling before, in the middle, and at the end of the campaign. A correlation of the PM readings for the two DustTraks shows that they are within 10% of each other ($y = 1.10x + 0.001$) and have an R^2 of 0.99. During the campaign, the DustTrak was maintained at its working flow rate of 1.7 lpm. In addition, the DustTraks were re-zeroed and their impaction plates were cleaned on a daily basis. The Q-Trak was calibrated by zero checking and re-zeroing, if necessary, before and during the campaign. The 9 PCIS used for the campaign were also tested by collocated sampling, and gravimetric analysis revealed that the PCIS agreed within 10-15% in mass concentrations. After sampling each day, the PCIS with filter substrates were sealed with parafilm and stored in a -4°C freezer.

2.2 Results and discussion

2.2.1 DustTrak correction factor

The PM measurements obtained from the DustTrak monitor form the basis of the results discussed in this study. The DustTrak monitor is a direct-reading photometer, operated based on aerosol light scattering. Thus, physical properties of the sampled aerosols such as density, index of refraction and size distribution strongly influence DustTrak measurements (Gorner et al. 1995). The DustTrak monitors were factory-calibrated against a gravimetric measurement of the International Organization for Standardization (ISO) 12103-1, A1 dust (Arizona Test Dust). When the physical characteristics of the sampled aerosols are significantly different from the test aerosol, a correction factor (CF) is needed to adjust the DustTrak readings to actual PM concentrations. Depending on the sampling environment and aerosol characteristics, DustTrak monitors typically read higher than the reference methods by a factor of 2-4 (Chung et al. 2001; Yanosky et al. 2002; Kim et al. 2004). In this study, impaction-based (PCIS) PM measurements and DustTrak $PM_{2.5}$ readings were collected simultaneously during the personal exposure campaign. The DustTrak CF was calculated based on the mass concentrations derived from the PCIS, which is shown in Table 2.1. The CFs are 1.43 and 1.86 for sampling periods 1 and 2 for the light-rail (gold) line, respectively, similar to CFs found in other environments (Heal et al. 2000; Kingham et al. 2006). Contrary to CF factors reported in literature, the CFs are somewhat low (0.85 and 1.11 for periods 1 and 2, respectively) for the subway line. Due to the number of DustTraks available for this campaign, a PM_{10} CF could not be calculated. All DustTrak data reported in this study have been corrected, in which PM_{10} data was adjusted with its corresponding $PM_{2.5}$ CF.

	Period	Dates of sampling	PCIS			Dust Trak	
			PM_{10} ($\mu g\ m^{-3}$)	$PM_{2.5}$ ($\mu g\ m^{-3}$)	Coarse PM ($\mu g\ m^{-3}$)	$PM_{2.5}$ ($\mu g\ m^{-3}$)	Correction factor
Subway system (red line)	1	May 3 - Jun 11, 2010	45.8	33.6	12.1	28.6	0.85
	2	Jun 14 - Aug 13, 2010	41.6	32.0	9.6	35.5	1.11
Ground-level light-rail system (gold line)	1	May 3 - Jun 11, 2010	22.7	16.6	6.1	23.9	1.43
	2	Jun 14 - Aug 13, 2010	23.3	20.1	3.2	37.3	1.86
Urban ambient site (USC)	1	May 3 - Jun 11, 2010	31.0	19.0	12.1	-	-
	2	Jun 14 - Aug 13, 2010	29.5	20.0	9.5	-	-

Table 2.1 Summary of the personal exposure campaign. Average PCIS and DustTrak PM concentrations. DustTrak correction factors are calculated based on $PM_{2.5}$ concentrations from the PCIS.

2.2.2 Overview of personal exposure concentrations of Metro red and gold line

Table 2.1 presents the results from the personal exposure campaign, which was designed to measure the PM exposure of a typical commute of a rider (75% of time spent inside train and 25% of time spent waiting at a station platform). The average PM_{10}, $PM_{2.5}$, and $PM_{10-2.5}$, or coarse PM, mass concentrations obtained from the PCIS, and the $PM_{2.5}$ mass concentrations obtained from the DustTrak are presented. Coarse PM is a subset of PM_{10} and is calculated as the difference of the adjusted PM_{10} and $PM_{2.5}$ values. The personal exposure PM_{10} and $PM_{2.5}$ concentrations on the subway line are 1.9 and 1.8 times greater than the corresponding concentrations for the light-rail line, indicating that subway commuters are exposed to almost double the PM concentrations of light-rail commuters. In comparison to the urban ambient site (USC), PM_{10} and $PM_{2.5}$ exposure concentrations for the subway line are on average 1.4 and 1.7 times higher, respectively; for the light-rail line, the concentrations are 0.76 and 0.94 times that of corresponding USC ambient concentrations. Using a paired t-test, the personal exposure $PM_{2.5}$ levels for the subway and light-rail line reported by the DustTrak are statistically different ($p<0.001$). Interestingly, personal exposure to coarse PM levels for the subway line are almost

equivalent to the urban ambient site, while light-rail levels are on average 0.43 times those of ambient levels. The lower coarse PM exposure is most likely due to the subject spending 75% of the time inside the train. This factor is further investigated in the next section.

2.2.3 PM concentrations at station platforms and inside trains

The results from the station/train intensive campaign for the subway line, light-rail line, and urban ambient site are summarized in Table 2.2. In general, the subway's platforms and train have PM_{10} and $PM_{2.5}$ concentrations that are approximately double those of the light-rail's platforms and train levels; however, coarse PM levels for the subway platforms and trains are 2.4 and 2.9 times greater than the light-rail platforms and train levels, likely a result of the enclosed tunnel environment of the subway line. The light-rail platform PM concentrations are comparable to the USC fixed site concentrations, while the subway stations have PM_{10}, $PM_{2.5}$, and coarse PM levels that are 2.5, 2.8, and 2.0 times greater than those at USC.

		PM_{10} ($\mu g\ m^{-3}$)	$PM_{2.5}$ ($\mu g\ m^{-3}$)	Coarse PM ($\mu g\ m^{-3}$)
Subway line (red)	Stations (all)	78.0 ± 16.5	56.7 ± 11.3	21.3 ± 5.6
	Train	31.5 ± 10.8	24.2 ± 6.9	7.3 ± 6.4
Light-rail line (gold)	Stations (all)	38.2 ± 4.1	29.4 ± 4.2	8.8 ± 1.4
	Train	16.2 ± 6.8	13.7 ± 5.3	2.5 ± 2.4
Urban ambient site (USC)		30.7	19.9	10.8

Table 2.2 Average PM_{10}, $PM_{2.5}$, and coarse PM concentrations of the station/train intensive sampling campaign.

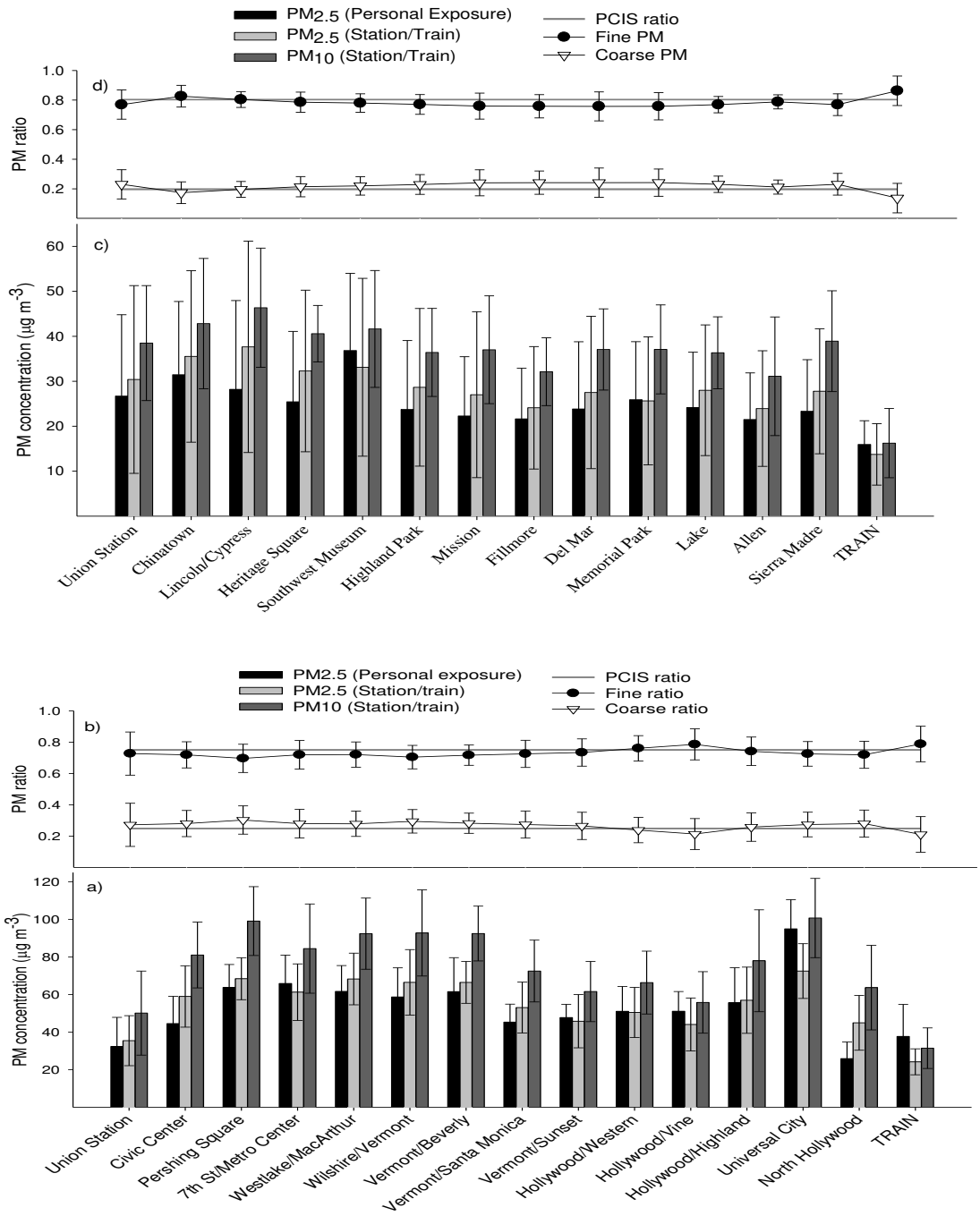

Figure 2.3 Mass concentrations of $PM_{2.5}$ for the subway line (a) and the light-rail line (c). Fine fraction ($PM_{2.5}/PM_{10}$) and coarse fraction ($PM_{10\text{-}2.5}/PM_{10}$) data from DustTrak are presented for the subway line (b) and light-rail line (d) with PCIS mass concentrations.

Figures 2.3a and 2.3c show the average PM_{10} and $PM_{2.5}$ concentrations from the station/train intensive campaign and the average $PM_{2.5}$ concentrations from the personal exposure campaign for the subway line and light-rail line, respectively, with error bars of one

standard deviation. Note that the values presented for the station/train intensive campaign are the average of bi-weekly concentrations. For the underground subway stations, the concentrations vary (i.e. PM_{10} values range from 50 to 100 $\mu g/m^3$) while the ground-level, light-rail station PM_{10} concentrations are distributed in a narrower range (31 to 48 $\mu g/m^3$). It is possible that the ventilation system installed at some stations along the subway line may be more efficient at removing PM than at other stations. Also, the bi-weekly variation of the light-rail line is much greater than the subway line variation; one standard deviation of the average PM values is 50% and 25% for the light-rail and subway line means, respectively. This indicates a greater temporal variation of PM levels in the light-rail line than the subway line. To further confirm this observation, a paired t-test was performed for each line between the mean $PM_{2.5}$ concentrations of the personal exposure and station/train intensive campaigns. At 95% confidence interval, the light-rail line mean data are significantly different ($p=0.001$), while the subway line mean data are not significantly different ($p=0.64$). This suggests that the light-rail line PM concentrations may vary according to seasonal and meteorological conditions, while the subway line PM concentrations are less influenced by temporal changes.

The fine fraction ($PM_{2.5}/PM_{10}$) and coarse fraction ($PM_{10-2.5}/PM_{10}$) of PM are shown for all stations and inside the train with corresponding error bars in Figures 2.3b and 2.3d for the subway line and light-rail line, respectively. The calculated PCIS fine and coarse fractions are also shown in the figures to demonstrate the agreement between the PCIS and DustTrak data. For the subway line, the station platforms and train have overall fine PM fraction averages of 0.73 and 0.79, respectively; for the light-rail line, the corresponding fine fraction averages are 0.78 and 0.86. In general, commuters are exposed to a somewhat lower fine PM fraction and thus a greater coarse fraction while they are waiting at the stations than while riding inside the train.

This is consistent with a subway study conducted in Taiwan, which also found $PM_{2.5}/PM_{10}$ to be higher inside the train (0.75-0.78) than at station platforms (0.67-0.75) (Cheng et al. 2008). A possible reason for the lower coarse fraction inside the trains is that the air conditioning system of the train may be more efficient at removing larger coarse mode particles than smaller particles in the fine mode. Another subway study in Hong Kong found that a non-air-conditioned transport system had a significantly lower fine fraction (0.63-0.68) than an air-conditioned system (0.71-0.78) (Chan et al. 2002).

Figures 2.4a and 2.4b show real-time $PM_{2.5}$, PM_{10}, and CO_2 concentrations collected simultaneously for an hour of sampling for the subway line and light-rail line, respectively. In general, $PM_{2.5}$ and PM_{10} levels follow each other consistently. A noticeable build-up of CO_2 occurs inside the train, whereas CO_2 levels drop rapidly as the commuter steps out of the train. The CO_2 measured inside the train is primarily from the exhaled breath of the riders. It is also important to note that when commuters stand right next to the train door, they are exposed to an immediate flux of particles and a reduction of CO_2 when the train door opens, which can be seen by the simultaneous peaks and dips in Figure 2.4a. Inside the train, CO_2 level reaches up to 1200 ppm, which is 3 to 4 times higher than the level of ambient CO_2 concentrations, but still not at a level of concern for commuters. A study in the Seoul subway system reported CO_2 levels ranging from 1153 to 3377 ppm (Park and Ha 2008). In Figure 2.4a, as the train departs from Union Station, CO_2 concentrations stay level until the train reaches 7^{th} St/Metro Center, where a large number of passengers enter the train, thus creating a surge in CO_2 levels. Although the number of passengers in the train car was not recorded, the accumulation of CO_2 depends strongly on this factor.

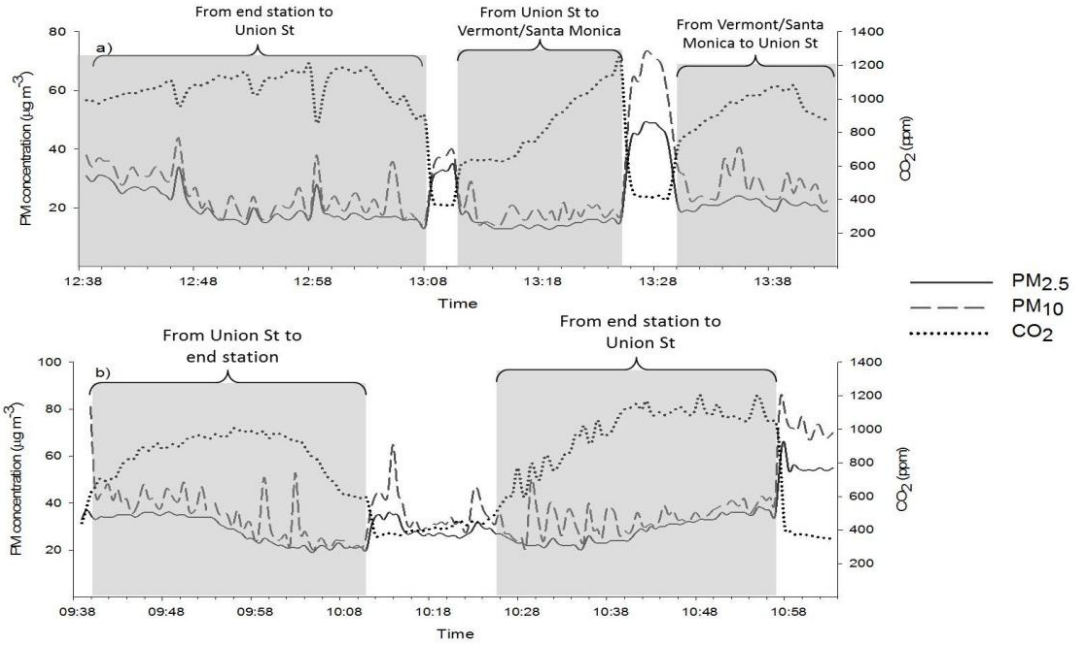

Figure 2.4 Continuous $PM_{2.5}$, PM_{10}, and CO_2 data for approximately one hour of sampling for the subway line (a) and the light-rail line (b). Shaded areas represent times when the subject was riding inside the train.

2.2.4 Comparison of red and gold line PM levels to nearby air monitoring sites

To investigate the influence of ambient PM concentrations on the two Metro lines, figures 2.5a-d show the association of personal exposure $PM_{2.5}$ concentrations of the subway line (a-b) and the light-rail line (c-d) with the $PM_{2.5}$ levels recorded at the two nearest monitoring sites in Downtown L.A. and Burbank (Figure 2.1). The sites are maintained by the South Coast Air Quality Management District (SCAQMD). Each data point represents a 3.5-hour average concentration from each day of sampling (N=54). The linear regression analysis reveals a moderately strong relationship between light-rail line personal exposure concentrations with ambient levels (R^2=0.62 and 0.59 for the Downtown L.A. and Burbank site, respectively) and a weaker relationship between subway line personal exposure concentrations with ambient levels (R^2=0.38 and 0.38). This suggests that the light-rail line is more influenced by ambient PM levels than the subway line. Also, given the relatively small y-intercept of the regression lines

(2.25 and 1.45 μg/m^3 in figures 2.5c and 2.5d, respectively), local emissions are presumably the main source of pollutants for the light-rail line. On the other hand, the subway line appears to have an almost constant background concentration of approximately 21 μg/m^3. The linear regression analysis implies that on a day with high episodic ambient PM concentrations, light-rail commuters may be subjected to comparable or higher personal exposure concentrations than subway commuters.

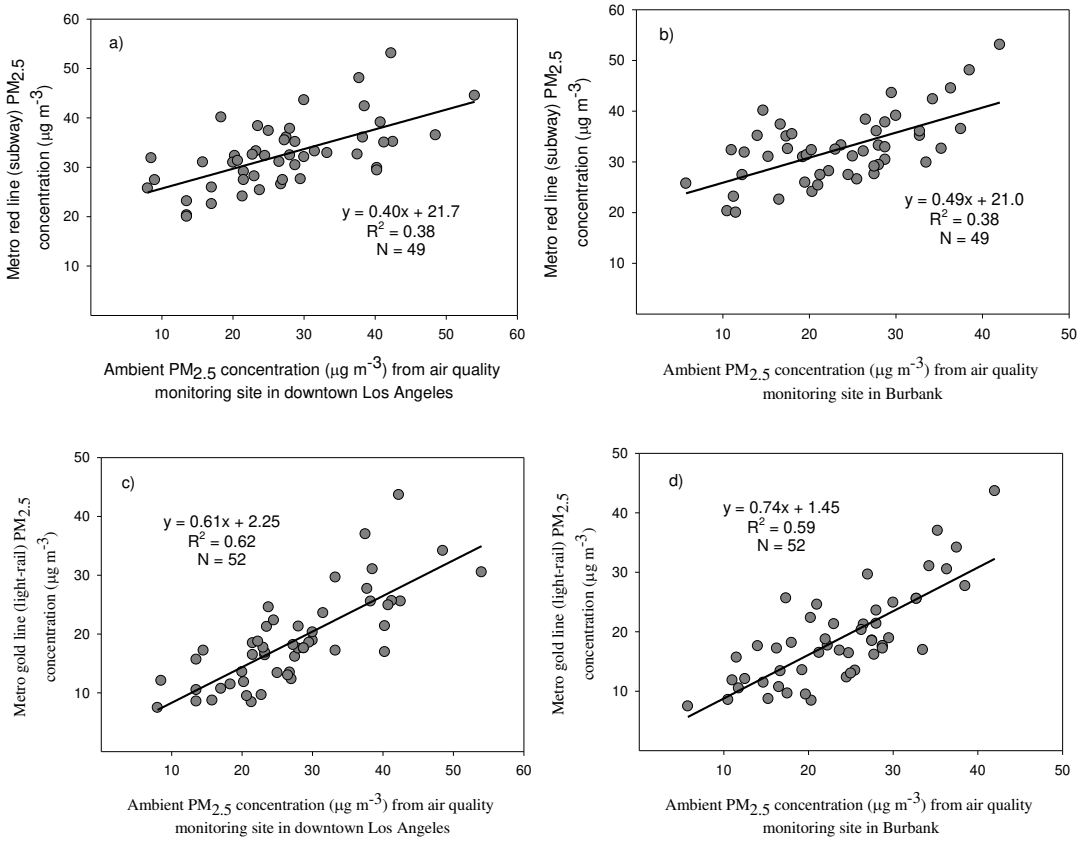

Figure 2.5 Comparison of $PM_{2.5}$ concentrations from personal exposure campaign with ambient levels from two stations (Downtown L.A. and Burbank). Each point represents a daily 3.5-hour average. (a) Red line (subway) vs Downtown L.A., (b) red line vs Burbank, (c) gold line (light-rail) vs Downtown L.A., and (d) gold line vs Burbank.

2.2.5 Inter-correlations of PM concentrations to investigate sources

To investigate the sources of PM in the two microenvironments, station platforms and trains, correlation analysis between $PM_{2.5}$ and coarse PM was done. In Figure 2.6a and 2.6b, the

data points represent the station/train intensive campaign average of the 7 days of sampling for each station and inside the train for the subway line and light-rail line, respectively. Since it was previously established that the two microenvironments have a common source of PM, a linear regression was performed for both the station and train data points. The high correlation (R^2=0.89) for the subway line scatter plot (Figure 2.6a) indicates that $PM_{2.5}$ and coarse PM have a common origin. Although this common PM source cannot be determined based on the data presented in this manuscript, previous studies have attributed metallic components of PM to originate from the friction of the wheels on the steel rails, the vaporization of metals due to sparking, wear of brakes (Pfeifer et al. 1999; Sitzmann et al. 1999), and particulate resuspension and dispersion from train and passenger movement (Chan et al. 2002; Raut et al. 2009). The upcoming chemical analysis of fine and coarse PM will help determine the degree to which the aforementioned sources may contribute to PM exposure in the underground environment.

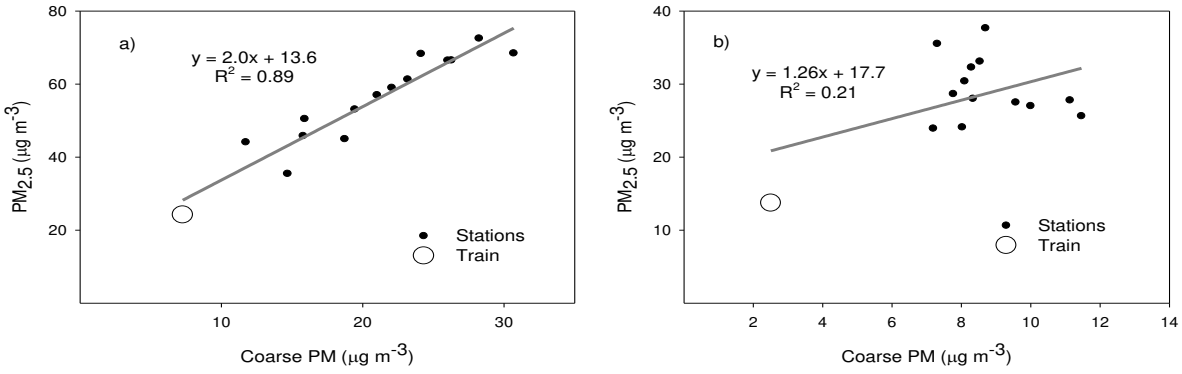

Figure 2.6 Correlation of $PM_{2.5}$ and coarse PM data at all stations and inside train for subway line (a) and light-rail line (b). Each data point represents an average of the 7 days of sampling from the station/train intensive campaign.

Figure 2.6b shows a weak correlation between $PM_{2.5}$ and coarse PM for the light-rail stations and train (R^2=0.21), suggesting that they do not share a common source. However, given the temporal variation of ambient air and its strong influence on the personal PM exposure levels of the light-rail line (Figure 2.5c and 2.5d), the data points presented in the figure, which

represent the average of the 7 days of sampling, do not account for this significant factor. To account for the day-to-day variation of light-rail line PM concentrations, a linear regression of the daily fine and coarse PM levels was conducted for each station and the train (N=7). The correlation coefficients are presented in Table 2.3, which range from 0.52 to 0.92. This moderate to strong correlation suggests that fine and coarse PM for the light-rail line may indeed have a common source. It is reasonable to hypothesize that the primary source of particulate pollution for the light-rail line is from local emissions (vehicular traffic, road dust, photochemical reactions, etc). The daily operations of the light-rail trains (i.e. movement of the train) may also affect PM levels, but their impact is expected to be considerably smaller, given its exposed environment.

	Gold line
	R
Union Station	0.81
Chinatown	0.80
Lincoln/Cypress	0.88
Heritage Square	0.77
Southwest Museum	0.82
Highland Park	0.85
Mission	0.74
Fillmore	0.73
Del Mar	0.68
Memorial Park	0.52
Lake	0.75
Allen	0.84
Sierra Madre	0.67
TRAIN	0.92

Table 2.3 Correlation coefficients between $PM_{2.5}$ and coarse PM for the light-rail line. N=7

2.2.6 Comparison to worldwide rail systems

The Los Angeles Metro system, which began operation in 1993, is a relatively new rail system compared to other systems around the world. Table 2.4 displays the average and range of PM_{10} and $PM_{2.5}$ concentrations and its fine fraction ($PM_{2.5}/PM_{10}$) for different rail systems. In

comparison to the PM levels of the subway systems presented, the particulate levels measured at the two rail lines of the Los Angeles Metro system fall on the relatively 'cleaner' side. On average, the underground stations of the Metro red line have PM_{10} and $PM_{2.5}$ levels that are 2.5 and 2.9 times greater than the USC urban ambient site, while an underground station in the Stockholm subway system had levels that are 4.8 and 11.2 times greater than its corresponding ambient site (Johansson and Johansson 2003). A study on the Seoul subway system reported levels of an underground station to be only 2.3 and 1.3 times greater than ambient concentrations, but the ambient PM_{10} and $PM_{2.5}$ concentrations were 155 $\mu g/m^3$ and 102 $\mu g/m^3$ respectively (Kim et al. 2008). The Seoul subway train PM levels are also exceptionally high because of the lack of a mechanical ventilation system inside the train (Park and Ha 2008). A study on the London subway system, the oldest rail system in the world, reported underground

City (study year)	Measurement location	$PM_{2.5}$ ($\mu g\ m^{-3}$)		PM_{10} ($\mu g\ m^{-3}$)		Fine fraction ($PM_{2.5}/PM_{10}$)	Reference
		average	range (min-max)	average	range (min-max)		
Los Angeles (2010)	in train (gold line - ground level)	14	3-38	16	6-53	0.88	Current study
	in train (red line - underground)	24	11-62	31	14-107	0.77	
	ground level station platforms (all stations)	29	4-77	38	8-184	0.76	
	underground station platforms (all stations)	57	9-130	78	14-197	0.73	
	urban ambient site	20	-	31	-	0.65	
Taipei (2007)	in train (underground)	31	19-51	40	22-71	0.78	*Cheng et al. (2008)*
	underground station platform	44	22-91	66	29-130	0.67	
	ground level station platform	33	7-94	44	11-131	0.75	
Paris (2006)	underground station platform (rush hours)	93	-	320	-	0.29	*Raut et al. (2009)*
	underground station platform (normal hours)	61	-	200	-	0.31	
Helsinki (2004)	in train (underground)	21	17-45	-	-	-	*Aarnio et al. (2005)*
	underground station platform	50	37-87	-	-	-	
Seoul (2004)	underground station platform	129	82-176	359	238-480	0.36	*Kim et al. (2008)*
	in train (underground)	126	115-136	312	29-356	0.40	
	urban ambient site	102	41-174	155	79-254	0.66	
Stockholm (2000)	underground station platform	258	105-388	469	212-722	0.55	*Johansson and Johansson (2003)*
	urban ambient site	23	3-89	98	6-454	0.23	
New York City (1999)	integration of 5h at station platform and 3h in train	62	-	-	-	-	*Chillrud (2004)*
Hong Kong (1999)	in train (mostly underground)	33	21-48	44	23-85	0.75	*Chan et al. (2002)*
	in train (mostly ground level)	46	29-68	60	41-89	0.77	
London (1999)	in train (underground line)	247	105-371	-	-	-	*Adams et al. (2001)*
	in train (above ground line)	29	12-42	-	-	-	

Table 2.4 A comparison of PM_{10} and $PM_{2.5}$ average concentrations for worldwide subway systems. Fine fractions ($PM_{2.5}/PM_{10}$) are also presented.

train $PM_{2.5}$ levels around 250 μg/m^3 (Adams et al. 2001). A study on the New York City subway system measured $PM_{2.5}$ levels on average of 62.5 μg/m^3 (Chillrud et al. 2004). The PM levels of the L.A. Metro system are comparable to the Taipei, Helsinki, and Hong Kong subway systems, which are generally newer systems and equipped with more efficient ventilation systems and advanced braking technologies. Higher fine fractions ($PM_{2.5}/PM_{10}$) are also observed for the newer rail systems, while the older systems (London, Paris, Stockholm) exhibit lower fine fractions, consistent with the fact that older ventilation systems may be less efficient at filtering larger particles.

2.3 Conclusion

An intensive particulate sampling campaign was conducted in spring and summer of 2010 to compare two types of rail systems on the L.A. Metro, an underground subway system (Metro red line) and a ground-level light-rail system (Metro gold line). In general, commuters of the subway line are exposed to greater PM concentrations than commuters of the light-rail line by almost two-fold. Regression analysis showed that the light-rail line is heavily influenced by ambient PM levels and its particulate pollutants originate from local sources, such as vehicular emissions and road dust. The subway line is less influenced by ambient PM levels and has an additional source of airborne particulate pollution that is generated from the daily operation of trains. Strong correlations of $PM_{2.5}$ and PM_{10} between train and stations reveal that PM from stations is the main source of PM inside trains. $PM_{2.5}$ and coarse PM are also highly correlated, suggesting they are also derived from the same source. The next chapter will provide a comprehensive chemical analysis that will be essential in determining the sources of PM in the two rail lines as well as their toxicological potential.

Chapter 3 Chemical characterization and redox potential of coarse and fine particulate matter (PM) in underground and ground-level rail systems of the Los Angeles Metro

3.1 Sample analysis

The Teflon filters were equilibrated for 24h and then weighed before and after sampling to determine gravimetric mass concentrations using a MT5 Microbalance (Mettler-Toledo Inc., Columbus, OH; uncertainty of ±5μg) in a temperature and relative humidity-controlled room. The filters were subsequently cut into 3 equal sections. The first section was analyzed by means of magnetic-sector Inductively Coupled Plasma Mass Spectroscopy (SF-ICPMS) to determine total elemental composition using an acid extraction (Zhang et al. 2008). The second section was extracted using Milli-Q water and aliquots were dispensed for SF-ICPMS analysis to determine water-soluble elemental composition and for ion chromatography (IC) analysis to determine the PM concentrations of inorganic ions (Kerr et al. 2004). For the third section, an alveolar macrophage assay was used to determine the reactive oxygen species (ROS) activity of aqueous suspensions of the collected PM. The location of the alveolar macrophage on the inner epithelial surface of the lung renders this assay an appropriate model of pulmonary inflammation in response to PM exposure. In addition, the fluorescent probe (DCFH-DA) used in the assay is sensitive toward a number of ROS. Details of the assay, extraction protocol, and detection methodology are explained in Landreman et al. (2008) (Landreman et al. 2008). The quartz substrates were prebaked at 550°C for 12h and stored in baked aluminum foil prior to sampling. Elemental and organic carbon (EC/OC) was determined using the Thermal Evolution/Optical Transmittance analysis (Birch and Cary 1996) and organic compounds were determined using

GC/MS (Schauer et al. 1999). Due to limitations in PM mass collection, only fine PM was analyzed for GC/MS.

3.2 Results and discussion

3.2.1 Mass balance

To reconstruct total PM mass concentration for the red line, gold line, and USC ambient site, chemical species were grouped into seven categories: water-soluble organic carbon (WSOC) and water-insoluble organic carbon (WISOC), elemental carbon (EC), inorganic ions, crustal metals less Fe (CM), elemental Fe, and trace metals. WSOC and WISOC were calculated using a multiplier of 1.8 to account for the oxygen, nitrogen, and hydrogen associated with organic carbon (Turpin and Lim 2001). Inorganic ions are the sum of Cl^-, NO_3^-, SO_4^{2-}, PO_4^{3-}, Na^+, K^+, and NH_4^+. The CM category represents the sum of Al, K, Ca, Mg, Ti, and Si, each of which were multiplied by appropriate factors to convert to oxide mass (Cheung et al. 2011). Because silicon data was not acquired, Si was estimated by multiplying Al with a factor of 3.41 (Hueglin et al. 2005). For the purpose of this study, all Fe data is presented as total elemental Fe. Coarse and fine PM mass reconstructions were calculated in the same manner under the assumption that chemical species in both modes originate from the same source.

Figure 3.1 shows the mass reconstruction based on the seven identified categories along with total gravimetric mass concentration for the gold line, red line, and USC ambient site for (a) coarse and (b) fine PM. Results are based on an average of the two periods sampled, except for the gold line coarse PM mode, which is a composite of the two periods. Error bars in this study represent one standard deviation. In coarse PM, the gravimetric mass concentration of the gold line is approximately 40% of the USC ambient site, while mass concentration for the red line is

almost equivalent to USC ambient site. Even though the gold line runs outdoors, the effect of being inside the train significantly reduces personal coarse PM exposure; however, this effect is not apparent for the red line, in which a previous study on the L.A. Metro has demonstrated an additional source of PM in the underground environment (Chapter 2). In fine PM, the red line gravimetric mass concentration is approximately 70% greater than both the gold line and USC ambient site concentrations, while concentrations for gold line are only 5% less than USC ambient site. This suggests that the additional source of PM for the red line has a greater influence in the fine mode than in the coarse mode, and that being inside the train for the gold line does not substantially reduce fine PM exposure.

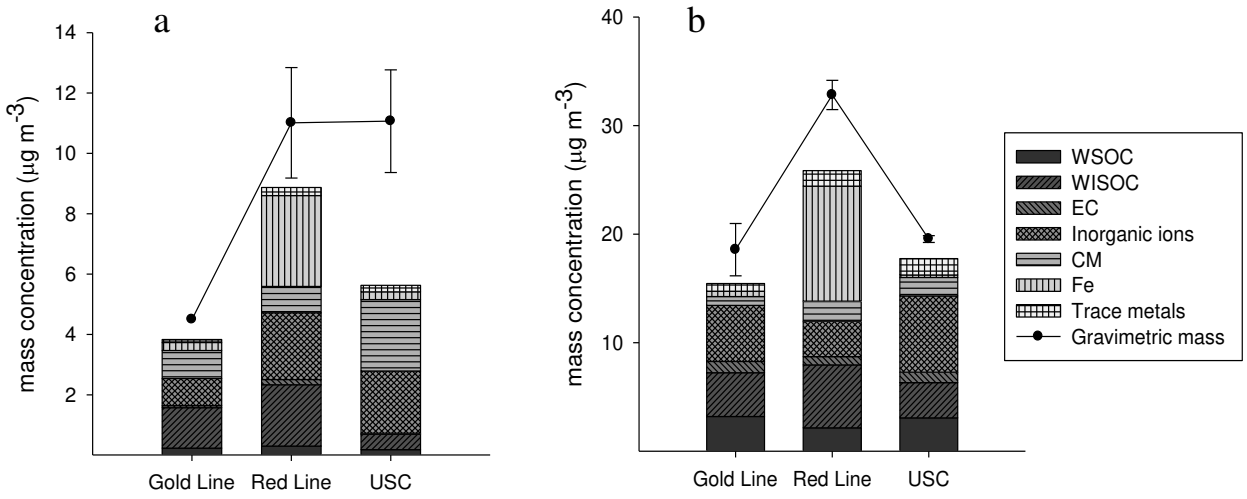

Figure 3.1 Mass reconstruction of the 7 identified categories (a) coarse and (b) fine PM. Gravimetric mass concentrations are also presented.

The most significant difference between the three sites is the abundance of Fe in the subway environment in both PM modes. In coarse PM, the gravimetric mass of red line, gold line, and USC ambient site contains 27%, 6%, and 2% Fe; fine PM in the corresponding sites

contains 32%, 3%, and 1% Fe. This significant presence of Fe in the subway air has major implications in terms of personal exposure of subway passengers. The mass reconstruction for USC ambient site in coarse mode shows that about 48% of the gravimetric mass is unidentified. This is consistent with a coarse PM study in the L.A. basin that found 20-50% unidentified mass in urban sites and attributed the fraction to the uncertainty of the OC multiplier coupled with conversion factors for crustal oxides (Cheung et al. 2011).

3.2.2 Crustal species

Crustal species are elements that are derived from soil origins. They account for a significant portion of urban aerosols, especially in the coarse mode. Table 3.1 shows the average concentration of crustal species in coarse and fine PM for the gold line, red line, and USC ambient site. Except for fine mode Al and Ca, the concentrations of the latter crustal species (Mg, K, and Ti) in both modes for the red and gold lines are remarkably similar. For the red line

		Coarse PM (ng m^{-3})					Fine PM (ng m^{-3})				
		Gold line	Red line	USC	Gold/ USC	Red/ USC	Gold line	Red line	USC	Gold/ USC	Red/ USC
Crustal	Mg	40.6	31.9 ± 18.1	147.3 ± 78.3	0.28	0.22	30.6 ± 20.7	63.7 ± 29.5	76.3 ± 6.6	0.40	0.84
	Al	75.2	70.4 ± 28.7	183.5 ± 34.8	0.41	0.38	61.7 ± 54.6	150.8 ± 47.5	133.3 ± 14.3	0.46	1.1
	K	36.0	26.7 ± 12.7	94.6 ± 21.0	0.38	0.28	57.6 ± 10.0	62.1 ± 12.0	95.3 ± 10.4	0.60	0.65
	Ca	80.0	91.8 ± 40.7	207.2 ± 55.1	0.39	0.44	74.2 ± 39.4	189.5 ± 61.2	144.6 ± 30.8	0.51	1.3
	Ti	6.5	5.6 ± 2.5	17.6 ± 0.7	0.37	0.32	9.4 ± 3.0	11.8 ± 2.8	18.3 ± 1.3	0.51	0.64
Non-Crustal	Cr	1.0	6.1 ± 1.7	0.9 ± 0.2	1.1	7.1	2.1 ± 0.9	23.1 ± 4.7	3.1 ± 2.2	0.68	7.4
	Mn	2.6	22.6 ± 6.8	3.7 ± 0.4	0.71	6.2	5.8 ± 2.2	84.9 ± 13.1	5.2 ± 0.8	1.1	16.2
	Fe	267.1	3010.8 ± 926.2	256.1 ± 43.8	1.0	11.8	490.5 ± 195.1	10599.2 ± 1723.7	236.8 ± 8.1	2.1	44.8
	Co	0.05	0.42 ± 0.14	0.09 ± 0.01	0.55	4.6	0.10 ± 0.03	1.24 ± 0.22	0.12 ± 0.03	0.87	10.5
	Ni	0.4	3.0 ± 1.0	0.6 ± 0.1	0.77	5.5	1.4 ± 0.5	11.9 ± 2.6	2.9 ± 1.5	0.49	4.1
	Cu	18.4	18.0 ± 5.6	12.6 ± 3.2	1.5	1.4	37.5 ± 2.5	64.8 ± 11.3	14.6 ± 0.9	2.6	4.4
	Zn	9.1	7.8 ± 4.0	6.0 ± 0.7	1.5	1.3	23.9 ± 5.5	29.7 ± 2.6	16.3 ± 3.6	1.5	1.8
	Mo	3.1	62.7 ± 23.4	0.6 ± 0.2	5.5	112.5	6.3 ± 2.1	155.6 ± 26.9	1.1 ± 0.1	5.9	146.2
	Cd	0.02	0.30 ± 0.11	0.02 ± 0.003	1.3	16.2	0.13 ± 0.07	0.99 ± 0.11	0.09 ± 0.02	1.5	11.5
	Ba	11.0	55.9 ± 16.8	14.6 ± 2.8	0.75	3.8	18.4 ± 11.5	215.6 ± 33.3	13.5 ± 0.9	1.4	16.0
	Eu	0.01	0.04 ± 0.01	0.01 ± 0.003	0.63	2.9	0.013 ± 0.009	0.15 ± 0.02	0.01 ± 0.001	1.1	12.8

Table 3.1 Average total mass concentrations (ng/m^3) and ratios relative to USC of crustal and non-crustal metals.

sample, crustal species in the coarse mode also exhibit the same patterns as the inorganic ions in which the concentrations follow each other in the two sequential sampling periods (not shown), indicating the influence of ambient crustal aerosols. However, crustal species in the fine mode did not exhibit this trend. It is important to note that the average red line concentrations of fine mode Al and Ca are greater than corresponding USC concentrations, suggesting these two species may have an additional non-crustal source, which will be discussed in greater detail in the following section.

3.2.3 Non-crustal species

Selected non-crustal species concentrations (ng/m^3) and gold and red line to USC ambient site concentration ratios are also shown in Table 3.1. The species were selected based on its elevated concentrations relative to USC concentrations and results from other subway systems (Salma et al. 2007; Murruni et al. 2009). Numerous studies have determined Fe to be ubiquitous in subway environments, and are present in elevated concentrations relative to street levels by up to 50 times (Nieuwenhuijsen et al. 2007). The current study has also observed a number of non-crustal species, particularly transition metals, to have significantly higher concentrations in the subway environment than USC ambient levels. It is important to note that the enrichment ratios of the red line relative to the gold line and USC are greater in the fine mode than in the coarse mode. For the red line, Fe concentrations (3.0 and 10.6 µg/m^3 in the coarse and fine mode, respectively) are 12 and 45 times greater than the corresponding USC concentrations and 11 and 22 times greater than those for the gold line. A study in Budapest found Fe concentrations at station platforms to be 33.5 and 15.5 µg/m^3 for $PM_{10-2.0}$ and $PM_{2.0}$, respectively, accounting for 40% and 46% of their corresponding total PM mass (Salma et al. 2007). Consistent with other worldwide subway studies, Mn, Cr, Co, Ni, Cu, and Ba were observed on the red line to have

concentrations that are at least 2 times higher than corresponding USC ambient levels. In comparison to the gold line personal exposure, passengers on the red line are exposed to substantially higher levels of most of these trace elements. In addition, Mo, Cd, and Eu have also been identified to be significantly enriched in the subway environment, especially in the fine mode. Mo exhibits the greatest enrichment ratios in both modes and both lines; for red line, Mo concentrations are 113 and 146 times greater than USC levels in coarse and fine mode, respectively; for the gold line, Mo concentrations are 5 and 6 times greater than USC levels. The enriched levels of these non-crustal species observed for the red line can be attributed to its enclosed environment and a significant underground source that has resulted in the accumulation and subsequent resuspension of PM dust.

Subway dust is primarily generated by the frictional processes of the wheels, rails, and brakes of the system as well as by the mechanical wearing of these parts. Particles can also be formed by the condensation of gaseous Fe species from the sparking between the third-rail and the train (Kang et al. 2008). Stainless steel, which is used for the rail tracks and the main body of the train for both lines, is an iron-based alloy mixed with chromium and other metallic elements to enhance its properties. However, the composition of the stainless steel employed by the red and gold line could not be found as it may be proprietary information of the manufacturer.

Linear regression analysis was conducted for the crustal and non-crustal species to determine the inter-correlation in coarse and fine PM. Table 3.2 shows the coefficients of determination (R^2) of these species. The regression analysis only includes total metals data from the gold and red line samples (N=7) based on the assumption that the selected non-crustal species from the gold and red line environment are derived from a different source than corresponding species from USC ambient site. The number of data points includes 3 coarse PM

data points (1 from gold line, 2 from red line) and 4 fine PM data points (2 from gold line, 2 from red line). While Table 3.1 established the elevated concentrations of Al and Ca for the red line relative to USC ambient site, bivariate linear regression analysis reveals that both species are strongly correlated with the majority of non-crustal species, suggesting that Al and Ca may have non-crustal sources for the gold and red line environments in addition to soil-derived sources. The strong correlation between Al, Ca, Cr, Mn, Fe, Co, Ni, Cu, Mo, Cd, Ba, and Eu suggests that these elements may share a common source, and may be components of stainless steel used by the subway and light-rail systems in this study.

		Crustal species					Non-crustal species										
		Mg	Al	K	Ca	Ti	Cr	Mn	Fe	Co	Ni	Cu	Zn	Mo	Cd	Ba	Eu
Crustal species	Mg	1															
	Al	0.94	1														
	K	0.43	0.42	1													
	Ca	0.90	0.96	0.40	1												
	Ti	0.68	0.68	0.92	0.64	1											
Non-crustal species	Cr	0.58	0.74	0.27	0.85	0.44	1										
	Mn	0.54	0.71	0.24	0.82	0.40	1.00	1									
	Fe	0.54	0.70	0.22	0.82	0.38	0.99	1.00	1								
	Co	0.55	0.70	0.21	0.83	0.38	0.99	0.99	1.00	1							
	Ni	0.59	0.74	0.30	0.86	0.47	1.00	0.99	0.99	0.98	1						
	Cu	0.52	0.61	0.75	0.67	0.79	0.73	0.70	0.67	0.66	0.76	1					
	Zn	0.35	0.42	0.92	0.42	0.86	0.40	0.38	0.34	0.33	0.43	0.86	1				
	Mo	0.52	0.67	0.15	0.80	0.31	0.96	0.97	0.98	0.99	0.95	0.56	0.25	1			
	Cd	0.54	0.71	0.26	0.82	0.43	0.99	0.99	0.99	0.99	0.99	0.72	0.41	0.96	1		
	Ba	0.57	0.73	0.26	0.84	0.43	1.00	1.00	1.00	0.99	0.99	0.72	0.40	0.96	0.99	1	
	Eu	0.56	0.73	0.26	0.83	0.43	1.00	1.00	0.99	0.99	0.99	0.72	0.40	0.95	0.99	1.00	1

Table 3.2 Coefficients of determination (R^2) of total crustal and non-crustal species. Correlation includes gold and red line data only for coarse and fine PM (N=7).

Cu exhibits lower R^2 values with the other stainless steel elements, but is still well correlated and also appears to be clustered with Zn, Ti, K, and Ca. Although Ba is strongly correlated with the other non-crustal elements (R^2>0.96), it is not typically used as an alloy in stainless steel, but has been identified with the wear of brakes (Furuya et al. 2001). Zn is the only

non-crustal species not strongly correlated with other non-crustal species, but instead exhibits strong correlation with K and Ti. Zn is typically used as a coating on steel for corrosion protection (Marder 2000), but our regression analysis suggests its elevated concentrations may be from another source. A subway study in Buenos Aires found that the main source of Zn was from street-level vehicular emissions (Murruni et al. 2009).

Figure 3.2 shows the crustal enrichment factors (EF) for 22 elements for the gold line, red line, and USC ambient site in the (a) coarse and (b) fine mode. The crustal ratios are calculated based on Upper Continental Crust (UCC) values from Taylor and McLennan (1985) (Taylor and McLennan 1985). Total elemental concentrations are first normalized by Al and then divided by

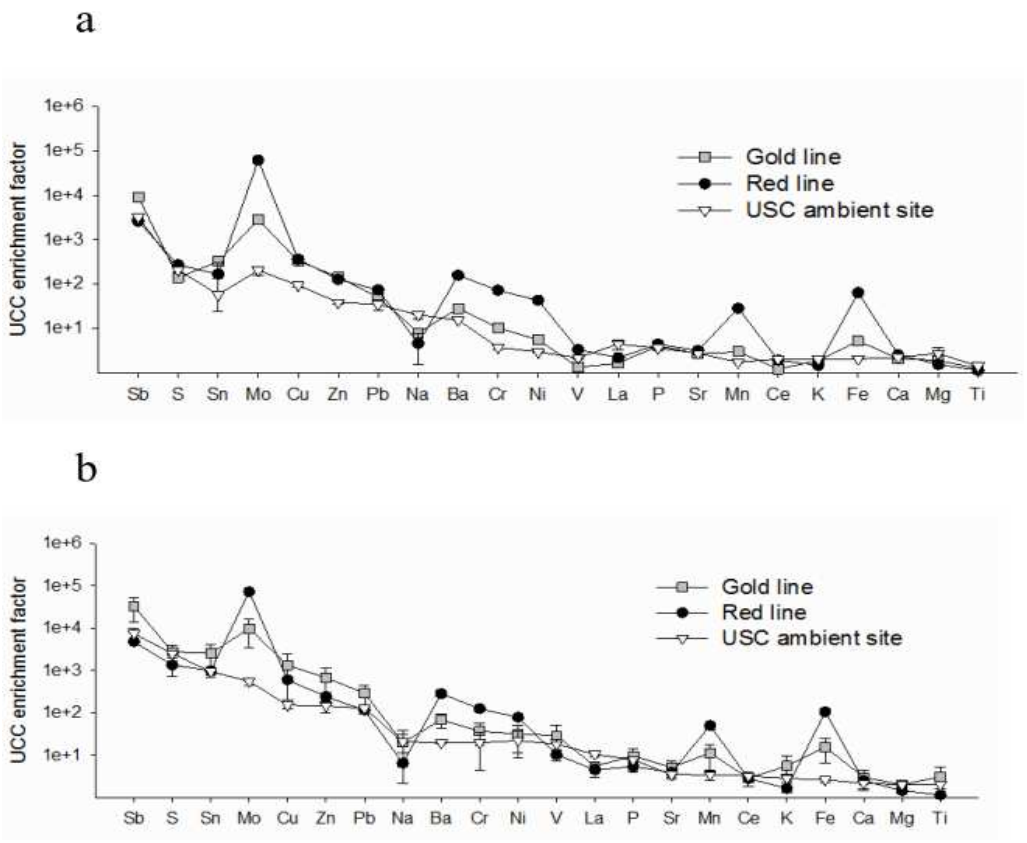

Figure 3.2 Upper Continental Crustal (UCC) enrichment factors (EFs) for (a) coarse and (b) fine mode using total elemental concentrations.

the relative abundance of the corresponding UCC ratio. A much higher crustal EF indicates anthropogenic origin, while an EF approaching 1 indicates crustal origin. The elements are sorted based on the decreasing order of the USC ambient site crustal EFs. The pattern in fine and coarse mode crustal EFs are remarkably similar to each other. Crustal EFs for Na, La, K, and Mg in both modes for the gold and red lines are lower than USC ambient site, suggesting the source is ambient air. In both modes, Mo has the highest crustal EF for the gold and red lines, followed by Fe, Mn, Ba, Cr, and Ni. It is evident that the source of these enriched elements is substantially greater on the red line than on the gold line. Table 3.1 showed that concentrations of Ni, Cr, and Ba for the gold line are lower or similar to corresponding concentrations at the USC ambient site, but the crustal EF analysis reveals that the EFs are actually greater than USC ambient site EFs by approximately 2-3 times. This suggests that these elements have indeed been influenced by additional sources (i.e. rail abrasion, brake wear, etc.), which are not affecting the vicinity of the USC ambient site.

3.2.4 Reactive oxygen species (ROS) activity

A number of transition metals that have been identified in this study to be present in elevated concentrations are known to contribute to the generation of reactive oxygen species (ROS), resulting in oxidative stress (Verma et al. 2010). Table 3.3 shows the ROS coefficients of determination (R^2) with WS crustal species, WS non-crustal species, OC, WSOC, EC, and ions. The analysis includes both PM modes for the red line, gold line, and USC (N=9). Non-crustal species, namely Fe (R^2=0.77), Ni (R^2=0.95), and Cr (R^2=0.84), show strong correlations with ROS activity, while most of the crustal species show poor correlations. Although Cd also shows a strong correlation with ROS activity, Cd is not redox active and its concentrations are below any toxicity threshold. Of the other PM components, OC exhibited the highest correlation with

ROS (R^2=0.92). A multiple linear regression (MLR) analysis was conducted to further investigate the contribution of PM components to ROS activity. We elected WS Fe and OC as our two independent variables to be predictors of ROS activity because they each represent distinct pollution sources and have also been shown to be redox active based on the ROS assay in previous studies (Hu et al. 2008; Verma et al. 2010). A fitted least-squares model was obtained using SigmaPlot resulting in the following equation:

$$ROS = -16.624 + 0.663 \times Fe + 0.0318 \times OC$$

The overall model is statistically significant ($p<0.001$) and has an adjusted R^2=0.94; the constant was reported not to be statistically significant ($p>0.05$). In addition, the correlation between the measured and predicted ROS values is excellent (R^2=0.96; y[predicted ROS]=0.96x[measured ROS]+3.41). The results suggest that WS Fe, a PM species present in elevated concentrations in rail environments, and OC, an indicator of ambient vehicular traffic, can explain 94% of the variance of the measured ROS activity.

WS Crustal species		WS Non-crustal species		Other PM components	
Mg	0.06	Cr	0.84	OC	0.92
Al	0.70	Mn	0.69	WSOC	0.69
K	0.14	Fe	0.77	EC	0.74
Ca	0.01	Co	0.65	ions	0.24
Ti	0.03	Ni	0.95		
		Cu	0.66		
		Zn	0.60		
		Mo	0.02		
		Cd	0.93		
		Ba	0.33		
		Eu	0.31		

Table 3.3 ROS coefficients of determination (R^2) with WS crustal and non-crustal species and other PM components. Data includes coarse and fine data for red line, gold line, and USC ambient site (N=9).

Figure 3.3 shows the ROS activity of particles for the gold line, red line, and USC ambient site in ng of Zymosan units (a) per volume (m^3) and (b) per mass (mg). The per volume basis is relevant for the personal exposure assessment of passengers, while the per mass basis is a measure of the intrinsic properties of the particles collected. On a per volume basis, fine PM accounts for 90-98% of total ROS activity. In addition, ROS activity observed on the red line is greater than USC ambient site and gold line activity by 65% and 55%, respectively. Even though total concentrations of ROS-active metals (Fe, Ni, and Cr) in both modes are 4-44 times greater on the red line than at USC ambient site (Table 3.1), ROS activity differs by less than 2 times. The opposite is observed when comparing the two PM modes, in which ROS activity differs by 7-29 times and total concentrations of Fe, Ni, and Cr only differ by 2-4 times. Based on these observations, it is clear that the soluble fraction of the metals plays a dominant role in ROS activity. On a per mg basis, gold line ROS activity in fine mode is 13% greater than red line and USC ambient site activity, while red line and USC ambient site ROS activity are comparable. Our results suggest that one unit of PM mass on the gold line may be as intrinsically toxic as one unit of PM mass from the red line, however, from a personal exposure perspective, PM originating from the red line generates greater ROS activity per m^3 of air than PM from the gold line and at USC ambient site.

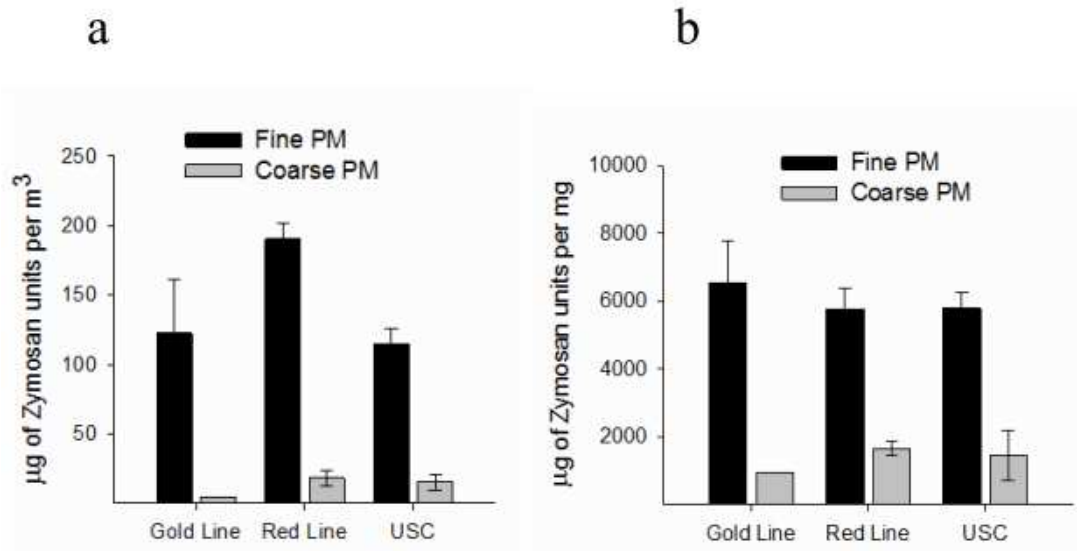

Figure 3.3 Reactive oxygen species (ROS) activity (a) per air volume (m^3) and (b) per gravimetric PM mass (mg).

Although our results suggest that subway and light-rail air may not be intrinsically more toxic than USC ambient air, it should be noted that a more appropriate personal exposure assessment of transport microenvironments in L.A. should be a comparison with the predominant mode of commute—private vehicles. Passengers of the L.A. Metro may actually be subjected to lower levels of PM and toxic co-pollutants such as EC and transition metals. To date, freeway commuter exposure assessments of on-road PM chemical composition measurements are limited. My future investigation will provide a comprehensive exposure assessment of "on-road" PM physical and chemical characterization of trafficked freeways and arterial roads of urban L.A. This will offer a greater understanding of the health impacts of different transport modes to the public health.

Chapter 4 Size-segregated composition of particulate matter (PM) in major roadways and surface streets

4.1 Introduction

The novelty of this study lies in the sampling instrumentation used to collect on-road PM. The use of portable, lightweight battery-operated pumps, which operate at relatively high flow rates coupled with cascade impactors made it possible to collect size-fractionated PM. A quasi-isokinetic inlet was deployed to collect time-integrated samples along three routes in Los Angeles: a major roadway dominated by light-duty vehicles (LDVs), a major roadway with a higher fraction of heavy-duty vehicles (HDVs), and two major surface streets. Concurrent samples were collected at a fixed site at the University of Southern California (USC), representing an urban background site. Other studies have provided measures of roadway ambient air pollutants which may be representative of a busy traffic area, but the current study focuses on assessing private commuter exposure by selecting three distinct commute environments which encompass various traffic volumes, traffic composition, and driving conditions. Chemical analysis has been performed for three size fractions of PM, including $PM_{10-2.5}$, $PM_{2.5-0.25}$, and $PM_{0.25}$. The objectives of this study are: 1) provide a chemical comparison of the three roadway environments and USC background site, 2) discuss factors that may contribute to the differences in chemical composition of the roadway environments, and 3) compare results to previous studies that have been conducted at fixed sites near the same roadways.

4.2 Experimental methodology

The in-vehicle sampling campaign was undertaken in Los Angeles in March-April 2011. Sampling was conducted for 11 hours per day on Monday - Friday, from 6:00 a.m. to 5:00 p.m. Figure 4.1 shows the three sampling routes that were selected to each represent a distinct

roadway environment. The I-110 is a high-traffic freeway that runs 51-km from the Port of Los Angeles through downtown Los Angeles to Pasadena and is composed mostly of light-duty vehicles (LDVs); the I-710 is a 43-km freeway and has a higher heavy-duty vehicle (HDV) composition than the I-110 because it serves as the main corridor for HDVs traveling to and from the Ports of Los Angeles and Long Beach; Wilshire/Sunset Boulevards is a 48-km major surface street route that traverses downtown Los Angeles, Koreatown, Miracle Mile, Beverly Hills, and Hollywood.

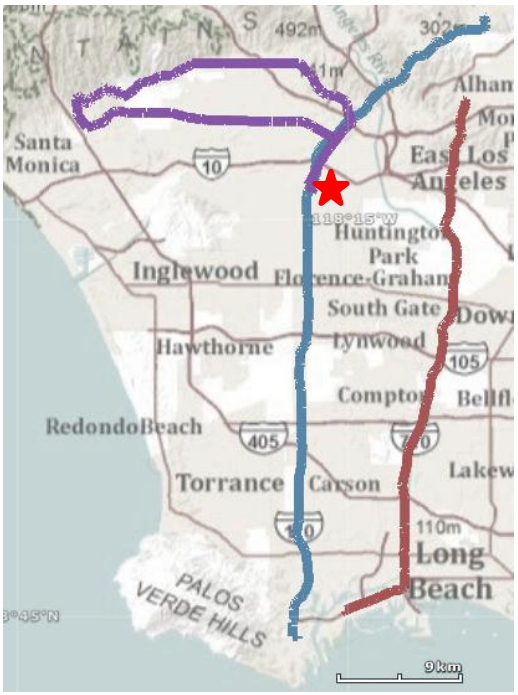

Figure 4.1 Map of the three sampling routes: 1) I-110 (blue), 2) I-710 (red), and Wilshire/Sunset (purple). The USC background site is denoted by the red star.

A summary of the traffic data is shown in Table 4.1, which is taken from the CalTrans Performance Measurement System (PeMS) database. The total vehicle flow for the I-110 (6378 vehicles/hr) is approximately 1.5 times higher than total flow for the I-710 (4247 vehicles/hr). However, the I-110 truck flow (243 trucks/hr) is approximately half of the I-710 truck flow (470 trucks/hr), yielding a truck composition of 3.9% and 11.3% for the I-110 and I-710, respectively.

In addition, the northern section of the I-110, which is approximately 12-km, is limited to LDVs only. It is important to note that even though traffic flows may differ for various parts of the freeway, the traffic sites were carefully selected to be located in the center of the freeway to characterize the entire freeway. The Wilshire/Sunset route had a total flow of 1,839 vehicles/hr with a negligible truck flow. Concurrent sampling was conducted at University of Southern California (USC) and served as our background site (Moore et al. 2007; Ning et al. 2007). Two samples were collected for the three routes and for the USC background site.

Route	Dates of sampling	Temp (deg C)	±	RH (%)	±	Prevailing wind direction	Wind speed (m/s)	±	Total/truck flow (vehicle/hour)	Truck composition (%)
110 S1	3/1-3/8/11	17.8	3.8	54.2	17.0	W	3.2	0.9	6378/243	3.9
110 S2	4/11-4/18/11	18.7	2.5	60.1	13.1	SW	3.1	0.8		
710 S1	3/17-3/25/11	15.8	3.2	55.3	16.2	W	3.6	0.9	4247/470	11.3
710 S2	4/19-4/25/11	18.7	1.7	64.5	8.3	W	3.4	0.9		
WS S1	3/9-3/16/11	21.7	3.8	48.3	16.0	SW	2.9	1.2	1839/NA	NA
WS S2	4/26-5/2/11	25.8	4.2	35.6	13.4	SW	3.7	1.0		

Table 4.1 Summary of meteorological parameters from nearby air quality monitoring sites (South Coast Air Quality Management District (SCAQMD)). Traffic data is from the CalTrans database.

4.2.1 Sampling instrumentation

The sampling vehicle (Honda Insight Hybrid 2011) was equipped with six Personal Cascade Impactor Samplers (PCIS) (Misra et al. 2002; Singh et al. 2003), each operated individually with a battery-powered Leland Legacy pump (SKC Inc., Eighty-Four, PA) at a flow rate of 9 liters per minute (lpm). The pumps were calibrated with a Gilian Gilibrator-2 Air Flow Calibrator (Sensidyne Inc., Clearwater, FL) before and after sampling, and pump flows were checked regularly with flow meters throughout the sampling campaign. Two PCIS units were operated concurrently at the USC background site. The inlet for roadway air was designed to have a 90° bend that is characterized by a 50% cutpoint of 10 μm (Peters and Leith 2004). Each PCIS had two impaction stages – the first with a cut point of 2.5 μm to collect $PM_{10-2.5}$ particles

and the second with a cut point of 0.25 μm to collect $PM_{2.5\text{-}0.25}$ particles– and an after-filter stage to collect $PM_{0.25}$. For the purpose of conducting comprehensive chemical analysis, three PCIS were loaded with PTFE (Teflon) filters and three were loaded with quartz filters. In the Teflon units, 25-mm Zefluor-supported PTFE filters (Pall Life Sciences, Ann Arbor, MI) were used as the impaction substrates and 37-mm PTFE membrane filter with PMP ring (Pall Life Sciences, Ann Arbor, MI) were used as after-filters; in the quartz units, quartz microfiber filters (Whatman International Ltd, Maidstone, England) were used as both the impaction substrates and after-filters. Two DustTrak (Model 8520, TSI Inc., Shoreview, MN) were also deployed to measure continuous $PM_{2.5}$ and PM_{10} mass concentrations. However, DustTrak results will not be presented in this paper.

Roadway air was supplied to the PCIS units and DustTrak monitors by a custom-designed, stainless steel inlet with an inner diameter of 0.95 cm (3/8 inch). The curved PM_{10} inlet directed roadway air into the vehicle window to a manifold with six branches (one for each PCIS) with the two DustTrak connected to the end (Figure 4.2). Total flow rate through the inlet was 57.4 lpm (6 PCIS * 9 lpm + 2 DustTrak * 1.7 lpm), yielding a velocity of 13.4 m/s (or 30 mph) at the inlet. Hence, isokinetic sampling was achieved when the vehicle was moving at 13.4 m/s. Anisokinetic sampling may result in the overestimation or underestimation of relatively larger particles (i.e. $PM_{10\text{-}2.5}$) and can be calculated based on the following equation (Belyaev and Levin 1974):

$$\frac{C}{C_o} = 1 + \left(\frac{U_o}{U} - 1\right)\left(1 - \frac{1}{1 + \left(2 + \frac{0.62U}{U_o}\right)St}\right)$$

where C is the estimated PM concentration, C_o is the actual PM concentration, U_o is the free stream velocity, or vehicle speed, U is the inlet velocity, and St is Stokes number. When the vehicle speed is above 13.4 m/s or $U_o > U$, sub-isokinetic sampling occurs; conversely, when vehicle speed is below 13.4 m/s or $U_o < U$, super-isokinetic sampling occurs. Considering the two most extreme cases for d_p=10 μm, when the vehicle speed is 22.3 m/s (or 50 mph), C/C_o=1.34, and when the vehicle speed is 4.5 m/s (or 10 mph), C/C_o=0.58. For particles smaller than 5 μm, the resulting over- or under- estimation of concentration in these two extreme cases of vehicle speed is less than 20%, and decreases rapidly with decreasing particle size. $PM_{2.5}$ is virtually unaffected by anisokinetic sampling.

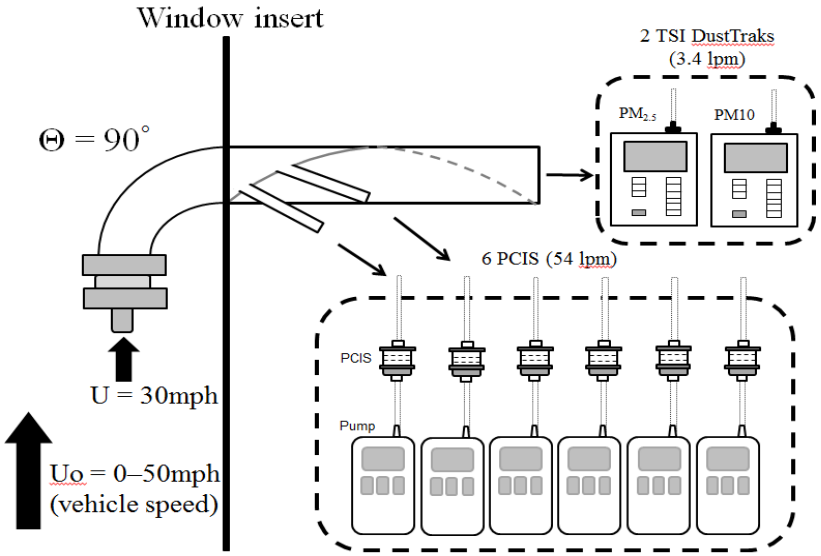

Figure 4.2 Sampling schematic of the inlet into the vehicle and the instrumental set up.

4.2.2 Sample analysis

After completion of sampling, Teflon filters were analyzed gravimetrically and chemically while quartz filters were only analyzed chemically. The Teflon filters were equilibrated for 24 hours, then pre- and post-weighed in a temperature and relative humidity-

controlled room using a MT5 Microbalance (Mettler-Toledo Inc., Columbus, OH) to determine gravimetric mass concentrations. The Teflon filters were analyzed by magnetic-sector Inductively Coupled Plasma Mass Spectroscopy (SF-ICPMS) using acid extraction to determine total elemental composition (Zhang et al. 2008) and ion chromatography (IC) to determine the PM concentrations of inorganic ions (Kerr et al. 2004). The quartz substrates were prebaked at 550°C for 12 hours and stored in baked aluminum foil prior to sampling. Elemental and organic carbon (EC/OC) content was determined using the Thermal Evolution/Optical Transmittance analysis (Birch and Cary 1996). Water extracts of OC yielded WSOC. Organic speciation analysis was conducted with gas chromatography mass spectroscopy (GC/MS) (Schauer et al. 1999). However, organics and metals speciation results are not discussed here and will be the topic of upcoming manuscripts.

4.3 Results and discussion

4.3.1 Overview of campaign

Table 4.1 provides the dates of sampling, a summary of the meteorological conditions, and the traffic flows on the sampled roadways. Meteorological data are obtained from the nearby Downtown Los Angeles and Long Beach air quality monitoring sites that are maintained by the South Coast Air Quality Management District (SCAQMD). Data presented are for the corresponding dates and times of sampling. Variation in both temperatures (°C) and relative humidities (%) were expected considering the daily sampling duration (6 a.m. to 5 p.m.). The prevailing wind direction during sampling hours was consistent across all samples with an onshore breeze from W or SW. Average wind speed (m/s) was also relatively consistent.

Figure 4.3 shows the size-fractionated PM mass concentrations of the two samples collected for each route and for USC background site. In terms of PM size composition, no PM mode is dominant and $PM_{10-2.5}$, $PM_{2.5-0.25}$, and $PM_{0.25}$ account for an average of 37.2±4.1%, 28.3±3.9%, and 34.6±3.6% of total PM mass, respectively, across all sites. Although there is some variation in total mass concentrations between the two sets of samples, the USC background site has the lowest levels of 24.1±2.8 μg/m^3 while the three sampled roadways exhibited comparable levels of 32.2±3.32 μg/m^3.

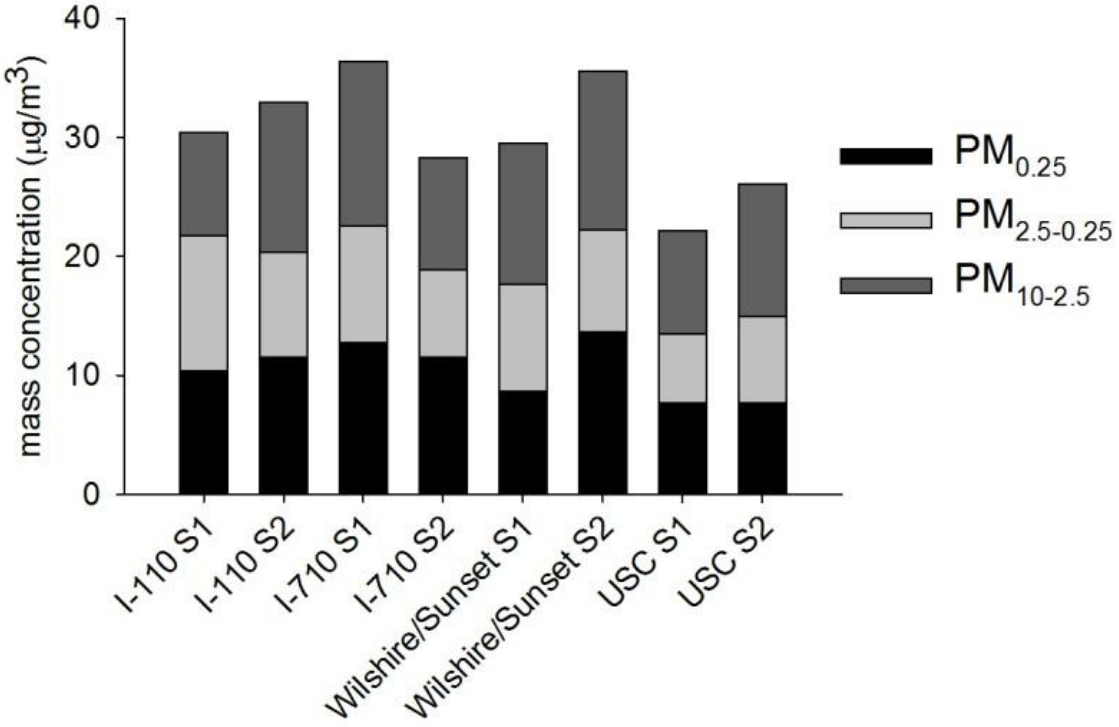

Figure 4.3 Size-fractionated mass summary the three roadways and USC background site. S1 and S2 represent the two sets of samples collected, with a sampling duration of approximately 50 hours for each set. Sampling dates are shown in Table 4.1.

4.3.2 Mass balance

Figure 4.4a-c shows the mass balance for each site (I-110, I-710, Wilshire/Sunset, and USC) and each size fraction. Gravimetric mass concentrations are shown with error bars representing one standard deviation. The mass balance was constructed based on 5 categories: inorganic ions, organic matter (OM), elemental carbon (EC), crustal metals, and trace metals. Inorganic ions consist of chloride, nitrate, phosphate, sulfate, sodium, ammonium, and potassium. Organic matter is calculated by multiplying OC by a correction factor of 1.8 (Turpin and Lim 2001). Crustal metals include Mg, Al, K, Ca, Ti, and Fe multiplied by a corresponding factor to account for oxide forms, with the exception of Si which is derived from Al (Chow et al. 1994; Marcazzan et al. 2001; Hueglin et al. 2005). Trace metals include the remaining elements. Individual metal mass concentrations (ng/m^3) for the three roadway environments and for USC background site are shown in Table 4.2, and will be discussed in more detail in Chapters 4 and 5.

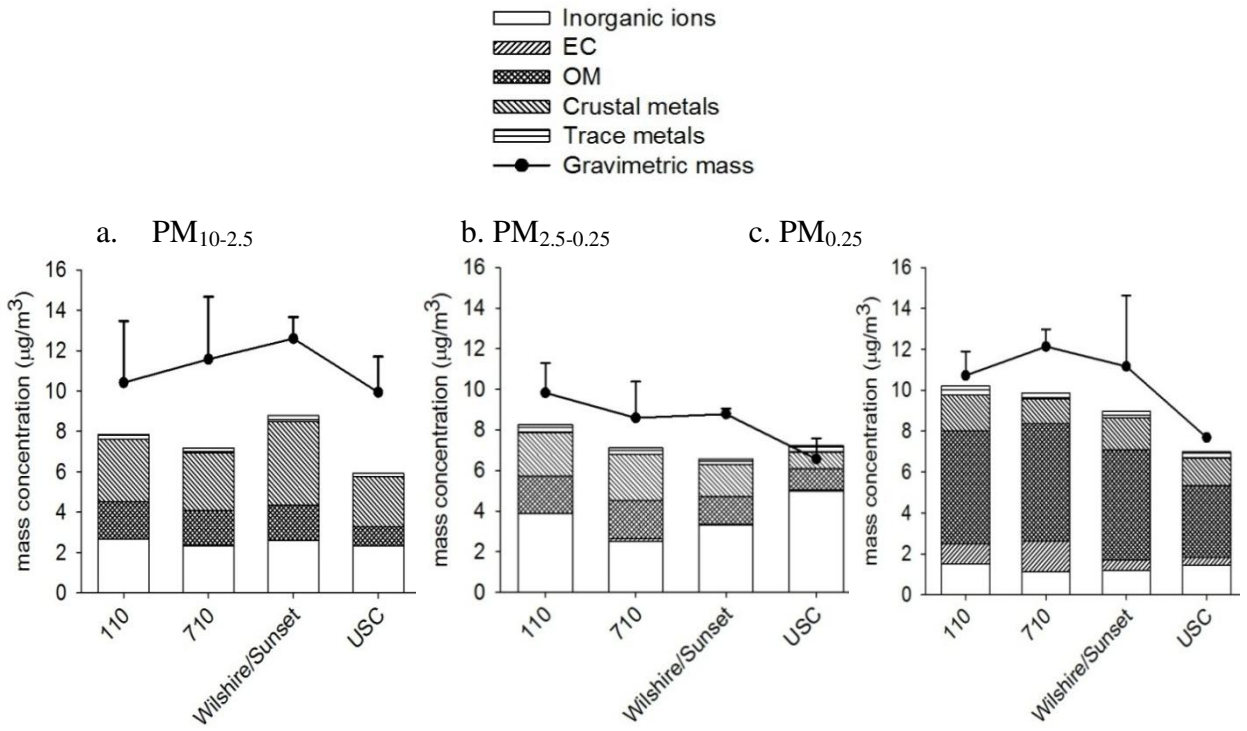

Figure 4.4 Mass balance constructed based on five identified categories for a) $PM_{10-2.5}$, b) $PM_{2.5-0.25}$, and c) $PM_{0.25}$. Error bars represent one positive standard deviation.

	$PM_{10-2.5}$								$PM_{2.5-0.25}$				$PM_{0.25}$			
	I-110	±	I-710	±	Wilshire/ Sunset	±	USC	±	I-110	I-710	Wilshire/ Sunset	USC	I-110	I-710	Wilshire/ Sunset	USC
Li	0.11	0.03	0.09	0.01	0.13	0.03	0.12	0.03	0.29	0.21	0.39	0.32	0.13	0.08	0.15	0.11
B	0.31	0.04	0.39	0.05	0.25	0.03	0.17	0.03	0.47	0.31	0.39	0.40	1.92	0.94	2.49	1.11
Mg	83.51	31.29	81.39	1.61	135.22	36.23	131.22	16.03	70.71	67.38	78.18	46.00	28.22	19.04	25.29	21.46
Al	151.81	49.86	147.60	29.13	224.66	50.56	149.13	76.88	97.24	113.60	80.06	39.25	100.19	68.56	90.20	101.64
P	5.20	0.63	4.72	1.05	3.80	2.24	1.83	1.45	10.64	8.76	6.90	7.28	9.03	7.88	7.04	4.74
S	114.07	26.20	109.38	19.00	124.97	9.60	109.59	1.71	264.42	191.58	210.31	312.35	336.90	231.42	221.81	286.22
K	82.56	24.10	89.01	11.78	99.20	10.74	99.98	14.35	56.27	54.40	49.19	49.18	61.19	34.82	52.06	38.43
Ca	206.40	37.27	203.28	8.89	272.08	24.61	192.02	64.12	113.93	131.81	97.32	56.82	106.66	77.71	97.37	68.60
Ti	31.99	0.48	26.28	3.13	35.30	2.06	21.13	0.44	23.66	20.97	12.35	7.82	22.84	13.45	15.72	8.53
V	0.54	0.10	0.74	0.03	0.58	0.04	0.49	0.05	0.56	0.73	0.45	0.60	0.86	1.19	1.01	1.04
Cr	2.70	0.10	2.00	0.14	3.68	0.18	1.04	0.31	2.02	1.92	1.48	0.66	2.10	1.52	1.79	2.18
Mn	6.93	0.45	6.40	0.11	7.73	0.05	3.78	0.36	5.65	5.74	3.72	2.49	4.32	3.42	3.73	2.34
Fe	765.05	139.84	651.78	31.05	893.98	40.27	318.14	15.33	598.85	598.40	338.31	136.67	356.75	267.31	328.50	134.49
Co	0.12	0.00	0.17	0.07	0.14	0.00	0.19	0.10	0.09	0.10	0.08	0.06	0.08	0.07	0.08	0.10
Ni	1.01	0.41	1.13	0.15	0.96	0.16	0.55	0.03	0.59	0.60	0.35	0.34	1.15	1.01	0.56	1.24
Cu	47.86	9.00	28.82	0.05	53.54	4.46	12.22	2.57	36.48	23.17	21.97	5.97	23.92	13.63	21.37	7.98
Zn	11.12	0.95	10.77	1.45	12.45	0.66	6.34	0.72	11.48	11.25	9.82	6.01	18.26	12.97	10.72	8.33
As	0.14	0.00	0.12	0.07	0.15	0.03	0.10	0.02	0.31	0.17	0.16	0.19	0.35	0.23	0.33	0.27
Rb	0.24	0.07	0.24	0.04	0.26	0.03	0.25	0.02	0.15	0.16	0.09	0.11	0.16	0.09	0.13	0.11
Sr	3.88	0.65	3.60	0.72	3.81	0.12	2.40	0.53	3.03	2.66	1.70	0.93	4.42	1.53	1.65	0.87
Mo	1.65	0.33	1.03	0.02	2.38	0.15	0.48	0.12	1.50	1.12	1.11	0.34	1.15	1.06	1.23	0.46
Ag	0.05	0.02	0.05	0.01	0.03	0.01	0.09	0.10	0.05	0.12	0.04	0.02	0.10	0.03	0.13	0.10
Cd	0.05	0.00	0.05	0.00	0.07	0.00	0.03	0.02	0.07	0.06	0.06	0.04	0.09	0.06	0.07	0.05
Sn	2.70	0.84	0.59	0.02	6.04	0.09	0.00	0.00	4.24	2.30	3.55	1.65	3.68	1.83	3.93	2.06
Sb	7.33	1.42	3.93	0.00	7.35	0.61	1.77	0.40	6.39	4.07	3.35	1.12	4.12	2.45	3.74	1.25
Ba	55.25	16.70	45.00	3.72	61.76	0.48	17.95	5.93	53.37	57.07	24.91	7.84	28.36	23.46	21.52	7.05
La	0.15	0.01	0.15	0.01	0.18	0.02	0.18	0.12	0.17	0.22	0.12	0.13	0.10	0.09	0.09	0.15
Ce	0.50	0.11	0.42	0.02	0.41	0.02	0.26	0.11	0.40	0.45	0.19	0.14	0.29	0.22	0.19	0.14
Pr	0.03	0.00	0.02	0.00	0.03	0.00	0.02	0.01	0.02	0.02	0.01	0.01	0.01	0.01	0.01	0.01
Nd	0.08	0.01	0.08	0.00	0.09	0.01	0.06	0.02	0.06	0.07	0.03	0.02	0.05	0.03	0.04	0.03
Eu	0.07	0.02	0.06	0.00	0.08	0.00	0.03	0.01	0.07	0.08	0.03	0.01	0.04	0.03	0.03	0.01
W	0.06	0.02	0.14	0.06	0.08	0.01	0.07	0.03	0.09	0.15	0.07	0.07	0.11	0.14	0.12	0.09
Pb	1.14	0.03	1.88	0.53	1.55	0.24	1.19	0.26	2.12	2.11	2.37	2.10	2.61	1.87	2.55	2.15

Table 4.2 Mass concentrations of metals (ng/m^3). For $PM_{10-2.5}$, N=2 with standard deviations; for $PM_{2.5-0.25}$ and $PM_{0.25}$, N=1.

4.3.2a $PM_{10-2.5}$

In $PM_{10-2.5}$, USC exhibited the lowest gravimetric and reconstructed mass concentrations while Wilshire/Sunset exhibited the highest in both (Figure 4.4a). In spite of the PM mass differences, the composition of the five designated PM components are relatively consistent across all routes and USC, with crustal metals accounting for 40-50% of reconstructed mass, ions

for 30-40%, OM for 15-25%, trace metals for 3%, and EC for 1%. This consistency demonstrates that the differential microenvironment of each roadway does not play a substantial role in the composition of $PM_{10-2.5}$. This can also be explained by the fact that the major sources of $PM_{10-2.5}$ are not from traffic sources (i.e. vehicular combustion), but rather from resuspension of road dust, large sea salt particles, mechanically generated particles, and biogenic particles (i.e. pollen, fungal spores).

The unidentified mass in this mode is the largest of the three PM size fractions, with I-110 having the lowest of 26% unidentified mass and USC site having the highest of 41%. This underestimation of reconstructed mass calculations can be attributed to the uncertainty in the OC multiplication factor and other mineral compounds that may exist in oxide form. Previous studies of this size fraction in urban areas of Los Angeles have also found that crustal metals and inorganic ions account for the majority of the mass balance (Sardar et al. 2005; Arhami et al. 2009) and that $PM_{10-2.5}$ may be characterized by a relatively high percentage of unidentified mass (Cheung et al. 2011).

4.3.2b $PM_{2.5-0.25}$

Figure 4.4b shows the PM composition for $PM_{2.5-0.25}$ for the 3 roadways and USC background site. Contrary to the $PM_{10-2.5}$ composition, there is more variability in some of the PM components, notably the inorganic ions, which account for 35% of reconstructed mass at I-710 and 69% at USC background site. Crustal metals also exhibited variability across the sites, with 11% for USC and 32% for I-710, and OM ranged from 14-26% with the lowest fraction at USC. This variability in composition suggests that this mode may be more influenced by sources in the immediate environment (i.e. vehicular resuspension, tire and brake wear). Inorganic ions

are primarily formed in the atmosphere in the presence of gaseous precursors (SO_2, NO_2), and thus secondary in nature (Seinfeld and Pandis 2006). Previous studies have also found that PM in $PM_{2.5-0.25}$ is dominated by inorganic ions (primarily sulfate and nitrate) in various regions of Los Angeles (Sardar et al. 2005; Arhami et al. 2009). Although there appears to be a greater difference in inorganic ions between the various roadways and USC background site, statistical analysis showed that the differences are not statistically significant ($p=0.17$). EC and trace metals are low contributors in this mode, accounting for 1-2% and 4-5%, respectively. Finally, 15-25% of gravimetric mass concentrations were unidentified for the roadway sites while USC exhibited an overestimation of 10% of mass.

4.3.2c $PM_{0.25}$

In $PM_{0.25}$, USC exhibits the lowest total PM mass concentrations (Figure 4.4c). On average, the three roadway environments have gravimetric PM concentrations that are 48.0±9.4% higher than levels observed at USC ($p<0.05$), which strongly suggests that vehicular emissions from both LDVs and HDVs are major contributors to PM in this mode. OM is the dominant component and its contribution is consistent across all sites, accounting for 50-60% of reconstructed mass. A previous study in Los Angeles also determined OM to be the dominant contributor of $PM_{0.25}$ (Arhami et al. 2009). Contrary to the larger size fractions, EC exhibited substantial variation across the three roadway environments, accounting for 15% for the I-710, 10% for the I-110, 6% for Wilshire/Sunset and 6% for USC. This observation is consistent with the application of using EC as a surrogate for primary emissions and as a tracer of diesel fuel combustion (Schauer 2003). The significantly higher contribution of EC in the two freeway environments relative to Wilshire/Sunset and USC ($p<0.05$) can be attributed to the fleet fraction of HDVs, of which the I-710 has the highest of 11.3%, the I-110 at 3.9%, and Wilshire/Sunset

with a negligible HDV fraction. Of the three size fractions, $PM_{0.25}$ appears to be most heavily influenced by traffic emissions. Inorganic ions' contribution exhibited slight variation, with the I-710 at a low of 11% and USC at a high of 21%; crustal metals' contribution ranged from 12% at I-710 and 19% at USC; trace metals' contribution were consistently low at 3-5% at all sites. $PM_{0.25}$ is characterized by the lowest fraction of unidentified mass, with 6% for the I-110 and 19% for both the I-710 and Wilshire/Sunset.

The authors acknowledge that quartz filters are subject to both positive (adsorption) and negative (volatility) artifacts of OC, especially for particles collected through filtration (i.e. $PM_{0.25}$) (Turpin et al. 2000). However, significant organic adsorption and volatility artifacts are not expected in this study due to the very high PM mass loadings (Kim et al. 2001) and the low pressure drop of the PCIS (Misra et al. 2002). Particles in $PM_{10-2.5}$ and $PM_{2.5-0.25}$ are collected by impaction and are thus less susceptible to sampling artifacts (Zhang and McMurry 1987).

4.3.3 Inorganic ions

Figure 4.5 shows the inorganic ions concentrations for five inorganic ions (nitrate, sulfate, sodium, chloride, and ammonium). Ion balance calculations showed that particles in $PM_{2.5-0.25}$ and $PM_{0.25}$ were almost fully neutralized; however, the calculation was not possible for $PM_{10-2.5}$ without information for calcium and carbonate.

4.3.3a $PM_{10-2.5}$

In $PM_{10-2.5}$, the average of total inorganic ion concentrations of the four sites is 2.5±0.2 $\mu g/m^3$ (Figure 4.5a). Nitrate is the dominant component and its contribution to total ions ranges from 31.9% on the I-710 to 50.1% for the I-110. A previous study in Los Angeles in this size

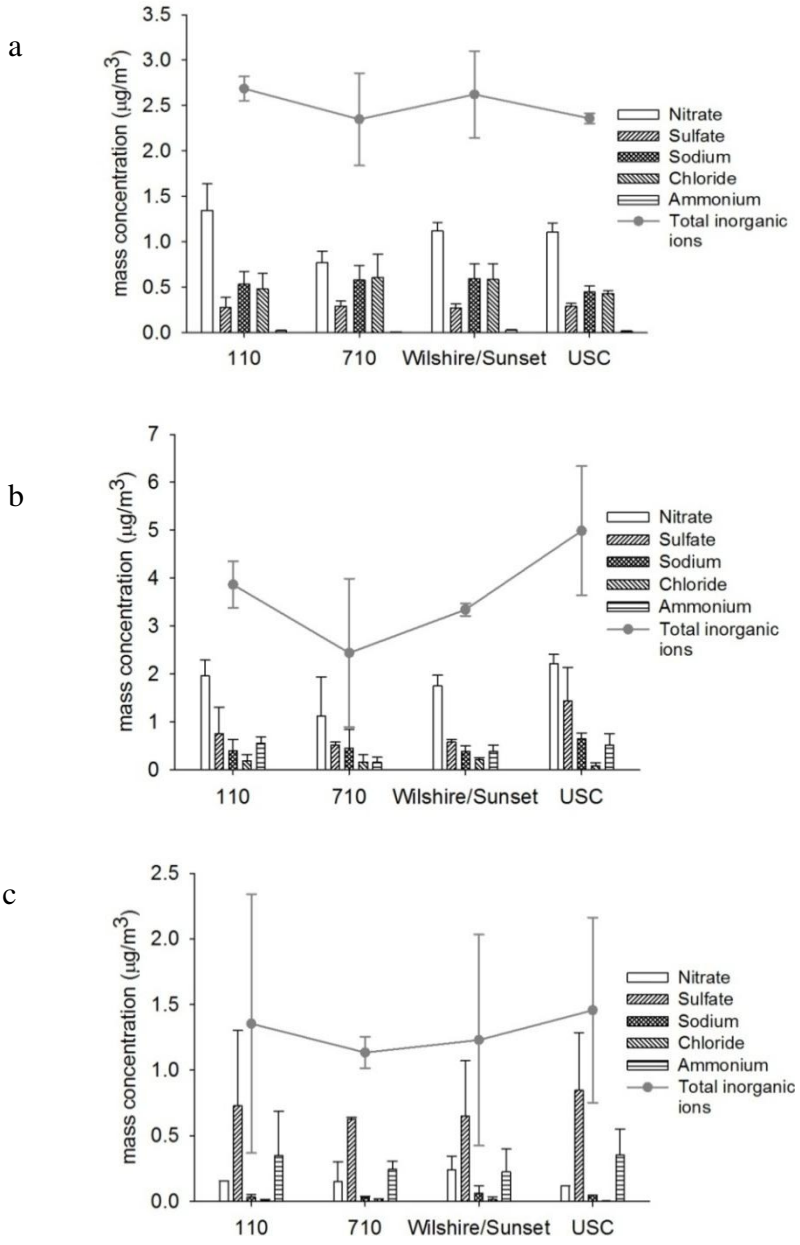

Figure 4.5 Inorganic ions concentrations for a) $PM_{10-2.5}$, b) $PM_{2.5-0.25}$, and c) $PM_{0.25}$. Error bars represent one standard deviation.

fraction also found nitrate to be the major component of inorganic ions (Cheung et al. 2011). Given the southwesterly sea breeze from the Pacific Ocean, sea salt is considered to be a contributor to $PM_{10-2.5}$ and its primary components, sodium and chloride, have concentrations of 0.9-1.2 μg/m^3 and make up 37-49% of total inorganic ions. On average, sea salt levels are

27.7±11.0% higher on roadways relative to USC levels, however, the difference is not statistically significant (p=0.43). Sulfate concentrations are relatively low (0.27-0.29 μg/m^3) and constitute 10-12% of total ions across all sites.

4.3.3b $PM_{2.5-0.25}$

It is clear from the mass balance that inorganic ions dominate the $PM_{2.5-0.25}$ mode (Figure 4.4b) and that its concentrations are highest in this mode ($p<0.05$) (Figure 4.5b). The I-110, I-710, Wilshire/Sunset, and USC sites have total inorganic ions concentrations of 3.9±0.5 μg/m^3, 2.4±1.6 μg/m^3, 3.3±0.1 μg/m^3, and 5.0±1.4 μg/m^3, respectively. However, the differences in inorganic ions concentrations are not statistically significant (p=0.17). With the exception of chloride, the concentrations of inorganic ions are comparable to or lower than USC levels. Although the total concentrations vary, the individual inorganic ion contributions are relatively consistent across all sites, with nitrate dominating and accounting for 44-52%, followed by sulfate (17-29%) and sodium (10-18%).

4.3.3c $PM_{0.25}$

Of the three size fractions, the $PM_{0.25}$ has the lowest total inorganic ion concentrations, with an average of 1.29±0.14 μg/m^3 across the four sites (Figure 4.5c). Overall, there is not a substantial amount of variation in concentration and composition among the three roadway environments. Sulfate is the dominant component and contributes 52-58% of total inorganic compounds across all sites, followed by ammonium (18-29%) and nitrate (8-19%). Previous studies in the Los Angeles basin also found sulfate to be the major inorganic component in $PM_{0.25}$ (Minguillon et al. 2008; Arhami et al. 2009). Similar to $PM_{10-2.5}$ and $PM_{2.5-0.25}$, the

inorganic ions concentrations in $PM_{0.25}$ at the roadway environments are generally comparable or less than USC background levels.

4.3.4 EC and OC

Figure 4.6 shows the average total carbon (TC), EC, OC, and water-soluble OC (WSOC) concentrations for the four sites. TC is the sum of EC and OC (Figure 4.6a). $PM_{0.25}$, $PM_{2.5-0.25}$, and $PM_{10-2.5}$ constitute 67-71%, 16-19%, and 11-15% of total TC, respectively. The I-710 exhibits the greatest TC concentration of 9.3±2.2 μg/m^3 and USC has the lowest of 4.1±0.2 μg/m^3. In terms of enrichment ratios relative to USC, the I-710, I-110, and Wilshire/Sunset are 2.2±0.4, 1.7±0.2, and 1.7±0.1, respectively. Of TC, OC accounts for 78-91% and EC accounts for 9-22%.

EC concentrations are significantly higher in $PM_{0.25}$ relative to the other two size fractions ($p<0.05$), and 80-95% of total EC is accounted for in this mode for all four sites (Figure 4.6b). The most substantial difference among the three roadway environments is the EC levels observed on the I-710, of which EC concentrations are 2.1±0.2 μg/m^3 and 4.1 times greater than USC, while levels on the I-110 and Wilshire/Sunset are 1.1±0.2 μg/m^3 and 0.6±0.02 μg/m^3 and 2.1 and 1.3 times greater, respectively. Given that EC is a primary pollutant and can be used as a tracer for diesel emissions at least in the Los Angeles Basin, the differences in EC concentrations may be explained by the truck density in each roadway. The I-710 and I-110 had truck flows of 470/hr and 243/hr, respectively, for the periods of sampling (CalTrans). Although the I-110 has a greater total vehicle flow than the I-710, the near two-fold difference in truck flows highlights the significant contribution of HDVs to EC. The Wilshire/Sunset traffic flow consists mainly of passenger cars and few compressed natural gas (CNG) buses, which emit lower levels of PM and

gaseous pollutants than conventional diesel buses (Hesterberg et al. 2008). The negligible HDV flow is evident in the comparable levels of EC on Wilshire/Sunset to the USC background site.

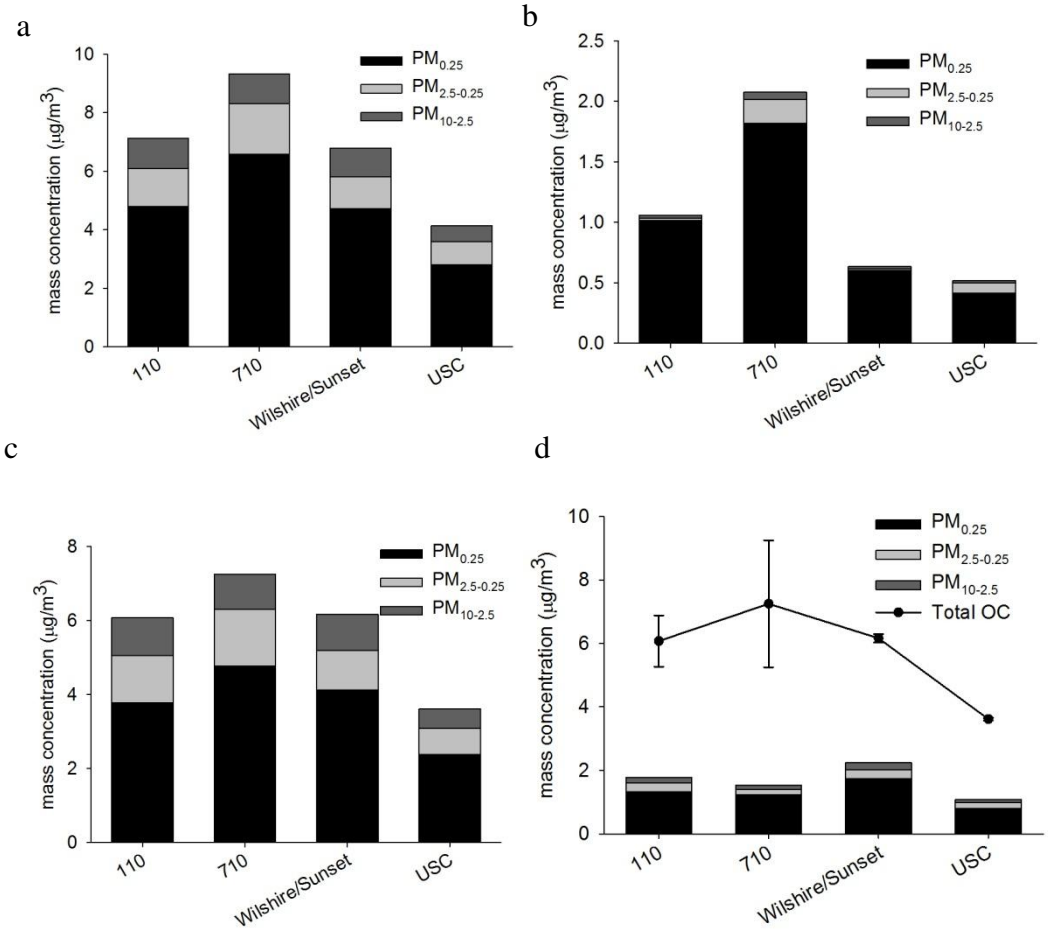

Figure 4.6 Size-segregated concentrations of a) total carbon (TC), b) elemental carbon (EC), c) organic carbon (OC), and d) water-soluble OC (WSOC).

Similar to EC, OC is significantly higher in $PM_{0.25}$ ($p<0.05$), of which 62-67% of total OC is accounted for in all 4 sites, while in $PM_{2.5-0.25}$ and $PM_{10-2.5}$, OC accounts for 17-21% and 13-17%, respectively (Figure 4.6c). Previous studies of ultrafine PM, $PM_{0.18}$, in Los Angeles also found OC to be the dominant PM component (Hughes et al. 1998; Arhami et al. 2009). Total OC concentrations for the I-110, I-710, Wilshire/Sunset, and USC are 6.1±0.8 μg/m^3, 7.3±2.0 μg/m^3, 6.2±0.1 μg/m^3, and 3.6±0.04 μg/m^3, respectively; enrichment ratios for the roadways relative to

USC are 1.7±0.2, 2.0±0.5, and 1.7±0.1, respectively. Organic mass originates from a mix of both primary (vehicular emissions) and secondary sources (photochemical reactions) (Kim et al. 2002). The more than two-fold difference in OC concentrations observed on the three roadway environments shows the significant contribution of vehicular traffic to OC.

Figure 4.6d shows WSOC concentrations, which are also significantly higher in $PM_{0.25}$ ($p<0.05$). Total WSOC concentrations for the I-110, I-710, Wilshire/Sunset, and USC are 1.8±0.02 $\mu g/m^3$, 1.5±0.1 $\mu g/m^3$, 2.2±0.2 $\mu g/m^3$, and 1.1±0.03 $\mu g/m^3$, and accounts for 29.4±3.8%, 21.9±5.6%, 36.3±3.1%, and 29.8±0.8% of total OC. The relatively low WSOC fractions observed are consistent with a previous study that showed OC in urban settings is less oxidized than OC in rural settings, and thus less water-soluble (Salma et al. 2007).

4.3.5 Comparison to previous studies in Los Angeles

Figure 4.7 shows a comparison of $PM_{2.5}$ mass, OC, and EC concentrations from the current study to previous studies conducted at fixed sites near the I-710 and I-110 (Kuhn et al. 2005a; Kuhn et al. 2005b; Phuleria et al. 2007). In Phuleria et al. (2007), the I-710 study was conducted directly adjacent to the roadway, at approximately 10 m from the centerline of the freeway and sampling took place in February and March 2006 from 11 a.m. to 7 p.m. Kuhn et al (2005a) was conducted in winter 2005 (January) and Kuhn et al. (2005b) was conducted in summer 2004 (May). However, the sampling site for these two studies was in the northern "gasoline-only" portion of the I-110 where HDVs were not allowed, while results from the current study are based on a 3.9% HDV fraction. OC concentrations in the ultrafine fraction were omitted due to positive adsorption artifacts from the Kuhn et al. (2005a and 2005b) studies. Differences in PM mass and OC concentrations are not substantial for either roadway

comparisons. However, average EC concentrations seem to have decreased by approximately 50% for both roadways in the last 5 years.

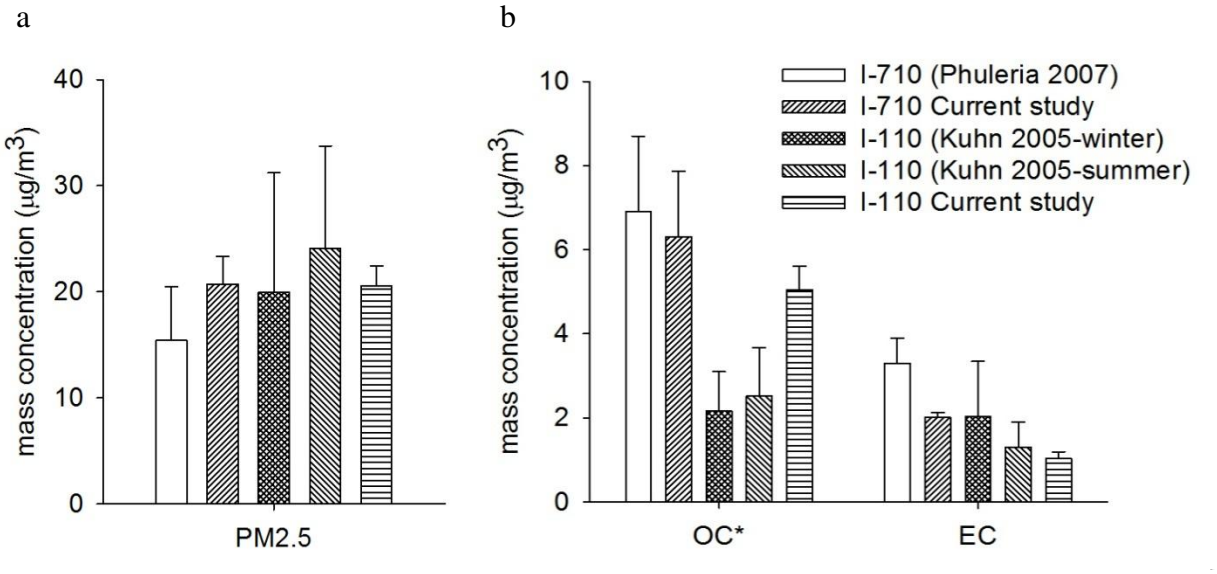

*OC in ultrafine fraction for Kuhn 2005 studies are omitted due to positive adsorption artifacts

Figure 4.7 Comparison of $PM_{2.5}$ concentrations of a) mass and b) OC and EC to previous studies conducted at fixed sites in the vicinity of the I-110 and I-710.

This improvement may be partially explained by differences in sampling conditions (i.e. time of year), but is most likely the result of the Port of Los Angeles Clean Truck Program, which calls for a progressive ban on older polluting drayage trucks (San Pedro Bay Ports Clean Air Action Plan (CAAP)). In October 2008, all pre-1989 drayage trucks were banned from entering the Port and in January 2010, all 1989-1993 drayage trucks were banned in addition to 1994-2003 drayage trucks that were not retrofitted. Finally, in January 2012, drayage trucks that do not meet the 2007 Federal Clean Truck Emission Standards will be banned. The impact of the program has been regional, and its effectiveness is illustrated in the decrease in EC levels of the current I-110 study (with 3.9% HDVs) in comparison to the previous I-110 study (no HDVs). This is consistent with a study that observed a reduction in BC emission factors after the

implementation of diesel particle filter (DPF) retrofit and truck replacement program in 2010 at the Port of Oakland (Dallmann et al. 2011).

4.4 Conclusion

An in-vehicle sampling campaign was conducted to assess the on-road chemical composition of PM in three roadway environments (I-110, I-710, and Wilshire/Sunset) for three size fractions ($PM_{10-2.5}$, $PM_{2.5-0.25}$, and $PM_{0.25}$). Based on average PM concentrations, $PM_{0.25}$ is heavily influenced by vehicular emissions, which is evident in its substantial contribution to TC, including both EC and OC components, while $PM_{2.5-0.25}$ and $PM_{10-2.5}$ are less impacted by on-road sources. Inorganic ions compositions (%) were found to be relatively consistent across the three roadways. Although concentrations in $PM_{2.5-0.25}$ and $PM_{0.25}$ at USC were higher than corresponding levels at roadways, the differences were not significant ($p=0.17$). The most notable finding from this study is the elevated levels of EC on the I-710, which were 4.0 times greater than the USC ambient site, while the I-110 and Wilshire/Sunset roadways were approximately 2.1 and 1.2 times greater, respectively. In comparison to previous studies, EC levels appear to have decreased substantially on both the I-110 and I-710, which may be explained by the effectiveness of the Port of Los Angeles Clean Truck Program that began in 2008.

Chapter 5 On-road emission factors of PM pollutants for light-duty vehicles (LDVs) based on real-world urban street driving conditions

5.1 Introduction

In this study, an on-road sampling campaign was conducted on two major surface streets in Los Angeles to assess the effect on PM emissions of urban street driving conditions, which are essentially intermittent stop-and-go driving. The major advantage of the on-road sampling methodology deployed in the current study is that it captures PM mass using a driving scheme that is much closer to urban driving conditions than the aforementioned studies. The dynamometer studies are based on standardized test cycles of individual vehicles and roadside samples can only cover localized driving conditions. The frequent acceleration and deceleration of a fleet of vehicles is expected to emit higher levels of PM than cruise conditions (Yanowitz et al. 1999). For the surface streets selected, the vehicle fleet is almost entirely composed of LDVs (passenger cars). Fuel-based emission factors of PM components species are determined and then compared to previous LDV studies. Lastly, *n*-alkane concentrations are discussed and carbon preference indices (CPIs) are calculated to assess the anthropogenic source contribution to *n*-alkanes. Results from this study are of great significance as they represent driving conditions on heavily trafficked surface streets typical of many urban locations throughout the United States.

5.2 Experimental methodology

5.2.1 Sampling route

The on-road sampling campaign was conducted on two major surface streets in Los Angeles, CA – Wilshire and Sunset Boulevards. The route was selected because it represents two important streets that are heavily trafficked on a daily basis and traverses major parts of Los Angeles including Hollywood, Miracle Mile, Beverly Hills and Downtown Los Angeles. The sampling route is approximately 47 km (29 mi), with each loop requiring 2-5 hours of sampling depending on traffic congestion. Concurrent sampling was conducted at a site located at the University of Southern California (USC), representing an urban background site which has been well documented in previous studies (Moore et al. 2007; Ning et al. 2007). Figure 5.1 shows the sampling route and the USC background site. Due to the time- and resource-intensive nature of this campaign, only two samples were collected, of which each sample represents over 50 hours of on-road PM sampling. Sampling was conducted on weekdays from 6am to 5pm; sample 1 was collected March 9-16, 2011 and sample 2 was collected on April 26-May 2, 2011. While the authors acknowledge that the sample size is small which may not provide an accurate estimate of the variability and uncertainty of on-road PM species presented in this study, the sampling period is very long and each sample corresponds to a fairly wide range of meteorological and traffic conditions of Los Angeles.

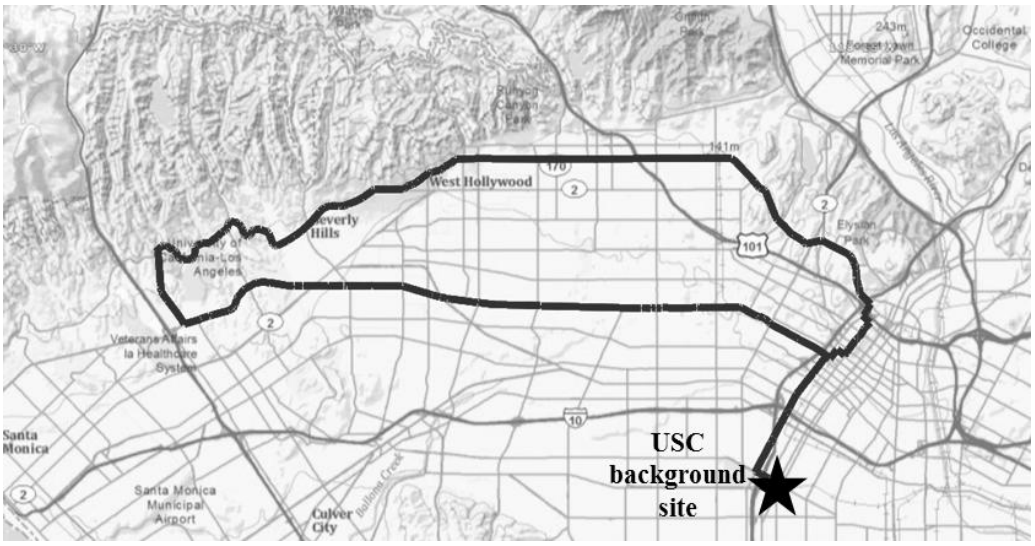

Figure 5.1 Map of sampling route (Wilshire/Sunset Boulevards) and USC background site.

5.2.2 Sampling methodology and analysis

A summary of the sampling methodology is described in this text. For a complete description, please refer to section 4.3. The mobile laboratory used in this study was a Honda Insight Hybrid 2011 vehicle, modified with a window insert for the aerosol inlet. PM mass was collected onto filter substrates for three size fractions: $PM_{10-2.5}$ ($10 > d_p > 2.5$ μm), $PM_{2.5-0.25}$ ($2.5 > d_p > 0.25$ μm), and $PM_{0.25}$ ($d_p < 0.25$ μm). Roadway PM was collected onto six Personal Cascade Impactor Samplers (PCIS) (SKC Inc., Eighty-Four, PA) (Misra et al. 2002) loaded with two impaction stages and an after filter through a PM_{10} ($d_p < 10$ μm) inlet into the vehicle. Each PCIS was operated with a battery-powered Leland Legacy pump (SKC Inc., Eighty-Four, PA) at a flow rate of 9 liters per minute. The resulting aerosol velocity at that flow rate through the inlet is 13.4 m/s (30 mph). Hence, isokinetic sampling was achieved when the vehicle was moving at 13.4 m/s. Anisokinetic sampling may result in the overestimation or underestimation of relatively larger particles (i.e. $PM_{10-2.5}$) due to sub-isokinetic flows at the aerosol inlet. For $d_p = 10$ μm, the estimated PM concentration is calculated to be 1.2 times greater than the actual concentration

when vehicle speed is 17.9 m/s (40 mph) whereas the estimated PM concentration is 0.6 times the actual concentration when vehicle speed is 4.5 m/s (10 mph) (Belyaev and Levin 1974). For particles smaller than 5 μm, the expected over- or under- estimation of concentration in these two cases of vehicle speed is less than 20%, and decreases with decreasing particle size. $PM_{2.5}$ is virtually unaffected by anisokinetic sampling. When the vehicle is stopped, there are no anisokinetic effects as the aerosol stream (roadway air) velocity is 0 m/s.

For the purpose of chemical analysis, two types of impaction substrates were used – PTFE (Pall Life Sciences, Ann Arbor, MI) and quartz (Whatman International Ltd, Maidstone, England) filters. The filters were stored overnight in a refrigerator until they were to be used the next sampling day. To determine total metal and trace elemental composition, the PTFE filters were extracted with acid to be analyzed by magnetic-sector inductively coupled plasma mass spectrometry (SF-ICPMS) (Zhang et al. 2008). Elemental and organic carbon (EC and OC, respectively) was determined from the quartz substrates using thermal evolution/optical transmittance analysis (Birch and Cary 1996). Water extracts of OC yielded WSOC. Organic speciation was conducted with gas chromatography mass spectroscopy (GC/MS) (Schauer et al. 1999).

5.2.3 Emission factors calculation

The emission factors presented in this study are based on fuel consumption. They are defined as the mass of pollutant emitted per mass of fuel burned and are calculated based on the following equation (Geller et al. 2005; Phuleria et al. 2006; Ning et al. 2008):

$$E_p = \left(\frac{[P]_{st} - [P]_{bg}}{[CO_2]_{st} - [CO_2]_{bg}} \right) w_c \times 10^6 \qquad (1)$$

where E_P is the emission factor of pollutant P expressed in mg/kg of fuel; $[P]_{st}$ and $[P]_{bg}$ are pollutant concentrations in $\mu g/m^3$ on streets and at the background site, respectively; $[CO_2]$ is the concentration of CO_2 in μg of C/m^3; w_c is the carbon weight fraction of the considered fuel, which is 0.85 for gasoline. This equation assumes that the carbon mass from vehicular exhaust is mostly in the form of CO_2, and that the mass of other carbon-containing compounds (i.e. CO, black carbon, hydrocarbons) are negligible relative to the total emitted carbon mass (Yli-Tuomi et al. 2005). A similar approach has been used in numerous studies to determine emission factors of various traffic environments including tunnels and freeways (Phuleria et al. 2006). It should be noted that the emission factors for species not associated with roadway emissions may not be accurately calculated from Eq. (1), the results of which should be interpreted with caution. In addition, PM species with very similar levels to corresponding background levels are not an important part of the roadway emissions profile.

5.3 Results and discussion

5.3.1 Emission factors for major PM components and species

Table 5.1 shows the emission factors of major PM components (mass, OC, EC, and WSOC) and metals and trace elements for three size fractions ($PM_{10-2.5}$, $PM_{2.5-0.25}$, and $PM_{0.25}$). The results are presented as the average of the 2 samples and its uncertainty. Emission factors for species with concentrations similar to or lower than corresponding background levels are not shown in the table. Overall, the $PM_{0.25}$ fraction has the greatest emission factors in all of the major PM components. The most substantial difference between the three size fractions is the OC emission factors, of which the $PM_{0.25}$ emission factors are 3.9 and 4.8 times greater than $PM_{10-2.5}$ and $PM_{2.5-0.25}$ emission factors, respectively. WSOC accounts for 55% of OC for $PM_{0.25}$,

while WSOC only accounts for 28% and 25% of OC, respectively. The relatively low emission factors for EC, which can be used as a surrogate for diesel emissions at least in urban settings (Schauer 2003) are expected, given that the traffic composition on the Wilshire/Sunset route consists primarily of LDVs. Chapter 4 reported the EC concentrations on the current route are approximately 3 times lower than the I-710, a freeway with 12% HDVs, and approximately 2 times lower than the I-110, a freeway with 4% HDVs.

	$PM_{10-2.5}$		$PM_{2.5-0.25}$		$PM_{0.25}$	
	Wilshire/Sunset	±	Wilshire/Sunset	±	Wilshire/Sunset	±
PM components (mg/kg of fuel)						
mass	75.8	18.8	62.7	35.8	99.4	98.9
OC	12.6	2.43	10.3	2.59	49.1	5.58
WSOC	3.51	0.82	2.59	0.57	26.8	5.20
EC	-	-	-	-	5.29	4.09
metals and trace elements (μg/kg of fuel)						
Mg	582	824	909	180	108	68.6
Al	2360	3330	1150	234	-	-
S	436	227	-	-	-	-
K	24.9	35.2	-	-	383	296
Ca	2270	2530	1140	267	808	280
Ti	401	49.4	128	33.3	202	40.7
Cr	74.6	4.55	23.2	3.12	-	-
Mn	111	9.73	34.6	7.41	38.9	7.25
Fe	16300	554	5700	641	5450	680
Ni	11.4	5.26	-	-	-	-
Cu	1170	42.6	452	32.7	376	32.7
Zn	173	3.14	108	35.8	67.3	43.4
Sr	40.1	11.8	21.8	4.99	21.9	4.7
Mo	53.9	0.38	21.8	3.08	21.4	3.33
Sb	158	4.56	63.1	5.43	70.0	6.26
Ba	1240	165	482	54.7	406	47.5
Eu	1.65	0.324	0.615	0.073	0.551	0.063
W	0.46	0.65	0.083	0.118	0.827	0.09
Pb	10.4	14.3	7.53	6.95	11.3	7.3

Table 5.1 Fuel-based emission factors (mass of pollutant emitted per kg of fuel) of PM components and metals and trace elements for three PM size fractions. Pollutants with concentrations close to or less than USC background levels have been omitted.

For metals and trace elements, the emission factors are highest in the $PM_{10-2.5}$ fraction, followed by $PM_{2.5-0.25}$ and lowest for the $PM_{0.25}$ fraction, consistent with previous studies in the Los Angeles basin that have found metals and trace elements to contribute most to larger size fractions of PM_{10} (Sardar et al. 2005; Krudysz et al. 2008). In general, emission factors for metals and trace elements in $PM_{10-2.5}$ are 2-5 times higher than corresponding emission factors in $PM_{2.5-0.25}$ and $PM_{0.25}$. The most notable observations are the emission factors of Fe, which are substantially higher than all other metals and trace elements in the three size fractions. Al, Ca, Cu, and Ba also have relatively high emission factors (>1000 μg/kg of fuel), followed by Mg, S, Ti, Mn, Zn, and Sb (>100 μg/kg of fuel).

In addition to road dust resuspension, numerous studies have associated metals with brake lining (Cu, Ba, Sb), automotive lubricant oil (Ca), and vehicular wear debris (Fe, Zn, Pb, S) (Sternbeck et al. 2002; Harrison et al. 2003; Lough et al. 2005). Catalytic converters can also be a source of precious metals (Pd, Pt, Rh) in the roadway environment (Prichard and Fisher 2012). In addition, a number of metals and trace elements may have both natural (crustal materials and soil) and anthropogenic sources. A previous study on $PM_{10-2.5}$ in the Los Angeles area reported that mineral and crustal metals and elements, most notably Fe, Ca, Al, Mg, K, Ti, and Mn contributed to 33% of total variance in mass, while abrasive vehicular markers such as Cu, Ba, and Sb, account for 16% of variance (Pakbin et al. 2011). Although crustal sources contribute to metals and trace elements, the on-road emission factors presented indicate that metal and trace elemental concentrations are substantially higher than our urban background levels and that vehicular abrasion is a major source of metals and trace elements in heavily-trafficked surface streets. Previous studies which have investigated the size distribution profile of metals in roadways environments have also identified vehicular combustion and lubricant oil to be a

source of metals and trace elements (i.e. Cu, Pb, Ca) in the sub-micrometer size range (Lin et al. 2005; Lough et al. 2005; Schauer et al. 2006). Lough et al. (2005) observed a local peak for Cu and Pb in the 0.1μm size range in a tunnel study and Lin et al. (2005) reported a bimodal distribution for K, Ca, Zn, and Pb in a roadway study. However, the only species that show an apparent peak in $PM_{0.25}$ is Pb and Sb. Given the 3 PM size fractions studied, it cannot be determined if there are local peaks in the sub-micrometer size range of the other species.

In roadway environments, while the greatest fraction of metals and trace elements are derived from vehicular wear products, organic compounds including PAHs, hopanes, steranes, and *n*-alkanes are mostly derived from lubricant oil and the incomplete combustion of fuel (Rogge et al. 1993a; Fine et al. 2004), and thus can be used as tracers for primary traffic emissions. Contrary to what was observed for metals and trace elements, Table 5.2 shows emission factors for PAHs are highest in $PM_{0.25}$ (1.4-6.5 μg/kg of fuel) while emission factors in $PM_{10-2.5}$ and $PM_{2.5-0.25}$ are comparably low (0.1-0.8 μg/kg of fuel). On average, emission factors in $PM_{0.25}$ are 18.9 and 19.7 times higher than corresponding PAHs in $PM_{10-2.5}$ and $PM_{2.5-0.25}$, respectively. This is consistent with observations in a study for a tunnel bore reserved for LDVs only that found gasoline engine-derived PAHs were found almost entirely in $PM_{0.12}$ (Miguel et al. 1998). Except for benzo(*ghi*)fluoranthene, a low molecular weight (MW) PAH, the emission factors for high MW PAHs (benzo(*ghi*)perylene and coronene) are greater than most of the lighter MW PAHs. Previous studies have also found that HDVs, which were a negligible part of the fleet composition of Wilshire/Sunset, are the major source of low MW PAHs, whereas both LDVs and HDVs contribute to higher MW PAHs (Schauer et al. 2002; Ning et al. 2008). The emission factors of benzo(*a*)pyrene have been omitted as the concentrations were below detection limit.

	$PM_{10-2.5}$		$PM_{2.5-0.25}$		$PM_{0.25}$	
	Wilshire/Sunset	±	Wilshire/Sunset	±	Wilshire/Sunset	±
PAHs (μg/kg of fuel)						
Pyrene	0.27	0.16	0.07	0.06	2.4	1.2
Benzo(*ghi*)fluoranthene	-	-	0.34	0.13	6.5	6.6
Benz(*a*)anthracene	0.13	0.19	0.10	0.15	1.4	0.46
Chrysene	0.24	0.04	0.32	0.08	2.2	0.32
Benzo(*b*+*k*)fluoranthene	0.08	0.11	0.79	0.62	4.2	1.0
Benzo(*e*)pyrene	0.19	0.07	0.08	0.12	2.9	0.37
Benzo(*a*)pyrene	-	-	-	-	-	-
Indeno(1,2,3-cd)pyrene	0.32	0.45	0.32	0.33	1.5	2.1
Benzo(*ghi*)perylene	0.25	0.13	0.30	0.27	4.3	0.93
Coronene	0.13	0.11	0.11	0.05	4.3	0.58
Hopanes and steranes (μg/kg of fuel)						
17α(H)-22,29,30-Trisnorhopane	0.38	0.32	0.11	0.16	-	-
17α(H)-21β(H)-30-Norhopane	0.81	1.0	0.14	0.19	2.5	2.0
17α(H)-21β(H)-Hopane	1.8	1.4	-	-	5.3	2.4
22S-Homohopane	1.3	0.83	0.16	0.22	2.3	3.2
22R-Homohopane	0.65	0.92	-	-	1.7	2.4
22S-Bishomohopane	0.86	1.2	0.56	0.80	-	-
22R-Bishomohopane	0.90	1.3	0.26	0.36	-	-
αββ-20R-C27-Cholestane	0.38	0.54	0.26	0.37	-	-
αββ-20S-C27-Cholestane	0.33	0.46	0.22	0.32	-	-
ααα-20S-C27-Cholestane	0.54	0.74	0.31	0.44	-	-

Table 5.2 Fuel-based emission factors (mass of pollutant emitted per kg of fuel) of polycyclic aromatic hydrocarbons (PAHs) and hopanes and steranes for three PM size fractions. Pollutants with concentrations close to or less than USC background levels have been omitted.

Lastly, emission factors of hopanes and steranes are shown in Table 5.2. These organic compounds have been used as reliable tracers of vehicular emissions as they are primarily derived from automotive lubricant oil (Schauer et al. 1996; Cass 1998). Similar to PAHs, the emission factors in $PM_{10-2.5}$ and $PM_{2.5-0.25}$ are generally low and are on average 0.8±0.5 and 0.3±0.1 μg/kg of fuel, respectively, while the average for $PM_{0.25}$ is 2.9±1.6 μg/kg of fuel. In comparison to the previously discussed PM components, hopanes and steranes have relatively low overall emission factors. A tunnel study which apportioned emission factors between LDVs and HDVs found that hopane and sterane emission factors for HDVs were approximately 8-14 times greater than LDVs for ultrafine PM (d_p < 0.18 μm) and 10-20 times greater for

accumulation PM ($2.5 > d_p > 0.18$ μm) (Phuleria et al. 2006). The following section will compare emission factors from the current study to previous LDV studies conducted in freeway, tunnel, and laboratory dynamometer environments.

5.3.2 Comparison of $PM_{2.5}$ emission factors to previous LDV studies

Table 5.3 shows the sampling/testing dates, location, and relevant results for previous $PM_{2.5}$ LDV emission factor studies to be compared to the current study. Ning et al. (2008) presents a study that was conducted at a fixed site downwind of the I-110 in Los Angeles at the northern portion of the freeway that allows LDVs only. Studies by Phuleria et al. (2006) and Geller et al. (2005) were conducted at the Caldecott Tunnel in Berkeley, CA in Bore 2, which is reserved for LDVs only. The dynamometer studies are based on a composite of LDV gasoline vehicles of various makes, models, and odometer values (Schauer et al. 2002; Fujita et al. 2007). Schauer et al. (2002) focused on 9 catalyst-equipped LDVs (model years 1981-1994) driven through the cold-start Federal Test Procedure (FTP) urban driving cycle; the Fujita et al. (2007) study is based on 14 LDVs (model years 1984-1997) driven through a modified unified driving cycle (UDC) from warm-start. Figure 5.2 shows a comparison of the driving cycles between the two dynamometer studies and the velocity profile of the current study. The FTP and UDC cycles have an average velocity of 9.5±7.1 m/s (21.2±15.9 mph) and 11.0±8.8 m/s (24.6±19.7 mph) (www.epa.gov) while the current study has an average of 7.1±4.7 m/s (16.0±10.5 mph). The

Sampling location/test cycle	Sample/test period	Relevant results for comparison	Reference
Wilshire/Sunset Blvds	March-May 2011	-	current study
LDV freeway (northern portion of I-110)	May-Jun 2004, Jan 2005	mass, EC, OC, metals, PAHs, hopanes and steranes	Ning et al. (2008)
LDV tunnel (Bore 2 of Caldecott Tunnel)	Aug-Sept 2004	PM mass, EC, OC, metals	Geller et al. (2005)
LDV tunnel (Bore 2 of Caldecott Tunnel)	Aug-Sept 2004	PAHs, hopanes and steranes	Phuleria et al. (2006)
LDV dynamometer study (warm-start UDC)	Summer 2001	mass, EC, OC, metals, PAHs, hopanes and steranes	Fujita et al. (2007)
LDV dynamometer study (cold-start FTP)	-	PM mass, PAHs, hopanes	Schauer et al. (2002)

Table 5.3 Description of previous light-duty vehicle (LDV) studies used for comparison.

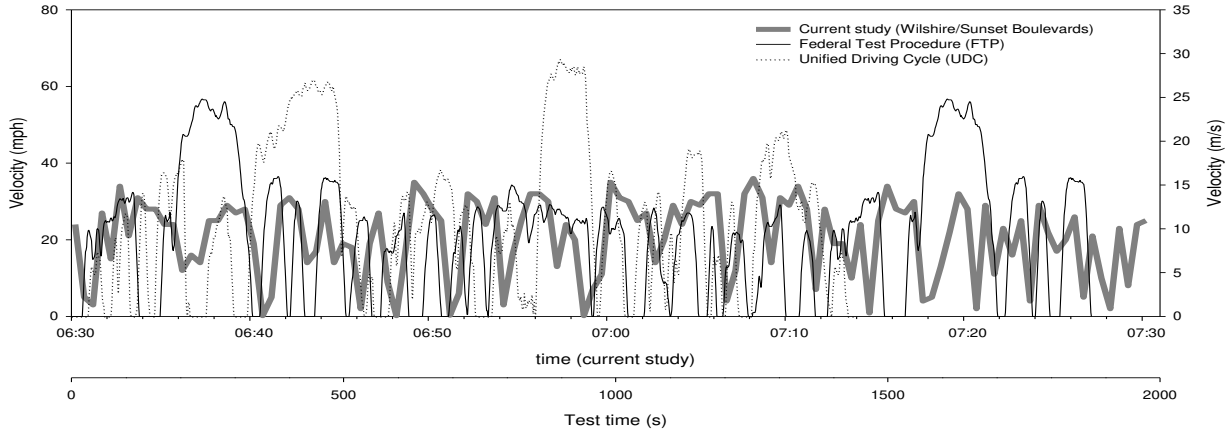

Figure 5.2 Comparison of the velocity profile of the current study (Wilshire/Sunset) and the two test cycles (FTP and UDC) of the dynamometer studies. The current study shows a typical sampling hour with a 30s resolution based on GPS data. The FTP and UDC driving schedules use a 1s resolution and can be found at www.epa.gov.

emission factors from the two dynamometer studies are distanced-based (mass of pollutant emitted per distance traveled), thus for the purpose of comparison, these factors are converted to fuel-based values. LDV gasoline properties used for conversion are fuel consumption (12L/100km) and density (740g/L) (Kirchstetter et al. 1999). All data shown are $PM_{2.5}$ emission factors, and the current data are calculated as the sum of $PM_{0.25}$ and $PM_{2.5-0.25}$.

Figure 5.3 shows the average emission factors of PM mass, OC and EC for the current study (shown as bars) and previous LDV studies (shown as markers). All positive errors bars for the current study represent the upper range of the data (N=2), negative error bars are not shown for visual clarity. On average, the PM mass emission factor for the current study is higher than earlier studies, but there is considerable variation in the values reported. The higher emissions of PM mass observed on the surface streets may be explained by the current on-road sampling methodology employed, which may capture road dust and vehicular abrasion emissions more

effectively than fixed roadside sampling and dynamometer testing, coupled with the frequent braking encountered on street driving conditions.

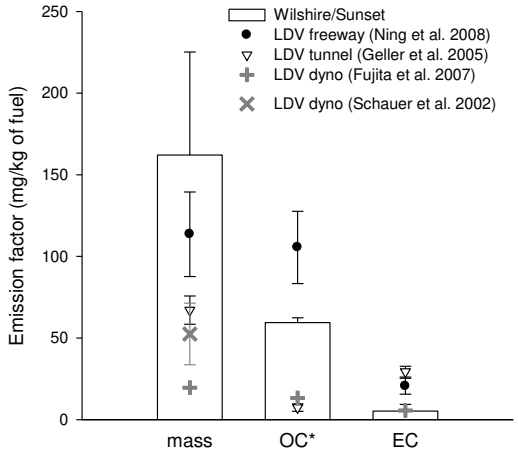

*Due to positive OC adsorption artifacts, Ning et al. (2008) reports a possible overestimation of OC and Geller et al. (2005) omits the ultrafine fraction of OC.

Figure 5.3 $PM_{2.5}$ emission factors for PM components for the current study (bars) and previous LDV studies (markers) for PM mass, OC and EC.

For OC, the emission factor for the current study lies in between the other studies. Due to positive organic vapor adsorption artifacts from the use of quartz substrates, Ning et al. (2008) reported an overestimation of the OC emission factors as they discuss in their analysis, whereas Geller et al. (2005) omitted the OC emission factors in the ultrafine fraction due to similar concerns about the effect of positive artifacts due to gas phase adsorption, which would be far more pronounced in the confined environments of a roadway tunnel. As in any study using quartz filters to capture PM for EC/OC analysis, we acknowledge the possibility of OC adsorption artifacts affecting our collections. These OC artifacts are only relevant for the after filter stage ($PM_{0.25}$), as the other size ranges ($PM_{2.5-0.25}$ and $PM_{10-2.5}$) are collected by impaction and thus are not susceptible to adsorption artifacts (Turpin et al. 2000). Two earlier studies in Los Angeles (Kim et al. 2001; Sardar et al. 2005) examined the effect of PM loading on positive

artifacts due to adsorption of vapor phase OC on quartz filters. Sardar et al. (2005), investigated the OC adsorption artifacts in ultrafine PM using micro-orifice uniform-deposit impactor (MOUDI) at 30 lpm, and showed that the adsorption process reaches saturation at a concentration of roughly 1.5 $\mu g/m^3$ for 24 hr sampling, corresponding to approximately 65 μg of OC. Similarly, Kim et al. (2001), who investigated artifacts at a rural site using the $PM_{2.5}$ Federal Reference Method (FRM) at 16.7 lpm, found that positive OC artifacts reach a saturation of approximately 2 $\mu g/m^3$ regardless of PM mass concentration, corresponding to a loading of 48 μg of OC. Thus, as the PM mass loadings increase, the OC adsorption artifacts tend to decrease. The $PM_{2.5}$ OC levels in this study are 5.2±0.3 $\mu g/m^3$ and correspond to over 400 μg of OC, which suggests that positive organic artifacts may be less of a concern in the current results given the high OC loadings. In addition, total $PM_{2.5}$ loadings were on the order of 1.5-2 mg. It is important to note that the other PM constituents (i.e. EC, metals) are not subject these artifacts. Lastly, because the samples were immediately stored in a refrigerator when not in use, we do not believe the filters were subject to additional negative artifacts due to volatilization.

For EC, the emission factors for all studies are relatively low (< 30 mg/kg of fuel). This is expected considering the negligible influence of HDVs, which are the major emitters of EC in an urban traffic environment (Schauer 2003). Geller et al. (2005), who also apportioned emission factors between LDVs and HDVs, found that HDVs emit 709±54 mg/kg of fuel compared to 29.4±3.3 mg/kg of fuel for LDVs.

Figure 5.4 shows a comparison of emission factors of metal and trace elements. The emission factors of Fe are shown on a separate axis due to their difference in magnitude compared to other studies. These metals and trace elements were selected on the basis they are associated with vehicular emissions or crustal materials based on the earlier discussion and have

been presented in the previous LDV studies as an essential part of the roadway emissions profile. The most important observation is that all of the emission factors from the current study are substantially higher than corresponding species of the previous studies. In comparison to the LDV freeway and tunnel studies, the current study's emission factors are approximately 12 times greater for Mg and Al, and 2-5 times greater for Fe and the remaining species. As discussed in the previous section, a number of the metals and trace elements presented may be derived from vehicular (tire and brake wear, lubricant oil, catalytic converters, etc.) and crustal sources. The higher emission factors of Mg and Al observed on the surface street are most likely from road dust resuspension, as these species are primarily from crustal sources (Grieshop et al. 2006). The differences in emission factors between the current study and the previous LDV tunnel and freeway studies can be explained by the on-road sampling methodology employed in the current study, which may capture substantially higher levels of metals and trace elements associated with vehicular abrasion and particulate resuspension. Measurements from Ning et al. (2008) were conducted at 3m downwind of the freeway while measurements from Geller et al. (2005) were conducted in the air ducts just above the tunnel ceiling at 50m from the tunnel exit, both of which are reasonable locations for measuring site-specific traffic emissions, but neither method captures the additional on-road metal and elemental concentrations that are observed on-road while driving with other vehicles. Another factor that may contribute to the elevated emission factors is that surface street driving is characterized by driving conditions involving frequent acceleration and decelerations, while the freeway and tunnel studies are measuring emission factors from vehicles moving primarily under cruise conditions (Ning et al. 2008; Geller et al. 2005). In comparison to the dynamometer study (Fujita et al. 2007), the emission factors of the current study are 80 times higher for Fe and 12-15 times higher for Mg, Ca, and Ba. This was not

surprising considering that, by design, dynamometer testing captures primarily tailpipe emissions and fails to capture any road dust and products of vehicular abrasion.

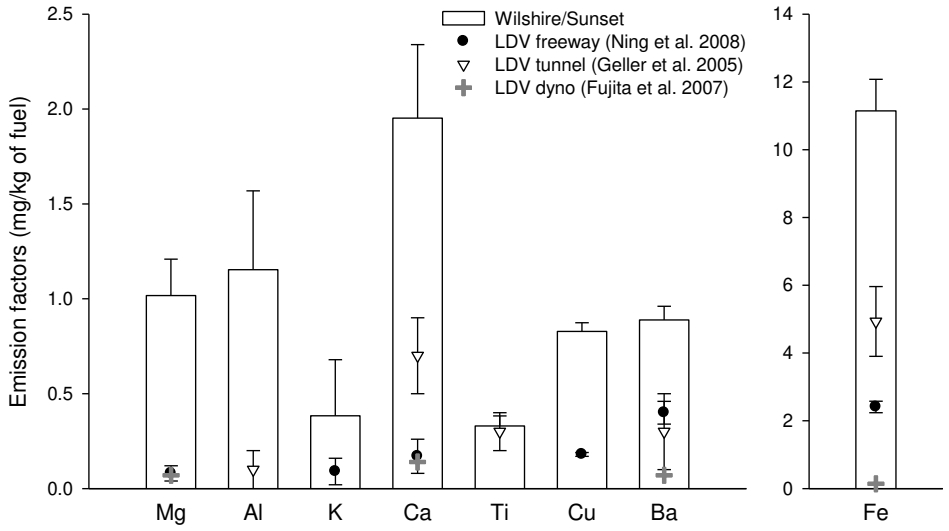

Figure 5.4 $PM_{2.5}$ emission factors for metals and elemental species for the current study (bars) and previous LDV studies (markers). Fe is shown separately due to its difference in magnitude.

Figure 5.5a shows the comparison of emission factors between PAHs. Overall, the emission factors from the current study are lower than EFs from the LDV tunnel (Phuleria et al. 2006) and higher than the fixed site downwind of the LDV freeway (Ning et al. 2008). The average ratio of emission factors of the current study to the LDV tunnel is 0.7±0.4; with the exception of the high MW PAHs (indeno(1,2,3-cd)pyrene, benzo(*ghi*)perylene, and coronene), the ratio to the LDV freeway levels is 3.8±1.6. Due to the semi-volatile nature of PAHs, this group of compounds can partition between gaseous and particulate phase depending on the vapor pressure of a particular PAH (Naumova et al. 2003). Since smaller PAHs (less than 5 aromatic rings) have higher vapor pressures than larger PAHs, they can be found in either phase depending on the environment. The enclosed nature and the lower, constant temperatures of the

tunnel environment may favor the partitioning of semi-volatile PAHs into the particulate phase. In contrast, the higher temperatures coupled with greater dilution conditions at the fixed site downwind of the freeway may shift PAHs into the gaseous phase, resulting in less PAHs in the particulate phase and lower PAH emission factors. Although the current study is also subject to

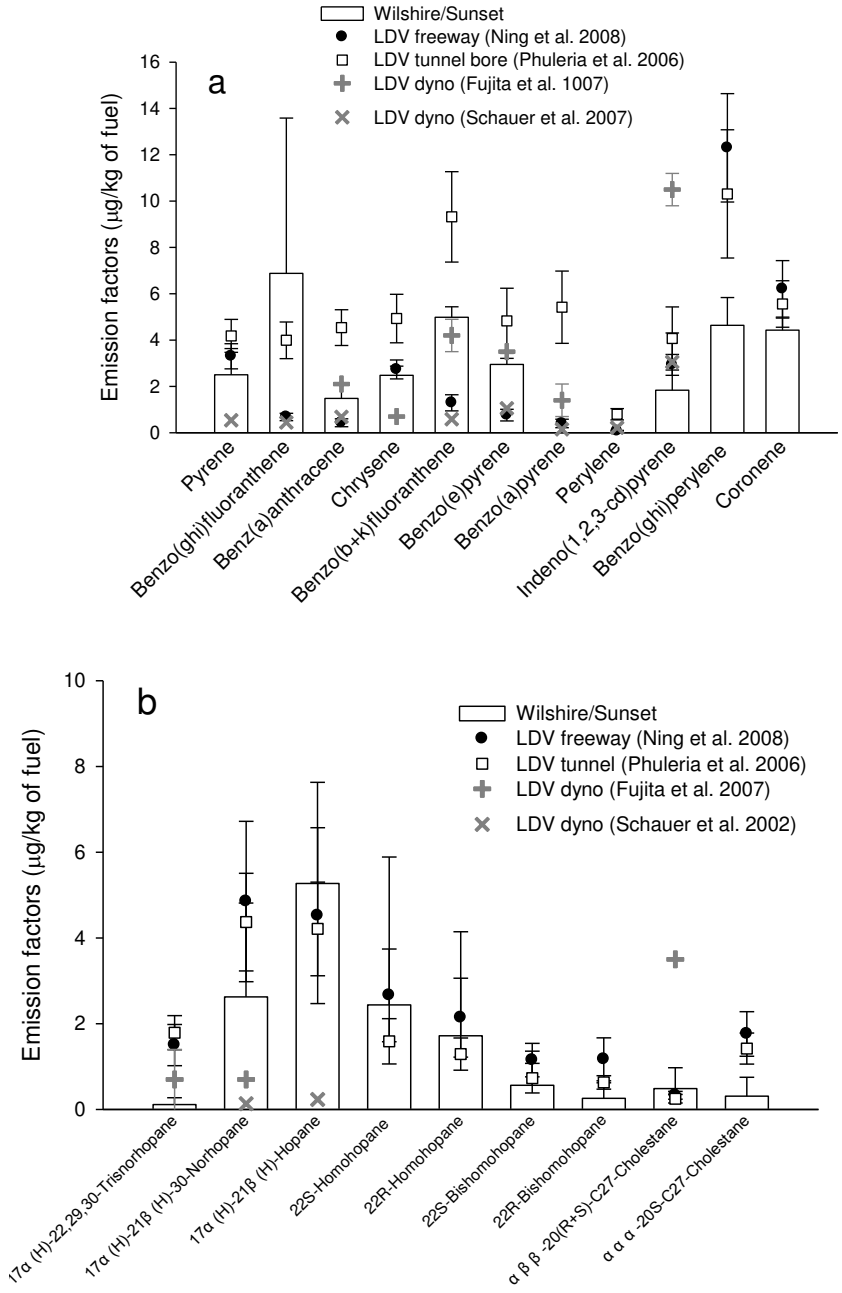

Figure 5.5 Comparison of $PM_{2.5}$ emission factors (µg/kg of fuel) between (a) PAHs and (b) hopanes and steranes.

open atmospheric conditions, the results are based on on-road sampling of major surface streets characterized by intermittent acceleration and deceleration of vehicles, as noted earlier. In comparison to the two dynamometer studies and with the exception of a few PAHs, the emission factors of the current study are generally higher. This may be explained by differences in driving conditions, composition of the LDV fleet as well as the sheer traffic volume on Wilshire/Sunset Boulevards, while results from the dynamometer studies represent only a composite of select vehicles.

Figure 5.5b shows the comparison of emission factors between hopanes and steranes. With the exclusion of 17α(H)-22,29,30-trisnorhopane and ααα-20S-C27-cholestane, the ratios of emission factors of the current study to the LDV tunnel and LDV freeway are 1.1±0.5 and 0.8±0.4, respectively. Contrary to observations for PAHs, emission factors of hopanes and steranes for the current study are substantially closer to corresponding emission factors for the LDV tunnel despite differences in sampling location and conditions. This is consistent with a previous study that found hopanes and steranes to be less sensitive to variations in temperature than PAHs (Zielinska et al. 2004). As mentioned earlier, the major source of hopanes and steranes is from automotive lubricating oil. In addition, this finding highlights the use of hopanes and steranes as reliable biomarkers of vehicular emissions for various traffic environments and driving conditions. Since these compounds are found to be generally stable, it is unlikely they will react fast enough in the atmosphere to compromise their use as a primary tracer on a regional time scale (i.e. a few hours) (Rogge et al. 1993a). However, in comparison to the two dynamometer studies, the current study's emission factors are generally higher, similar to PAHs. As previously mentioned, this observation further shows how results from dynamometer tests

represent idealized driving conditions and may be considerably different from actual traffic environments.

5.3.3 n-Alkanes and calculation of carbon preference index (CPI)

Particulate *n*-alkane homologues (C19-C40) were quantified in this study to further assess anthropogenic influence of organic PM composition for the two major surface streets in Los Angeles. Figure 5.6 shows the mass concentrations (ng/m^3) of *n*-alkanes in $PM_{10-2.5}$, $PM_{2.5-0.25}$, and $PM_{0.25}$ for Wilshire/Sunset Boulevards and USC background site. In $PM_{10-2.5}$, overall *n*-alkane concentrations are comparable between Wilshire/Sunset and USC background site; however, *n*-alkane concentrations in $PM_{2.5-0.25}$ and $PM_{0.25}$ between the surface street and USC are significantly different ($p<0.05$). It is interesting to note that peak concentrations in all size fractions are observed at C29 and C31 *n*-alkanes for both Wilshire/Sunset and USC. Biogenic debris, namely leaf abrasion products, is characterized by high odd-carbon number predominance of C29-C33 *n*-alkanes while fine particulate *n*-alkanes emitted from combustion processes show no carbon number preference but rather high concentrations of *n*-alkanes in C19-C25 (Rogge et al. 1993b). The same study also found that *n*-alkanes derived from tire wear debris have no carbon number preference, but observed greater concentrations for high molecular weight *n*-alkanes (>C30) with peak concentrations at C37. This suggests that, in $PM_{0.25}$, *n*-alkanes observed on Wilshire/Sunset may be influenced by an additional source of biogenic and vehicular combustion products than *n*-alkanes at the USC background site; in $PM_{2.5-0.25}$, *n*-alkanes on Wilshire/Sunset may be influenced by biogenic sources and tire wear debris and less by combustion sources. These results are not surprising considering that the on-road sampling methodology deployed in this study can capture substantially greater amounts of

PM derived from combustion and tire wear as well as biogenic products that have been pulverized and subsequently resuspended in the form of road dust from vehicular turbulence.

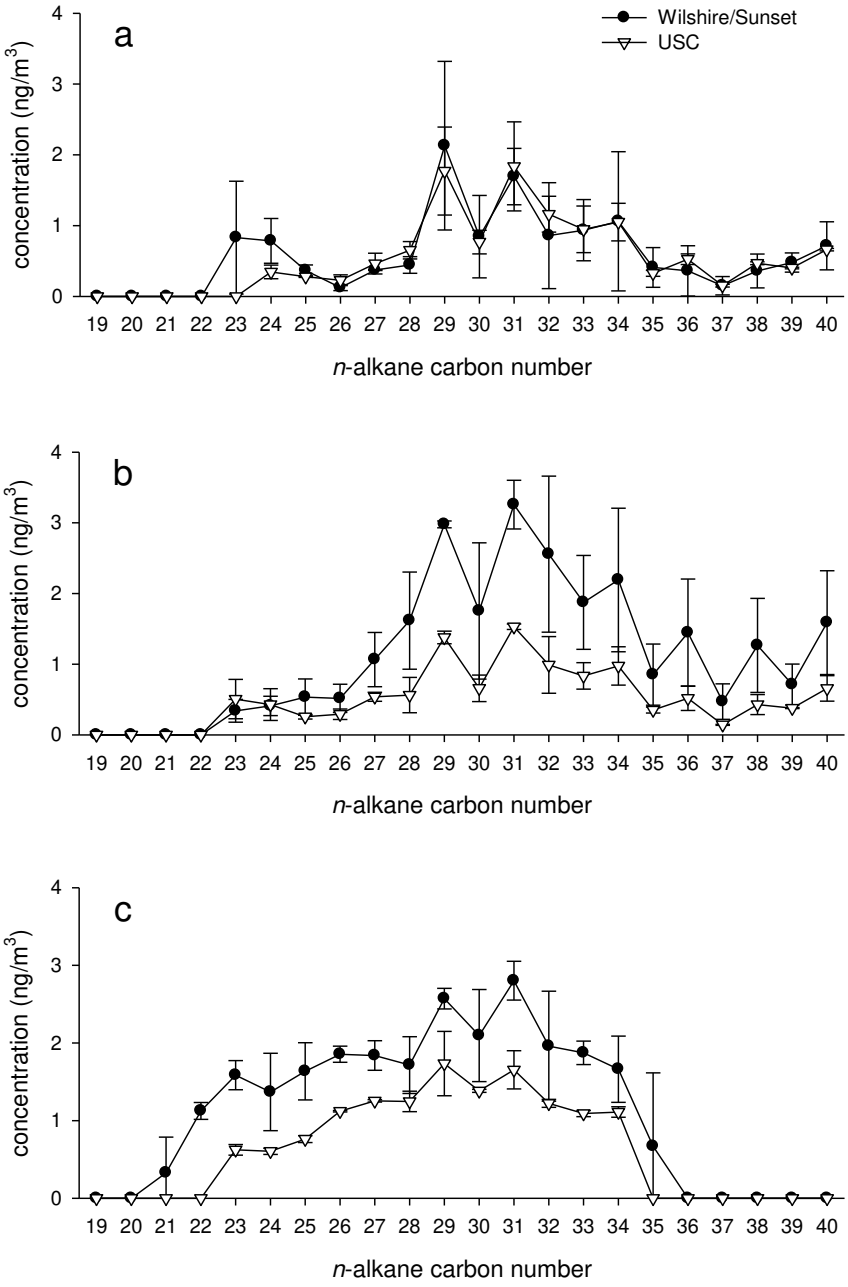

Figure 5.6 *n*-alkane concentrations (C19-C40) for (a) $PM_{10\text{-}2.5}$, (b) $PM_{2.5\text{-}0.25}$, and (c) $PM_{0.25}$.

The carbon preference index, CPI, is an indicator that can be used to determine the contribution of biogenic organic matter and anthropogenic sources to organic aerosol. The alkane CPI is defined as the sum of the concentrations of odd carbon number alkanes divided by the sum of the concentrations of even carbon number alkanes (Simoneit 1989; Brown et al. 2002; Arhami et al. 2009). Biogenic products have an odd carbon preference and have a high CPI (up to 7), while organic matter with a high anthropogenic contribution will not have a carbon number preference and have CPIs ranging from 1 to 2. C_{max} is defined as the carbon number of the alkane which has the highest concentration of the *n*-alkanes. Table 5.4 shows the sum of the concentrations of *n*-alkanes (C19-C40), C_{max} and its corresponding concentration, and CPI values for Wilshire/Sunset and USC in the three PM size fractions. Overall, all CPIs are in the range of 1-2, indicating a substantial anthropogenic influence for both environments and all size ranges. For Wilshire/Sunset, although the concentration sums of *n*-alkanes in $PM_{2.5-0.25}$ and $PM_{0.25}$ are approximately 2 times higher than $PM_{10-2.5}$, the CPIs are comparable.

	$PM_{10-2.5}$		$PM_{2.5-0.25}$		$PM_{0.25}$	
	Wilshire/Sunset	USC	Wilshire/Sunset	USC	Wilshire/Sunset	USC
Σn-alkanes (ng/m^3)	12.9 ± 4.0	12.0 ± 2.7	25.4 ± 9.1	11.4 ± 1.2	25.1 ± 5.0	13.8 ± 0.7
Cmax (ng/m^3)	C29 (2.1 ± 1.2)	C31 (1.8 ± 0.6)	C31 (3.3 ± 0.3)	C31 (1.5 ± 0.04)	C31 (2.8 ± 0.2)	C29 (1.7 ± 0.4)
CPI	1.7 ± 1.1	1.0 ± 0.1	1.0 ± 0.2	1.1 ± 0.3	1.1 ± 0.0	1.1 ± 0.1

Table 5.4 Sum of the concentrations of n-alkanes (C19-C40), Cmax and its corresponding concentrations, and CPI values. Values shown include uncertainty of one standard deviation.

5.4 Conclusion

To investigate on-road emission factors of PM pollutants for two major surface streets in Los Angeles (Wilshire and Sunset Boulevards), a sampling campaign was conducted and size-segregated PM was collected. The current study is the first on-road study to report comprehensive chemical speciation data including metals and trace elements, PAHs, hopanes

and steranes, and *n*-alkanes based on time-integrated data. The fuel-based PM emission factors essentially represent emissions from a LDV fleet with frequent acceleration and deceleration driving conditions. Previous studies have only reported chemical speciation data from PM collected at fixed sites in the proximity of a LDV freeway (Ning et al. 2008) and a LDV tunnel bore (Phuleria et al. 2006; Geller et al. 2005). Results from the current study revealed that the on-road sampling methodology deployed can capture higher levels of PM compared to earlier studies, in particular, higher levels of metals and trace elements associated with vehicular abrasion (Fe, Ca, Cu, and Ba) as well as with crustal origins (Mg and Al). Overall, the $PM_{2.5}$ emission factors of PAHs from the current study are lower than the LDV tunnel and higher than the LDV freeway while hopane and sterane emission factors are comparable between the studies. Finally, alkane CPIs were calculated and were indicative of substantial anthropogenic source contribution for surface streets in Los Angeles.

Chapter 6 A comparative assessment of $PM_{2.5}$ exposures in light-rail, subway, freeway, and surface street environments in Los Angeles and estimated lung cancer risk

6.1 Introduction

The focus of this study is to assess and compare $PM_{2.5}$ exposures between five different transport environments in the Los Angeles area (subway, light-rail, surface street, two major freeways with a low and high truck fraction). Key species for comparison are EC, OC, total and water-soluble metals and trace elements, and PAHs. They are presented as mass per m^3 of air. Sources of PM components and species will be discussed in detail as well as its contribution from the commute environment. Lastly, estimates of lung cancer risk based on concentrations of PAHs are calculated to determine risk associated with each commute environment. The novelty of the current study lies in its focus on the exposure risk assessment for commuters of various microenvironments of Los Angeles. The PM species presented and discussed in this study have either been identified as carcinogens or as hazardous to human health. In addition, results from this study are of primary interest not only for commuters of these specific commute environments, but also for residents and pedestrians who are in the vicinity of major roadways that are sources of these pollutants.

6.2 Experimental methodology

This study represents the integration of two major campaigns that were conducted independently but with common measurement methods. The two campaigns will be referred to as the METRO study and the on-road study. Table 6.1 shows a summary of the sampling dates and times, routes, and meteorological parameters including average temperature, relative

humidity (RH), prevailing wind direction, and wind speed. Meteorological data is based on South Coast Air Quality Management District (SCAQMD) monitoring site. Average temperatures varied from 17 – 24 °C for the two campaigns due to different sampling periods. Note that the differences in the variation of relative humidity were due to the longer sampling time period for the on-road campaign (6:00AM-5:00PM) as compared to the METRO campaign (9:30AM-1:00PM). Overall, the wind direction and wind speed are comparable in the two campaigns. The University of Southern California (USC) site, which is centrally located near downtown Los Angeles, was sampled concurrently during both campaigns as a reference site. Previous studies have also been conducted at this site (Moore et al. 2007; Ning et al. 2007). Figure 6.1 shows a map of the five commute environments, USC reference site, and SCAQMD monitoring site.

Route	Dates of sampling	Sampling times	Temperature (°C)	RH (%)	Prevailing wind direction	Wind speed (m/s)
METRO study						
METRO lines	5/3-8/13/10	9:30am - 1:00pm	24.0 ± 3.5	55 ± 9.7	SW	3.2 ± 0.9
on-road study						
110	3/1-3/8/11, 4/11-4/18/11	6:00am - 5:00pm	18.3 ± 4.5	57.2 ± 21.5	W	3.2 ± 1.2
710	3/17-3/25/11, 4/19-4/25/11	6:00am - 5:00pm	17.3 ± 3.6	59.9 ± 18.2	W	3.5 ± 1.3
Wilshire/Sunset	3/9-3/16/11, 4/26-5/2/11	6:00am - 5:00pm	23.8 ± 5.7	42.0 ± 20.9	SW	3.3 ± 1.6

Table 6.1 Summary of sampling dates and times and meteorological parameters for the METRO and on-road studies. Meteorological parameters are based on South Coast Air Quality Management District (SCAQMD) monitoring site.

6.2.1 Sampling methodology

Both campaigns used the same instruments to collect PM for the purpose of comparing results. $PM_{2.5}$ was collected using the compact Personal Cascade Impactor Sampler (PCIS) (SKC Inc., Eighty-Four, PA) (Misra et al. 2002; Singh et al. 2003), which was operated with portable Leland Legacy pumps (SKC Inc., Eighty-Four, PA). The PCIS was prepared using an impaction

Figure 6.1 Map of five commute environments: 110 (green), 710 (blue), Wilshire/Sunset (purple), METRO red line (red), and METRO gold line (yellow). The USC reference site is denoted by the star and the South Coast Air Quality Management District (SCAQMD) monitoring site is denoted by the triangle.

stage with a cutpoint of 2.5 μm and an after filter stage, which collected $PM_{2.5}$. For the purpose of comprehensive chemical analysis, two types of filters were used—PTFE (Teflon) filters (Pall Life Sciences, Ann Arbor, MI) and quartz microfiber filters (Whatman International Ltd, Maidstone, England). Two sets of samples (N=2) were collected for both campaigns.

For the METRO campaign, subjects used suitcases to carry the instruments and spent 25% of their time waiting at stations and 75% of their time inside the train to simulate a typical commuter. The sampling duration for the METRO campaign was on weekdays from May to August 2010 from 9:30AM to 1:00PM. For the on-road campaign, the sampling vehicle was a Honda Insight Hybrid 2011 equipped with a curved inlet for roadway air entry to the sampling instruments. Since anisokinetic effects, which may result in the overestimation or

underestimation of relatively larger particles (i.e. $PM_{10-2.5}$) (Hinds 1999) need to be considered for on-road PM measurements, it was determined that $PM_{2.5}$, the PM fraction of interest in this study, is largely unaffected by anisokinetic sampling (refer to Chapter 4). The sampling duration for the on-road campaign was on weekdays from March to April 2011 from 6:00AM to 5:00PM.

6.2.2 Route description

A detailed description of the methodology of the METRO study has been described in section 2.2, so only a brief description follows. In the METRO study, two lines (the red line and gold line) were sampled concurrently using identical instruments. The red line is a subway line powered by electric third-rail that connects Downtown Los Angeles to North Hollywood and has the highest ridership of the METRO system; the gold line is a ground-level light rail line powered by overhead electric lines that connects Downtown Los Angeles to Pasadena. Trains pass every 8-12 minutes depending on the hour.

The on-road study has been described in detail in Chapters 4 and 5, so a summary of the routes and methodology follows. On-road sampling was conducted for three roadways during different time periods (Table 6.1). The three roadways each represent differential private commute environments. The 110 is a high-traffic freeway that runs from the Port of Los Angeles through Downtown Los Angeles to Pasadena, and is composed mostly of light-duty vehicles (LDVs); the 710 is less trafficked but serves as the main corridor for heavy-duty vehicles (HDVs) traveling to and from the Port of Los Angeles; Wilshire/Sunset Boulevards are major surface street routes that are composed primarily of LDVs and negligible HDVs and characterized by "stop-and-go" (frequent acceleration and deceleration) driving conditions. In the Los Angeles Basin, the 110 and 710 represent the lowest HDV (3.9%) and highest HDV (11.3%) traffic composition of the freeways in the area, respectively. Traffic data from the CalTrans PeMS 2011

database showed that total traffic flows for the 110 and 710 in one direction are 6,378 and 4,247 vehicles/hr, respectively, and truck flows are 243 and 470 trucks/hr. Wilshire/Sunset has a total flow of 1,839 vehicles/hr and negligible truck flows.

6.2.3 Sample analysis

Both campaigns were analyzed using the same analytical methodology. The Teflon filters were gravimetrically analyzed to determine mass concentration using a MT5 Microbalance (Mettler-Toledo Inc., Columbus, OH). For chemical analysis, Teflon filters were extracted by acid and subsequently analyzed by magnetic-sector Inductively Coupled Plasma Mass Spectroscopy (SF-ICPMS) to determine metals and trace elements (Zhang et al. 2008). The quartz filters were analyzed using the Thermal Evolution/Optical Transmittance analysis to measure elemental and organic carbon (EC/OC) (Birch and Cary 1996). Water extracts of the samples determined WSOC and water-soluble metals and trace elements. Quartz filters were also analyzed for polycyclic aromatic hydrocarbons (PAHs) concentrations by gas chromatography mass spectroscopy (GC/MS) using an established solvent extraction and molecular quantification analysis protocol as initially developed by Mazurek et al. (1987) and subsequently advanced by other studies (Schauer et al. 1999; Schauer et al. 2002).

6.3 Results and Discussion

6.3.1 Comparability of the two campaigns

The interpretation of results of this study largely depends on the comparability of PM components and chemical speciation data across the two sampling campaigns. Chemical speciation results from PM collected at the USC site (N=2) were compared for the two campaigns since sampling there occurred concurrently as a reference site, while using the same

sampling instrumentation and analyzed with the same methodology. To distinguish the two data sets, 'USC on-road' refers to reference results from the on-road campaign and 'USC METRO' refers to the reference results from the METRO campaign. Figure 6.2 shows the average concentrations ($\mu g/m^3$) of major PM components and the range, unless otherwise noted. Organic carbon (OC) is a major component of $PM_{2.5}$ in the Los Angeles Basin, and can constitute approximately 30-40% of $PM_{2.5}$ in the Basin (Sardar et al. 2005). According to mass balance analysis from the previously published manuscripts at the USC site, organic matter (OM), which is OC multiplied by a correction factor of 1.6±0.2 for an urban aerosol (Turpin and Lim 2001), constitutes the second largest component of $PM_{2.5}$ after inorganic ions (section 4.4.2). The

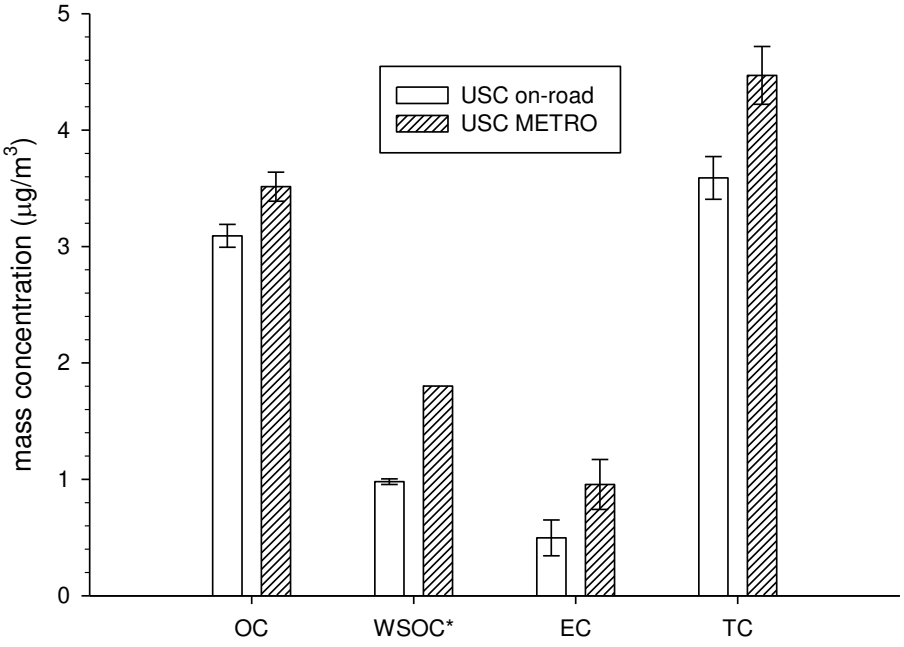

*N=1 for USC METRO data

Figure 6.2 Comparison of major PM components at the USC reference site for the two campaigns to assess comparability of data. All bars presented in this study represent upper and lower data points (N=2).

current study presents OC with no correction factor. The OC levels at USC are 3.5 and 3.1 $\mu g/m^3$ for the METRO and on-road campaigns, respectively, varying by 11%; and water-soluble OC (WSOC) constitutes 51% and 32% of OC, respectively. Elemental carbon (EC) for the USC METRO is approximately 2 times higher than the USC on-road campaign, which could be the result of reductions in EC due to the implementation of the recent Port of Los Angeles Clean Truck program that started in 2008. Total carbon (TC), which is the sum of EC and OC, is 4.5 and 3.6 $\mu g/m^3$ for the USC METRO and USC on-road campaigns, respectively, thus varying by 20%.

A table of comparison of metals and trace element and PAH concentrations at USC during the two campaigns is shown Table 6.2. The major difference observed between the two campaigns are the sulfur levels which are 2.4 times higher during the METRO campaign than during the on-road campaign, consistent with the higher and more variable levels of S observed at the light-rail and subway lines. This can be explained by the fact that the METRO campaign was conducted in the summertime, the photochemical period in Los Angeles. In Los Angeles, S in the particulate phase is mostly in the form of ammonium sulfate, which is primarily formed from gaseous precursors of SO_2 in the presence of sunlight and reaches its highest levels in summertime. Another important element, Na, which is influenced by sea salt, differs by 30% between the two campaigns. Otherwise, most of the other metals and trace elements differ by less than 20%. For PAHs, chrysene exhibits the highest concentration during the USC METRO campaign and is 3.6 times greater than during the on-road study. All other PAHs are generally less than 0.1 ng/m^3.

	USC METRO		USC on-road			USC METRO		USC on-road	
	average	±	average	±		average	±	average	±
Metals and trace elements (ng/m^3)					*PAHs* (ng/m^3)*				
Na	780.5	289.6	591.5	46.2	Pyrene	0.05	-	0.04	0.01
Mg	76.3	6.6	67.5	3.6	Benzo(*ghi*)fluoranthene	0.04	-	bdl	bdl
Al	133.3	14.3	140.9	9.7	Benz(*a*)anthracene	0.03	-	0.01	0.00
S	1412.4	188.9	598.6	38.7	Chrysene	0.18	-	0.05	0.005
K	95.3	10.4	87.6	9.3	Benzo(*b*)fluoranthene	0.11	-	0.09	0.08
Ca	144.6	30.8	125.4	7.4	Benzo(*k*)fluoranthene	0.05	-	0.02	0.01
Ti	18.3	1.3	16.3	1.0	Benzo(*e*)pyrene	0.08	-	0.05	0.06
Cr	3.1	2.2	2.8	0.1	Benzo(*a*)pyrene	bdl	-	bdl	bdl
Mn	5.2	0.8	4.8	0.2	Indeno(*1,2,3-cd*)pyrene	0.05	-	0.03	0.002
Fe	236.8	8.1	271.2	12.0	Benzo(*ghi*)perylene	0.11	-	0.14	0.05
Co	0.12	0.0	0.16	0.0	Coronene	0.06	-	0.02	0.01
Ni	2.9	1.5	1.6	0.2					
Cu	14.6	0.9	13.9	0.5					
Zn	16.3	3.62	14.3	1.16					
Mo	1.06	0.1	0.80	0.1					
Cd	0.09	0.0	0.09	0.0					
Sn	3.5	0.6	3.7	0.1					
Sb	2.4	0.55	2.4	0.09					
Ba	13.5	0.9	14.9	0.8					
Eu	0.011	0.001	0.021	0.001					
Pb	2.9	0.0	4.3	0.2					

bdl denotes below detection limit
*only one sample analyzed for USC METRO for PAHs

Table 6.2 Average concentrations of metals and trace elements and PAHs at USC site during the two campaigns. (N=2)

In addition to PM species, meteorological parameters (temperature, relative humidity, wind direction and speed) and gaseous pollutants (NOx, CO, and O_3) were compared during the two campaigns based on measurements at the SCAQMD monitoring site (Table 6.3). Average temperatures are warmer during the METRO campaign since it is during the summertime while the on-road campaign is in the spring; average relative humidity (%) and wind speed is similar. NOx and CO concentrations are greater by about 20-25% on average during the on-road campaign because these species are emitted by traffic sources and are typically higher in the morning hours (6:00-9:00AM) and decline throughout the day. On the other hand, O_3, a

secondary pollutant, is 12% higher during the METRO campaign because O_3 levels are typically lower in the morning hours (6:00-9:00AM). Overall, there is more variability in the meteorological parameters and gaseous pollutants due to the longer sampling period during the on-road campaign, but corresponding p-values demonstrate that none of the parameters are statistically significant between the two campaigns ($p>0.05$). Overall, considering the differential sampling dates and times of the two campaigns and less a few PM species, the $PM_{2.5}$ components and species do not vary substantially. As a result, concentrations (mass per m^3 of air) will be presented in this manuscript as the metric of comparison among the five commute microenvironments.

	Dates of sampling	Sampling times	Temperature (°C)	RH (%)	Prevailing wind direction	Wind speed (m/s)	NOx (ppm)	CO (ppm)
METRO campaign	5/3-8/13/10	9:30am - 1:00pm	24.0 ± 3.5	55 ± 9.7	SW	3.2 ± 0.9	0.035 ± 0.016	0.47 ± 0.14
on-road campaign	3/1-5/2/11	6:00am - 5:00pm	19.8 ± 8.1	53.0 ± 35.1	W	3.3 ± 2.4	0.043 ± 0.043	0.58 ± 0.32
p-value (α=0.05)	-	-	0.25	0.82	-	0.22	0.61	0.28

Table 6.3 Meteorological parameters and gaseous pollutant measurements at South Coast Air Quality Management District (SCAQMD) monitoring site in downtown Los Angeles.

6.3.2 Major PM components

Figure 6.3 shows the concentrations of major PM components (OC, WSOC, TC, and EC) for the five microenvironments. The bars represent the upper and lower data points. Overall, the 710 exhibits the highest concentrations of OC and EC, and thus TC, while the two METRO lines have the lowest concentrations of OC and TC. The relatively higher levels observed on the 710 can be attributed to its higher volume of heavy-duty vehicles (HDVs), which are the greatest emitters of EC (Schauer 2003) and OC (Geller et al. 2005; Ntziachristos et al. 2007; Phuleria et al. 2007) in a traffic environment. For OC, the concentrations of the 110 and Wilshire/Sunset are comparable and are approximately 20% higher than the METRO lines even though reference OC levels at USC were 11% higher during the METRO campaign. It is also important to note that

EC is largely from primary emissions while OC has a primary and secondary component (Schauer 2003), and thus less influenced by primary emissions. As discussed in Chapter 3, the source of OC in the METRO red line is primarily from the entrance of ambient air through the ventilation system. For WSOC, the concentrations of the microenvironments range from 1.2-2.0 $\mu g/m^3$, with the METRO red line exhibiting the lowest concentration and Wilshire/Sunset exhibiting the highest. For EC, the 710 concentrations are 2.0-3.3 times higher than the other commute microenvironments. Similar to OC, the main source of EC for the METRO lines is the influence of ambient air. Although Wilshire/Sunset is a highly-trafficked roadway environment, its low levels of EC can be explained by its negligible HDV volumes, designating it as a primarily LDV roadway. Moreover, Geller et al. (2005) showed that the fuel-based emission factors (mg of pollutant emitted per kg of fuel burned) for HDVs and LDVs for $PM_{2.5}$ is 710 and 29 mg/kg of fuel, respectively, which means HDVs emit almost 25 times more EC than LDVs per kg of fuel burned.

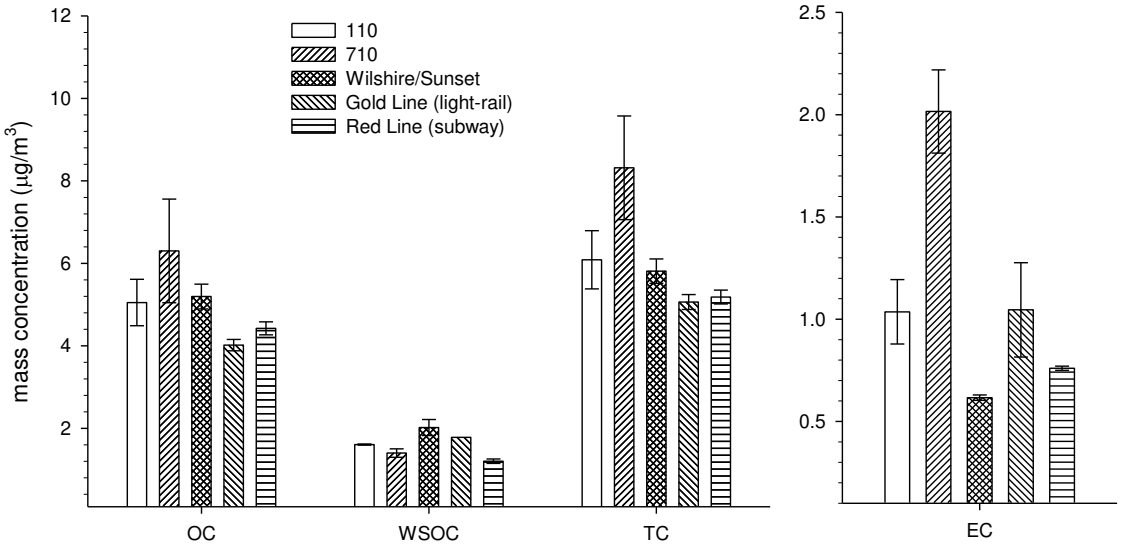

Figure 6.3 Comparison of major PM components (OC, WSOC, EC, and TC) for the five commute microenvironments. EC appears on a separate axis to highlight differences.

6.3.3 Metals and trace elements

A number of metals and trace elements that have been quantified in this study are identified as hazardous air pollutants under the U.S. EPA Clean Air Act Amendments of 1990, which includes Sb, Cd, Cr, Co, Pb, Mn, and Ni compounds. The U.S. EPA states that these airborne pollutants are known to cause or possibly cause cancer or other serious health effects, including birth defects, further emphasizing the importance of understanding the exposure of metals and trace elements for public and private commuters as well as residents who are in the vicinity of major roadways. Figure 6.4 and Table 6.4 shows the concentrations (ng/m^3) of total metals and trace elements for the commute microenvironments, and are presented based on concentration levels. Overall, the METRO red line (subway) exhibits the highest concentrations for Fe, Mn, Mo, Ba, Cr, Co, Ni, and Cd. For Fe, the red line is approximately 10 times higher than the 110 and 710, 15 times higher than Wilshire/Sunset, and 20 times higher than the gold line (light-rail). The sources of these enriched species have been discussed extensively in section 3.3, thus only a brief summary follows. In the enclosed underground environment, subway dust is generated mainly from the abrasion processes between the rail, wheels, and brakes as well as by the mechanical wearing of the parts. The rail tracks and the main body of the train are composed of stainless steel, an Fe-based alloy mixed with other metallic elements to enhance its properties. The same study also demonstrated that Fe is strongly correlated with Cr, Mn, Co, Ni, Mo, Cd, and Eu ($R^2 > 0.9$, $p < 0.05$), indicating that these species may be components of stainless steel. In addition, PM may be resuspended due to train and passenger movement. Although the gold line (light-rail) exhibits relatively low concentrations of these steel-associated elements, the study determined that based on crustal enrichment factors (Taylor and McLennan 1985), of which values close to 1 indicates crustal origins and greater values indicate

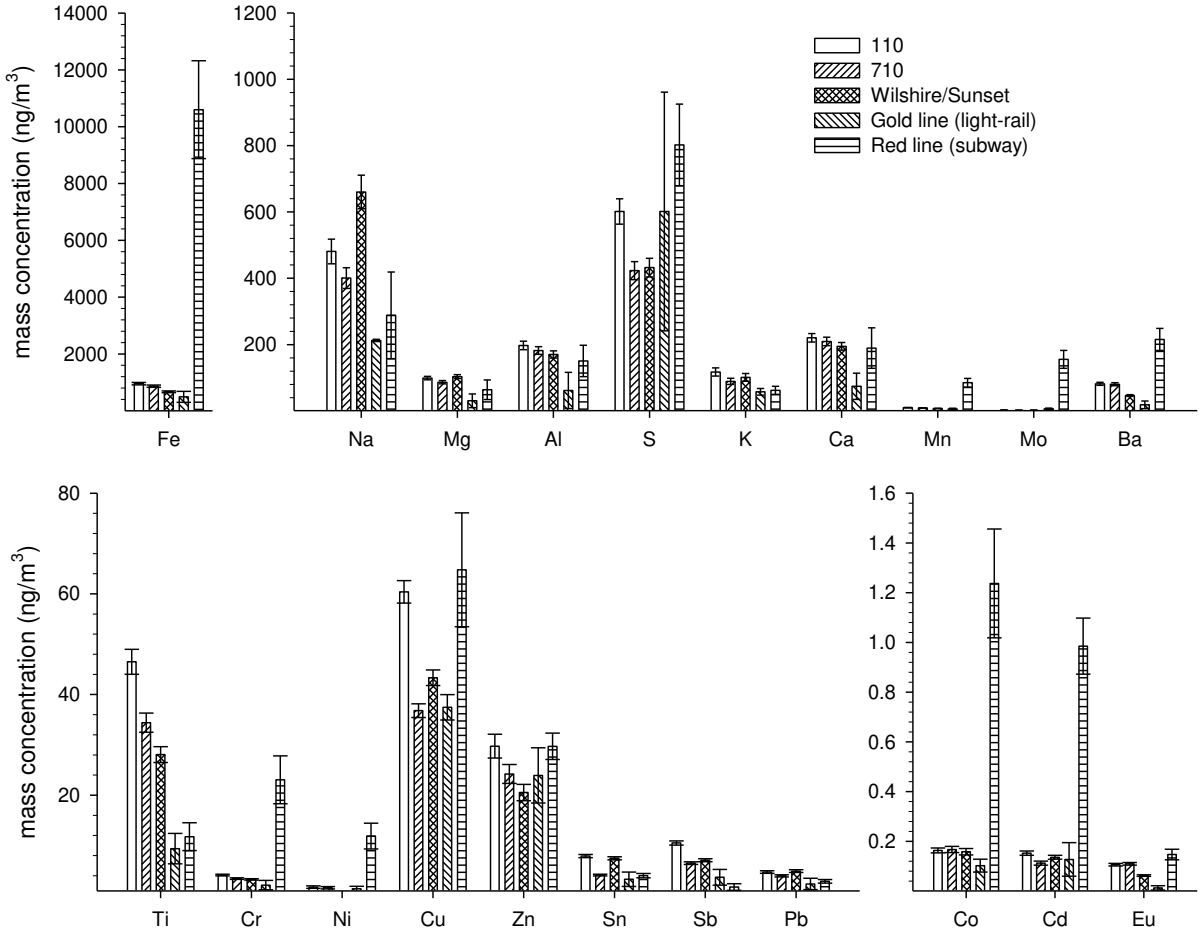

Figure 6.4 Comparison of concentrations of total metals and trace elements for the five commute environments.

anthropogenic sources, these elements have enrichment factors that are 2-3 times greater than the USC reference site. This suggests that these elements have indeed been influenced by additional sources (i.e. steel abrasion, wear of rail parts, etc.) that do not influence USC. Regardless of its additional source, the concentrations of metals and trace elements on the gold line (light-rail) are the lowest of the five commute environments, meaning commuters of this light-rail line are exposed to the lowest amounts of these airborne toxics.

	110	±	710	±	Wilshire/ Sunset	±	METRO Gold line	±	METRO Red line	±
PM components (μg/m3)										
OC	5.0	0.6	6.3	1.3	5.2	0.3	4.0	0.1	4.4	0.2
WSOC	1.6	0.01	1.4	0.1	2.0	0.2	1.8	-	1.2	0.1
EC	1.0	0.2	2.0	0.2	0.6	0.01	1.0	0.2	0.8	0.01
TC	6.1	0.7	8.3	1.3	5.8	0.3	5.1	0.2	5.2	0.2
metals and trace elements (ng/m3)										
Fe	955.6	43.6	865.7	42.0	666.8	30.8	490.5	195.1	10599.2	1723.7
Na	480.9	37.2	400.7	31.2	660.1	50.7	212.5	3.2	288.0	130.8
Mg	98.9	5.3	86.4	5.0	103.5	5.8	30.6	20.7	63.7	29.5
Al	197.4	12.6	182.2	11.7	170.3	11.1	61.7	54.6	150.8	47.5
S	601.3	38.3	423.0	27.3	432.1	28.0	601.2	359.8	802.1	123.1
K	117.5	12.5	89.2	9.4	101.3	11.8	57.6	10.0	62.1	12.0
Ca	220.6	12.9	209.5	12.8	194.7	11.6	74.2	39.4	189.5	61.2
Mn	10.0	0.4	9.2	0.4	7.4	0.3	5.8	2.2	84.9	13.1
Mo	2.6	0.2	2.2	0.1	2.3	0.1	6.3	2.1	155.6	26.9
Ba	81.7	4.5	80.5	4.6	46.4	2.4	18.4	11.5	215.6	33.3
Ti	46.5	2.5	34.4	1.9	28.1	1.6	9.4	3.0	11.8	2.8
Cr	4.1	0.2	3.4	0.2	3.3	0.1	2.1	0.9	23.1	4.7
Co	0.2	0.0	0.2	0.01	0.2	0.01	0.1	0.03	1.2	0.2
Ni	1.7	0.2	1.6	0.2	0.9	0.2	1.4	0.5	11.9	2.6
Cu	60.4	2.2	36.8	1.4	43.3	1.5	37.5	2.5	64.8	11.3
Zn	29.7	2.4	24.2	1.9	20.5	1.6	23.9	5.5	29.7	2.6
Cd	0.2	0.0	0.1	0.0	0.1	0.01	0.1	0.1	1.0	0.1
Sn	7.9	0.3	4.1	0.2	7.5	0.3	3.3	1.4	4.0	0.4
Sb	10.5	0.4	6.5	0.3	7.1	0.3	3.7	1.6	1.8	0.7
Eu	0.1	0.01	0.1	0.01	0.1	0.003	0.01	0.01	0.1	0.02
Pb	4.7	0.3	4.0	0.2	4.9	0.3	2.4	1.1	2.9	0.4
PAHs (ng/m3)										
Pyrene	0.21	0.02	0.83	0.10	0.13	0.05	0.06	-	0.08	0.01
Benzo(GHI)fluoranthene	0.22	0.04	0.32	0.09	0.24	0.24	bdl	-	0.06	0.00
Benz(a)anthracene	0.10	0.03	0.16	0.06	0.06	0.02	bdl	-	0.02	0.00
Chrysene	0.23	0.06	0.25	0.07	0.14	0.01	0.14	-	0.19	0.02
Benzo(b)fluoranthene	0.31	0.05	0.30	0.09	0.23	0.07	0.10	-	0.12	0.01
Benzo(k)fluoranthene	0.10	0.01	0.10	0.07	0.05	0.02	0.05	-	0.04	0.00
Benzo(e)pyrene	0.21	0.01	0.24	0.09	0.15	0.05	0.04	-	0.08	0.05
Benzo(a)pyrene	bdl	-	0.09	0.05	bdl	-	bdl	-	bdl	-
Indeno(1,2,3-cd)pyrene	0.09	0.06	0.04	0.01	0.09	0.09	0.06	-	0.05	0.00
Benzo(GHI)perylene	0.45	0.10	0.51	0.16	0.30	0.10	0.12	-	0.10	0.00
Coronene	0.10	0.10	0.17	0.14	0.17	0.03	0.06	-	0.06	0.01

Table 6.4 Mass concentrations of major PM components, metals and trace elements, and PAHs at the five microenvironments (N=2). Only one sample for PAHs was analyzed for the METRO gold line.

The differential microenvironments play a major role in the contribution of various sources of metals and trace elements presented in this study. For example, Na may be part of soil dust, but because Los Angeles is largely affected by the southwesterly onshore breeze from the Pacific Ocean, sea salt is a substantial source of Na in the Basin. The higher Na concentrations observed on the three roadways relative to the METRO lines are expected in light of its major

sea salt influence. Moreover, the higher levels of Na observed at Wilshire/Sunset relative to the 110 and 710 (average of 33% higher), can be explained by the proximity of the Wilshire/Sunset route to the coast, while the 110 and 710 routes are located more inland, and thus less influenced by sea salt. The average concentrations of Mg, Al, and K for the three roadways are 96.3±8.8, 183.3±13.6, 102.6±14.2 ng/m^3, respectively, and are all higher than average corresponding concentrations on both METRO lines (47.2±23.4, 106.2±63.0, and 59.9±3.2 ng/m^3). This is consistent with previous studies which determined that these species are primarily of crustal origin and derived from resuspension rather than from vehicular sources (Sternbeck et al. 2002).

Studies have shown that Fe, Al, Ca, Mg, K, Na are abundant in crustal materials, but road dust may be enriched with some of these elements, indicating anthropogenic sources (Harrison et al. 2003; Lough et al. 2005). While the focus of this study is not to quantify the enrichment of these species relative to a reference site, our data is consistent with earlier roadside studies for elements which have a contribution from traffic sources (i.e. Cu, Ba, Pb, Fe, Ca, Sb, etc.). The most obvious observations are the elements that are associated with vehicular traffic but not rail abrasion or wear, which are Ca, Ti, Sn, Sb, and Pb. These elements are primarily derived from vehicular wear processes such as brake and tire wear (Ti, Sb, and Pb) and motor oil additives (Ca) (Lough et al. 2005; Grieshop et al. 2006). The average concentrations for the three roadways are 208.3±13.0 ng/m^3 for Ca, 36.3±9.4 ng/m^3 for Ti, 6.51±2.1 ng/m^3 for Sn, 8.0±2.2 ng/m^3 for Sb, and 4.6±0.5 ng/m^3 for Pb, while corresponding averages for the two METRO lines are 131.9±81.6, 10.6±1.7, 3.7±0.5, 2.7±1.4, and 2.6±0.4 ng/m^3. HDVs are known to be greater emitters of elements associated with brake wear due to the greater mechanical force required to decelerate relative to LDVs (Sternbeck et al. 2002). However, our results found no statistically

significant differences for Ca, Ti, Sn, Sb, and Pb between the 110, which is composed of 3.9% HDVs, and 710, which is composed of 11.3% HDVs (p=0.42).

Elements associated with both steel and vehicular sources include Fe, Ba, Cu, and Zn. Traffic sources for these elements include engine wear (Fe), brake wear (Ba and Cu), and tire wear (Zn) (Sternbeck et al. 2002; Sanders et al. 2003). $BaSO_4$ is known to be commonly used in brake linings (Garg et al. 2000). The overall trend for these four elements is substantially higher concentrations in the red line (subway) relative to the other environments except for Zn, which exhibit comparable levels for the five environments. For Fe, Ba, and Cu, concentrations on the three roadways vary within 50% of each other (with averages of 829.4±147.8 ng/m^3 for Fe, 69.6±20.0 ng/m^3 for Ba, and 46.8±12.2 ng/m^3 for Cu), and are generally higher than the gold line (490.5 ng/m^3 for Fe, 18.4 ng/m^3 for Ba, and 37.5 ng/m^3 for Cu).

Sulfur, which is the predominant element in all environments, shows unexpectedly high concentrations for the METRO lines relative to the three roadways. As discussed earlier, since S is in the form of ammonium sulfate in the Los Angeles Basin (Hughes et al. 2000), this is most likely explained by the warmer temperatures observed during the METRO campaign, which would lead to greater formation of sulfate from the increase in photochemical reactions. A previous study in the basin also found that sulfate levels were higher in the summer than in the winter (Sardar et al. 2005). Another source of S is from fuel, which is known to be emitted at higher rates from HDVs due to higher S content in diesel fuel (Lowenthal et al. 1994), or S can be emitted from fuel, motor oil, and additives such as zinc dithiophosphate (Lough et al. 2005).

6.3.4 Water solubility of metals and trace elements

In regards to PM exposure, water solubility of particle-bound elements is an important property that contributes to its bioavailability to human cells. In particular, soluble transition metals have been shown to mediate cardiopulmonary injury (Costa and Dreher 1997). Numerous studies have also shown that soluble transition metals (i.e. Fe, Ni, Cr) may generate reactive oxygen species (ROS) through Fenton-like reactions, resulting in oxidative stress (Loft et al. 2005; Verma et al. 2010). Figure 6.5 shows the water solubility (%) of selected metals and trace elements in this study grouped by high and low solubility classes. Solubility of elements for the METRO campaign has been discussed in section 3.3, so only a brief discussion follows. Overall, elements in the METRO red line are the least soluble but have the highest total elemental concentrations, while the METRO gold line has the highest solubility of the five environments but the lowest total elemental concentrations. A number of these metals and trace elements quantified in this study are typically in the form of oxides or other compounds in the urban environment (Chow et al. 1994), and thus have varying solubility depending on their specific form. In addition, various isotopes have different solubility as well. The most notable observation is the differential solubility of Fe, which exhibited total Fe concentrations of 10.6 $\mu g/m^3$ for the red line (subway) but is only 0.8% soluble, while the gold line (light-rail) exhibited total Fe concentrations of 0.5 $\mu g/m^3$ but is 11.5% soluble. This yields water-soluble concentrations of 79.8 and 57.9 ng/m^3 for the red line and gold line, respectively, which differs only by 1.4 times as opposed to the 20 times difference for total concentrations. For elements that are typically salts (i.e. Na, Mg, S in the form of sulfate) generally have higher solubilities, as expected. Except for a few elements, solubility of elements for the three roadway environments

are comparable and lie in between the solubilities of the gold and red line for a number of transition metals including Cr, Mn, Fe, Co, Ni, Cu, Zn, and Cd.

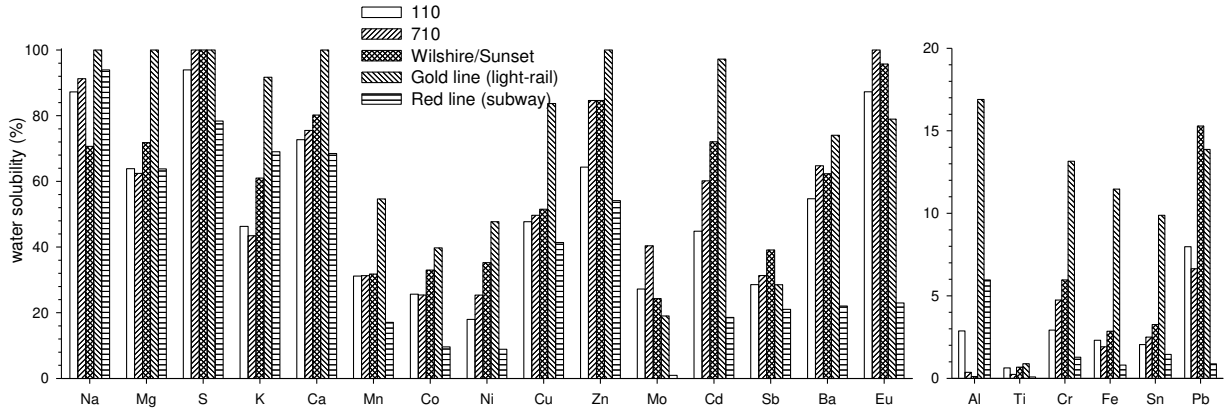

Figure 6.5 Comparison of water-solubility (%) of metals and trace elements for the five microenvironments separated into high and low solubility species.

6.3.5 Polycyclic aromatic hydrocarbons (PAHs)

The U.S. EPA classifies 16 PAHs as priority pollutants based on their carcinogenicity and mutagenicity. Many PAHs and their derivatives are identified as probable (Group 2A) or possible (Group 2B) carcinogens as defined by the International Agency for Research on Cancer (IARC). Therefore, it is essential to identify and quantify the concentrations of PAHs of which public and private commuters are exposed to on a daily basis. Figure 6.6a and 6.6b and Table 6.4 shows the average and range of concentrations of 11 PAHs (ng/m^3) and total PAH concentrations for the five commute environments. It is important to note that the temporal and seasonal differences in sampling times may affect PAH concentrations to a certain degree. Total PAH concentrations are substantially higher on the roadway environments than on the two METRO lines. Specifically, the 710, 110, and Wilshire/Sunset roadways are 4.2, 2.8, and 2.2 times higher than the average of the two METRO lines, respectively. For most of the individual PAH species,

the 710 levels are generally 2-3 times higher than the other two roadway environments, except for pyrene, where levels are 4-8 times higher. Although the 710 has the highest total PAH concentrations, statistical analysis using a t-test showed that the concentrations of all the PAHs (N=11) on the 710 were not significantly different with the 110 (p=0.37) or Wilshire/Sunset (p=0.18). PAH concentrations for the two METRO lines are consistently lower than the roadways, which is expected considering the main source of PAHs in the subway and light-rail environment is most likely entrainment from ambient air. Pairwise multiple comparison tests (Tukey test) was performed to further investigate statistical significance, which determined that only two pairs (710 and red line, 710 and gold line) were significantly different ($p<0.05$).

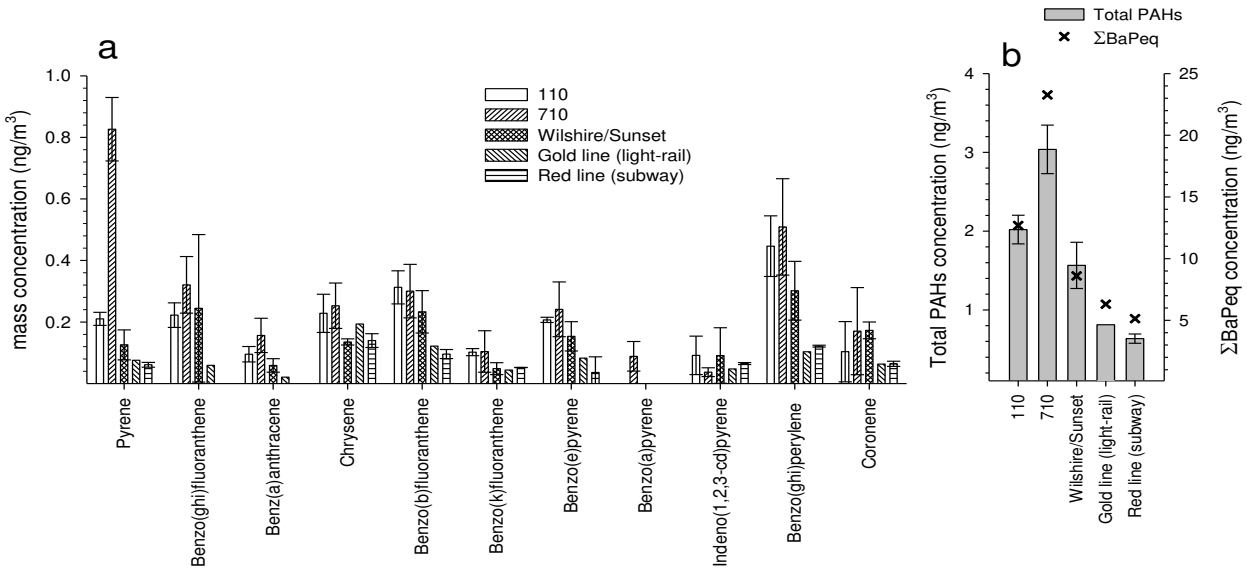

Figure 6.6 a) Concentrations of 11 PAHs and b) sum of PAHs concentrations and ΣBaPeq for the five commute environments.

In urban environments, the main source of PAHs is from fuel and combustion processes (Miguel et al. 1998). Both LDVs and HDVs emit PAHs, but HDVs emit PAHs at substantially higher amounts than LDVs (Phuleria et al. 2006; Ning et al. 2008). Numerous studies which have apportioned PAH emission factors (μg of pollutant/kg of fuel burned) for HDVs and LDVs

through tunnel studies (Phuleria et al. 2006) and dynamometer studies (Schauer et al. 1999; Schauer et al. 2002) have found that HDVs can emit up to 50 times more PAH levels than LDVs. The same studies also found that low molecular weight (MW) (MW ≤ 228) PAHs (i.e. pyrene) are primarily emitted by HDVs and high MW (MW ≥ 276) PAHs (i.e. benzo(*ghi*)perylene, indeno(*1,2,3-cd*)pyrene) are emitted by both HDVs and LDVs, which is consistent with the results of our current study. Although the 110 has high total traffic flows but low HDV flows (6378 veh/hr and 243 trucks/hr) and the 710 has a lower total traffic flow but higher truck flow (4247 veh/hr and 470 trucks/hr), the near 2-fold difference in truck volumes present on the 710 is most likely responsible for the higher concentrations of light MW PAHs.

An important property of PAHs is their semi-volatile nature. PAHs can be found in the urban environment in the gaseous phase or adsorbed onto particles in the solid phase based on its vapor pressure. Ambient temperatures can also play a role in the presence of particle-bound PAHs (Eiguren-Fernandez and Miguel 2012). Generally, high MW PAHs have lower vapor pressures than low MW PAHs. Thus, pyrene (MW = 202), can partition between the gas and particle phase depending on ambient temperatures, while indeno(1,2,3-cd)pyrene (MW = 276) and coronene (MW = 300) are found almost entirely in the particle phase. This is consistent with a previous study which found that emission factors for high MW PAH based on roadside sampling at the 110 and 710 were comparable to the reconstructed LDV and HDV emission factors based on tunnel sampling in spite of the different temperatures and dilution conditions, while low MW PAH emission factors differed by over two times (Ning et al. 2008). For the current study, the ambient temperatures for the two campaigns varied from 17 to 24 °C (Table 6.1). Of the 3 roadway environments, Wilshire/Sunset exhibited the lowest PAH levels, consistent with the higher observed temperatures. Although the METRO campaign also had

higher average ambient temperatures, the PAH levels for the red and gold lines are also influenced by the particle removal efficiency of the subway and train ventilation systems and thus particle penetration into the train.

6.3.6 Lung cancer risk for commuters

As mentioned earlier, PAHs are a major public health concern due to its carcinogenicity, and more specifically, to lung cancer risk. A number of PAHs identified in this study are classified as priority pollutants under the U.S. EPA. According to the IARC, benzo(a)pyrene, or BaP, is classified as a probable carcinogen (Group 2A). Since BaP has been studied and its cancer potency values have been well established, it is commonly used as the index compound for which potency activity of other PAH compounds and its derivatives are compared to. Relative potency values are referred to as potency equivalent factors (PEFs), for which BaP has a PEF of 1. Benz(a)anthracene has a PEF of 0.1, meaning it has $1/10^{th}$ the potency of BaP. PEFs for other PAH compounds are from OEHHA. The calculation of lung cancer risk follows the method in Sauvain et al. 2003, and a brief summary follows. The PEFs are multiplied by the corresponding PAH concentration to determine the BaP equivalent concentrations (BaPeq). The sum of the individual BaPeq (ΣBaPeq) is subsequently multiplied by its unit risk factor $(\mu g/m^3)^{-1}$, which has been determined based on rodent or epidemiology studies (Collins et al. 1998; Bostrom et al. 2002; Sauvain et al. 2003). Unit risk factors based on rodent and epidemiology studies are 1.1E-4 and 2.1E-3 $(\mu g/m^3)^{-1}$, respectively. Figure 6.6b shows ΣBaPeq as a marker for each of the 5 microenvironments. Since the unit risk factors in Sauvain et al. (2003) are based on occupational continuous exposures (45 years for 8 hr/day), the current unit risk factors are determined by a multiplication factor of 0.18 to account for the lower risk for a commuter's lifetime on the road, which is considered to be 45 years for 5 days/week for 2 hours/day.

Table 6.5 shows the concentrations of ΣBaPeq and corresponding unit risk factors and lung cancer risk based on earlier rodent and epidemiology studies. Note that the unit risk factors between the rodent and epidemiology studies differ by approximately 19 times, yielding cancer risk values that differ by the same factor. Overall, the 710 exhibits the highest cancer risk. The 710 is greater than the two METRO lines by an average of 4.2 times, and is greater than the 110 and Wilshire/Sunset by 1.9 and 2.7 times, respectively. Although the results offer meaningful insight into the cancer risk that various commuters face on a daily basis, the authors acknowledge that there are relatively large uncertainties associated with the results as seen with the differences in unit risk factors between the rodent and epidemiology studies. In addition, concentrations of PAHs may exhibit temporal variation. For example, a previous study in Wilmington, CA, which is located between the 110 and 710 and in the proximity of the Ports of Los Angeles and Long Beach found that lung cancer risk is highest during rush hour traffic (around 8:00AM) and lowest in the late afternoon (around 5:00PM) (Polidori et al. 2008), whereas the current study represents results based on time-integrated samples from 6:00AM to5:00PM. Nonetheless, results from this study are substantive in assessing the lung cancer risk for commuters on the light-rail, subway, freeway, and surface street environments in Los Angeles.

	ΣBaPeq (ng/m^3)	lung cancer risk ($x10^{-6}$)	
		rodent	epidemiology
110	12.7	1.4	27.1
710	23.3	2.7	49.7
Wilshire/Sunset	8.6	1.0	18.4
Gold line (light-rail)	6.3	0.7	13.5
Red line (subway)	5.1	0.6	11.0

Table 6.5 Lung cancer risk calculations based on a commuter lifetime of 45 years, 2 hours/day, and 5 days/week. Unit risk factors for rodent and epidemiology are 1.1E-4 and 2.1E-3 $(\mu g/m^3)^{-1}$, respectively.

6.4 Conclusion

This study compares the major PM components (EC, OC, WSOC), metals and trace elements, and PAHs in $PM_{2.5}$ for public and private commuters in five differential environments: subway (METRO red line), light-rail (METRO gold line), surface street (Wilshire/Sunset), and two freeways which represent the highest (710) and lowest (110) truck compositions in Los Angeles. The 710 exhibited the highest EC and OC levels most likely due to its higher volume of HDVs, while the two METRO lines had the lowest EC and OC levels. Metals and trace elements quantified in this study are derived from a variety of sources depending on the commute environment. Substantially high levels of Fe and other steel-associated elements (Mn, Mo, Ba, Cr, Co, Ni, and Cd) were observed on the red line (subway) and substantially low levels were observed on the gold line (light-rail). Major sources in the rail environment are steel abrasion and wear of parts. Another group of elements (Ca, Ti, Sn, Sb, and Pb) was identified to be associated with urban traffic sources only, which are generated from vehicular wear processes and emitted from motor oil additives. Additionally, a number of the elements are primarily of crustal (i.e. Mg, Al) or sea salt (Na) origins, and not influenced by rail or traffic sources. In the roadway environment, PAHs are primarily derived from vehicular emissions and total PAHs were found to be substantially higher on the 710, consistent with earlier studies which found HDVs to be significantly greater emitters of PAHs than LDVs (Phuleria et al. 2006; Ning et al. 2008). Lastly, lung cancer risk was estimated and the 710 was determined to have the greatest cancer risk, while the two METRO lines had the lowest risk. Since the gold line (light-rail) was observed to have low concentrations of both PAHs and metals and trace elements, this suggests that commuting on a light-rail may have potential health benefits due to lower PM exposure levels as opposed to driving on freeways and major roadways. Results from this study are especially

important for understanding $PM_{2.5}$ exposure not only for daily commuters but also for residents and pedestrians who are in the proximity of roadways and can be subjected to these pollutants and its inherent health risks.

Chapter 7 Conclusions and recommendations for future research

This thesis focuses on the size-fractionated PM exposure for five different commute environments in Los Angeles (light-rail, subway, freeway with highest HDV fraction, freeway with lowest HDV fraction, and major surface streets). Individual routes were selected to represent unique microenvironments within a local region of Los Angeles and to highlight various sources that contribute to the emissions profile of PM depending on commute environment. A comprehensive chemical analysis was conducted to assess the chemical composition of PM collected in the various microenvironments, including OC, EC, WSOC, inorganic ions, total and water-soluble metals, and speciated organics. Implications to health were also discussed including toxicological results and estimates to lung cancer risk based on particle-bound PAHs.

7.1 METRO study conclusion

Chapters 2 and 3 presented the results from the METRANS campaign. Chapter 2 focused on the mass concentrations of $PM_{2.5}$ and PM_{10} based on continuous measurements on the light-rail (METRO gold line) and subway (METRO red line). Results showed that subway commuters are exposed to greater PM concentrations than light-rail commuters, and the light-rail environment is heavily influenced by ambient PM while the subway environment has an additional source of airborne PM from the daily operation of trains. Correlation analysis was also conducted to show that $PM_{2.5}$ and coarse PM are highly correlated, and thus from the same source. Due to the enclosed nature of the subway line, PM concentrations are inherently higher Chapter 3 focused on the chemical composition of PM collected on the subway and light-rail lines. A mass balance was conducted and showed that iron constitutes approximately 30% of total mass for the subway line for both coarse and fine PM fractions. Bivariate regression

analysis investigating ROS activity showed that ROS is strongly correlated with water-soluble Fe, Ni, and OC. A multiple linear regression model using water-soluble Fe and OC to be predictors of ROS was developed and explained 94% of the variance in ROS. In addition, on a per volume basis, commuters on the red line exhibit 55% more ROS activity than riders on the gold line. Results also showed that a number of metals, including Cr, Mn, Co, Ni, Mo, Cd, and Eu were elevated for the red line and, to a lesser degree, the gold line. This campaign is the first to make time-integrated and continuous measurements of PM for the Los Angeles METRO.

7.2 On-road study conclusion

Chapters 4-6 present the results from the on-road study. This study's novelty lies in the sampling methodology deployed to collect size-fractionated on-road PM. While numerous on-road studies have been conducted in various roadway environments, none of the previous have collected time-integrated PM for the purpose of a comprehensive chemical analysis. Three roadways (HDV freeway, LDV freeway, and major surface streets) were selected to represent different commute environments that are typical of Los Angeles commuters. The mobile laboratory was a hybrid vehicle, and was selected for its low emission. The aerosol inlet was specially designed to account for anisokinetic effects, which may underestimate or underestimate PM collection depending on size range. Calculations in section 4.3.1 showed that coarse particles less than 5 μm in diameter are affected by anisokinetic effects by less than 20%, while $PM_{2.5}$ is virtually unaffected.

Chapter 4 presents the first of the results from this major on-road sampling campaign. This chapter focuses on the mass balance of three size fractions ($PM_{10-2.5}$, $PM_{2.5-0.25}$, and $PM_{0.25}$) of the three roadway environments. It is clear that each size fraction is influenced by different source contributions varying from vehicle emissions, road dust resuspension, and natural sources

such as sea salt. For all roadways, $PM_{0.25}$ is heavily influenced by vehicular emissions, as expected since particles from combustion are typically in the ultrafine size fraction. The other two size fractions are less influenced by roadway emissions. $PM_{2.5-0.25}$ is dominated by inorganic ions which are secondary pollutants formed from gaseous precursors (SO_2 and NOx) in the presence of sunlight. In an urban environment, the gaseous precursors are typically emitted from anthropogenic sources such as tailpipe emissions. $PM_{10-2.5}$ is dominated by crustal metals, most likely from the resuspension of road dust generated from the turbulence of on-road traffic. Major PM components (EC, OC, and WSOC) were investigated and the most notable observation are the elevated EC concentrations on the HDV freeway (710). Although elevated, EC concentrations are lower in comparison to previous studies, which may be due to the implementation of the Clean Truck Program that started in 2008.

Chapter 5 presents the second part of the results from the on-road campaign, and focuses on the surface street environment (Wilshire and Sunset Boulevards). On-road emission factors are calculated for LDVs since the surface streets selected are predominantly trafficked by LDVs. The surface street environments differ from the other two roadway environments is that it is characterized by stop-and-go driving conditions due to frequent acceleration and deceleration of vehicles. Emission factors are based on a urban reference site (USC), where concurrent sampling was conducted, and are presented for metals and trace elements, PAHs, and hopanes and steranes. Results are compared to earlier an earlier LDV tunnel and LDV freeway study for $PM_{2.5}$ only. Overall, results show that the on-road sampling methodology deployed may capture higher levels of PM compared to earlier roadside studies. It is also observed that the overall emission factors of PAHs are lower than the LDV tunnel study and higher than the LDV freeway study. This is most likely due to the semi-volatile nature of PAHs which has the ability to partition between the

gaseous and particulate phase depending on ambient conditions. Due to the cooler temperatures and enclosed nature of the LDV tunnel environment, PAHs will most likely to partition to the particulate phase, thus contribute to higher levels of PAHs, while the warmer temperatures and open atmospheric conditions of the LDV freeway will like shift PAHs to its gaseous phase. While the two surface streets are also subject to open atmospheric conditions, as noted earlier, the LDV fleet on surface streets is subject to frequent stop-and-go conditions while the LDV fleet on freeways is mostly under cruise conditions. Emission factors for hopanes and steranes were comparable between the current study and the two earlier LDV studies, as expected since hopanes and steranes are relatively stable regardless of environment.

7.3 Integration of the METRO and on-road study conclusion

The last part of the thesis presents an integration of the results of the METRO study and the on-road study and essentially ties the entire thesis together. In addition to comparing the chemical composition of the five commute microenvironments, this chapter of the thesis focuses more on the health implications of commuter exposure to PM. Since $PM_{2.5}$ is the most relevant in terms of health and risk assessment, results and discussions are limited to this size fraction. Since a number of metals and trace elements are listed as hazardous air pollutants and a number of PAHs are classified as priority pollutants under the U.S. EPA, these two major groups of species become the focus of this integrative chapter. Due to the various commute environments studied, three major sources contribute to the levels of metals and trace elements depending on the environment. These three sources include vehicular emissions (tire and brake wear), rail abrasion, and natural (crustal or sea salt sources). For example, Fe, Mn, Mo, Ba, Cr, Co, Ni, and Cd were observed on the subway line to be substantially higher, indicating these elements may be associated with stainless steel and become airborne due to the steel abrasion and wear of train

and rail parts. Another group of elements including Ca, Ti, Sn, Sb, and Pb was identified to be associated with traffic sources only and mostly arise from vehicle wear processes and from engine oil, for which they are additives. Elements including Mg, Al, and Na originate from crustal or sea salt, otherwise natural, origins and not influenced by either rail or traffic sources. PAH concentrations were highest in the HDV freeway environment, as expected since HDVs are substantially greater emitters of PAHs relative to LDVs (Phuleria et al. 2006; Ning et al. 2008). Since PAHs are classified as probable or possible carcinogens under the IARC, lung cancer risk was estimated based on speciated PAHs. Results show that the HDV freeway exhibits the greatest cancer risk while the two METRO lines exhibit the lowest risk since they have lower levels of PAHs. Based on the results from this study, commuting on the light-rail line may have potential health benefits since it has low concentrations of both metals and trace elements and PAHs, and thus lower risk of lung cancer.

7.4 Recommendations for future research

7.4.1 Limitations of the current studies

Size-fractionated PM was collected in five differential commute environments in Los Angeles and a comprehensive chemical analysis was conducted to compare major PM components, metals and trace elements, inorganic ions, and speciated organics. Two separate campaigns were conducted at different time periods and dates. The METRO campaign was conducted during the summer of 2010 from 9:30AM to 1:00PM while the on-road campaign was conducted in the spring of 2011 from 6:00AM to 5:00PM. Due to the time-, resource-, and labor-intensive nature of the two campaigns, it was not possible to conduct concurrent sampling at all five commute microenvironments. This is inherently one of the limitations of the current study, for which there may be temporal or seasonal variations that may contribute to the differences in

PM components and species that were compared in Chapter 6. It was shown that at the USC reference site, which was sampled during both campaigns, differences in PM components, metals and trace elements, organic species, atmospheric conditions less a few parameters (i.e. temperature), and gaseous pollutants were not significantly different during the two campaigns ($p>0.05$). While measures were taken to ensure results would be consistent as possible (i.e. using same sampling instruments and chemical analysis), given the limitations, concurrent sampling of all microenvironments would have been the ideal method of conducting this massive campaign.

Numerous studies have shown that while ambient PM is dynamic and may vary on a daily basis, PM trends have been observed on a seasonal, diurnal, and temporal basis (Sardar et al. 2005; Hughes et al. 2000). The studies are conducted for a few months out of the entire year and are only representative of the time period sampled. Although PM exposure in other similar commute environments or during another time period can be extrapolated based on the results of this study, PM exposure will vary depending on regional and temporal differences. Regardless of this limitation, this study represents an extensive emissions profile that may be typical of many urban commute environments that are dominated by a mix of anthropogenic and natural sources.

7.4.2 Recommendations for future research

The research presented in this manuscript has valuable implications to public risk assessment as well as developing a comprehensive emissions profile for various common commute microenvironments. Although the results are limited to a certain time period and to the localized region of Los Angeles, researchers looking to investigate PM chemical composition and exposure for commuters can use the current study as a foundation for developing similar future research projects. Further studies can be designed to investigate a more intensive campaign that focuses on on-road diurnal trends (i.e. morning vs evening commute time periods).

Since the current study represents the integration of 11-hour time intervals on weekdays, the results cannot take into account the variability that occurs in the course of the day. Studies can also be conducted to focus on the seasonal differences throughout a year where an on-road can be conducted during preferential time periods that represent the extreme weather conditions (i.e. summer and winter). This would be a great extension of the current on-road research that has been conducted and it would be especially interesting to investigate the diurnal on-road variation of PM exposure for commuters during their morning and evening commutes.

Similar future studies can also be conducted on other light-rail and subway systems. It would be interesting to investigate time-integrated PM composition inside the train and while waiting at stations to differentiate between the two locations. The current study represents and integration of waiting at the stations (25% of time) and sitting inside the train (75%) of the time to represent a typical commuter environment. It may also be worthwhile to investigate a line that is partially underground and partially ground-level or a line that is entire above ground. The PM composition may be slightly different from ground-level PM due to elevation differences.

In addition to the future research proposals, a greater sample size (N) would enhance the analysis of the data set in providing a greater understanding of the variability that may occur in different time periods. A greater sample size would also benefit epidemiologists investigating exposure risk for commuters in various microenvironments.

7.4.3 Recommendations for regulatory control

It was determined in the METRO study that a number of metals were elevated especially in the subway system, and to a lesser degree, in the light-rail system. Levels were substantially higher in the subway system due to its underground environment and enclosed nature, thus

particles generated may accumulate in the underground stations. Certain stations exhibited higher concentrations than other stations (Chapter 2), which could be due to the age of the station where some stations may be more recent and thus have improved ventilation systems built in. In regards to controlling PM pollutants, namely Fe and other stainless steel associated elements, ventilation systems should be upgraded to enhance airflow of subway air to ambient air and to increase entrainment of ambient air into the subway station. In-train exposure can also be improved by upgrading the ventilation system or installing an air conditioning system. Since Chapter 2 showed that PM concentrations inside the train are correlated with PM concentrations at the station, this suggests that PM at the stations is the main source of PM inside the train. Thus, to ultimately improve rider exposure to PM inside the train, where commuters spend most of their time, measures should be taken to improve air quality at the stations.

In regards to controlling on-road PM pollutants, the major source of these pollutants must be taken into account as well as the PM size fraction of interest. In the traffic environment, it is clear that the major sources of elevated PM species are from vehicular wear, tailpipe emissions, and resuspended road dust. The smallest PM size fraction, $PM_{0.25}$, is dominated by OC and is most likely a result of incomplete combustion byproducts; the larger PM size fraction, $PM_{10\text{-}2.5}$, is dominated by crustal materials, which is most likely from natural sources. While there may not be any control technology to reduce resuspension of road dust (nor may be necessary to), it is essential to target effective controls towards the reduction of tailpipe emissions, specifically from older model vehicles that are less efficient and heavy polluters. A more effective control method would be to target HDVs, which are substantially greater emitters of EC, OC, metals, and organic species (Phuleria et al. 2007; Geller et al. 2005).

The Port of Los Angeles, which is responsible for the majority of HDVs that travel along the 710 (HDV freeway), has already implemented the Clean Truck Program in 2008. The objective of the program is to establish a progressive ban of older model HDVs (www.portoflosangeles.org). In October 2008, all pre-1989 trucks were banned from entering the Port; in January 2010, all 1989-1993 trucks were banned, in addition to 1994-2003 trucks that had not been retrofitted; in January 2012, all trucks that did not meet the 2007 Federal Clean Truck Emissions Standards were banned from the Port. The program has been extremely effective in reducing emissions and improving overall air quality in the region. A recent study showed that health costs from PM emitted from HDVs exceeded 440M dollars in 2005, but decreased by 36%, 90%, and 96% after meeting the 2008, 2010, and 2012 program deadlines (Lee et al. 2012). The study shows that the Clean Truck Program has been effective in that it exceeded its target goal, with substantive reductions in the cost of health outcomes.

In addition to reductions in health costs, emissions have also decreased on the roadways. Based on results of the current studies, EC levels (Figure 4.7b), which can be used as a tracer of HDVs at least in an urban environment (Schauer 2003), has decreased nearly 50% in the last 5 years based on comparison of the current HDV freeway study that was conducted in 2011 in comparison to an earlier study that was conducted in 2006 (Phuleria et al. 2007). The previous study and current study represents two years before and three years after the implementation of the Clean Truck Program, respectively. Section 4.4.5 also showed that conditions on the 110 freeway, which has a lower truck fraction, may also have improved based on EC levels. Overall, there have been obvious improvements in the overall air quality for roadways in Los Angeles in the past five years. After the implementation of the last stage of the Clean Truck Program in 2012, it would be worthwhile to further investigate PM emissions on the 710 roadway.

Publications from this thesis

Chapter 2:

Kam W., Cheung K., Daher N., and Sioutas C. (2011) "Particulate matter (PM) concentrations in underground and ground-level rail systems of the Los Angeles Metro." *Atmospheric Environment*, 45(8): 1517-1524.

Chapter 3:

Kam W., Ning Z., Shafer M. M, Schauer J. J., and Sioutas C. (2011) "Chemical characterization of coarse and fine particulate matter (PM) in underground and ground-level rail systems of the Los Angeles Metro." *Environmental Science and Technology*, 45(16): 6769–6776.

Chapter 4:

Kam W., Liacos J., Schauer J. J., Delfino R. J., and Sioutas C. (2012) "Size-segregated composition of particulate matter (PM) in major roadways and surface streets." *Atmospheric Environment,* 55: 90-97.

Chapter 5:

Kam W., Liacos J., Schauer J. J., Delfino R. J., Sioutas C. (2012) "On-road emission factors of PM pollutants for light-duty vehicles (LDVs) based on urban street driving conditions." *Atmospheric Environment*, 61: 378-386.

Chapter 6:

Kam W., Delfino R.J., Schauer J.J., Sioutas C. (2013) "A comparative assessment of PM2.5 exposures in light-rail, subway, freeway, and surface street environments in Los Angeles and estimated lung cancer risk." *Environmental Sciences: Processes and Impacts,* doi: 10.1039/c2em30495c.

Bibliography

Aarnio, P., T. Yli-Tuomi, et al. (2005). "The concentrations and composition of and exposure to fine particles (PM2.5) in the Helsinki subway system." *Atmos. Environ.* **39**(28): 5059-5066.

Adams, H. S., M. J. Nieuwenhuijsen, et al. (2001). "Fine particle (PM2.5) personal exposure levels in transport microenvironments, London, UK." *Sci. Total Environ.* **279**(1-3): 29-44.

Arhami, M., M. Sillanpaa, et al. (2009). "Size-Segregated Inorganic and Organic Components of PM in the Communities of the Los Angeles Harbor." *Aerosol Sci. Technol.* **43**(2): 145-160.

Belyaev, S. P. and L. M. Levin (1974). "Techniques for collection of representative aerosol samples." *J. Aerosol Sci.* **5**: 325-338.

Birch, M. E. and R. A. Cary (1996). "Elemental carbon-based method for monitoring occupational exposures to particulate diesel exhaust." *Aerosol Sci. Technol.* **25**(3): 221-241.

Bostrom, C. E., P. Gerde, et al. (2002). "Cancer risk assessment, indicators, and guidelines for polycyclic aromatic hydrocarbons in the ambient air." *Environ. Health Persp.* **110**: 451-488.

Brinkman, M., K. Cowen, et al. (2008). "Sioutas PCIS with Leland Legacy Pump: Environmental Technology Verification Report." Mickey Leland National Urban Air Toxics Research Center (NUATRC). Number 12.

Brown, D. M., M. R. Wilson, et al. (2001). "Size-dependent proinflammatory effects of ultrafine polystyrene particles: A role for surface area and oxidative stress in the enhanced activity of ultrafines." *Toxicol. Appl. Pharmacol.* **175**(3): 191-199.

Brown, S. G., P. Herckes, et al. (2002). "Characterization of organic aerosol in Big Bend National Park, Texas." *Atmos. Environ.* **36**(38): 5807-5818.

Brunekreef, B., N. A. H. Janssen, et al. (1997). "Air pollution from truck traffic and lung function in children living near motorways." *Epidemiology* **8**(3): 298-303.

Bukowiecki, N., J. Dommen, et al. (2002). "A mobile pollutant measurement laboratory-measuring gas phase and aerosol ambient concentrations with high spatial and temporal resolution." *Atmos. Environ.* **36**(36-37): 5569-5579.

Campbell, A., M. Oldham, et al. (2005). "Particulate matter in polluted air may increase biomarkers of inflammation in mouse brain." *Neurotoxicology* **26**(1): 133-140.

Cass, G. R. (1998). "Organic molecular tracers for particulate air pollution sources." *Trac-Trends in Analytical Chemistry* **17**(6): 356-366.

Chakrabarti, B., P. M. Fine, et al. (2004). "Performance evaluation of the active-flow personal DataRAM PM2.5 mass monitor (Thermo Anderson pDR-1200) designed for continuous personal exposure measurements." *Atmos. Environ.* **38**(20): 3329-3340.

Chan, L. Y., W. L. Lau, et al. (2002). "Commuter exposure to particulate matter in public transportation modes in Hong Kong." *Atmos. Environ.* **36**(21): 3363-3373.

Chan, L. Y., W. L. Lau, et al. (2002). "Exposure level of carbon monoxide and respirable suspended particulate in public transportation modes while commuting in urban, area of Guangzhou, China." *Atmos. Environ.* **36**(38): 5831-5840.

Cheng, Y. H., Y. L. Lin, et al. (2008). "Levels of PM10 and PM2.5 in Taipei Rapid Transit System." *Atmos. Environ.* **42**(31): 7242-7249.

Cheung, K., N. Daher, et al. (2011). "Spatial and temporal variation of chemical composition and mass closure of ambient coarse particulate matter (PM10-2.5) in the Los Angeles area." *Atmos. Environ.* **45**(16): 2651-2662.

Chillrud, S. N., D. Epstein, et al. (2004). "Elevated airborne exposures of teenagers to manganese, chromium, and iron from steel dust and New York City's subway system." *Environ. Sci. Technol.* **38**(3): 732-737.

Cho, A. K., C. Sioutas, et al. (2005). "Redox activity of airborne particulate matter at different sites in the Los Angeles Basin." *Environ. Res.* **99**(1): 40-47.

Chow, J. C., J. G. Watson, et al. (1994). "Temporal and Spatial Variations of Pm(2.5) and Pm(10) Aerosol in the Southern California Air-Quality Study." *Atmos. Environ.* **28**(12): 2061-2080.

Chung, A., D. P. Y. Chang, et al. (2001). "Comparison of real-time instruments used to monitor airborne particulate matter." *J. Air Waste Manag. Assoc.* **51**(1): 109-120.

Collins, J. F., J. P. Brown, et al. (1998). "Potency equivalency factors for some polycyclic aromatic hydrocarbons and polycyclic aromatic hydrocarbon derivatives." *Regul. Toxicol. Pharm.* **28**(1): 45-54.

Costa, D. L. and K. L. Dreher (1997). "Bioavailable transition metals in particulate matter mediate cardiopulmonary injury in healthy and compromised animal models." *Environ. Health Persp.* **105**: 1053-1060.

Creason, J., L. Neas, et al. (2001). "Particulate matter and heart rate variability among elderly retirees: the Baltimore 1998 PM study." *J. Expo. Anal. Environ. Epidemiol.* **11**(2): 116-122.

Dales, R., A. J. Wheeler, et al. (2009). "The Influence of Neighborhood Roadways on Respiratory Symptoms Among Elementary Schoolchildren." *J. Occup. Environ. Med.* **51**(6): 654-660.

Dallmann, T. R., R. A. Harley, et al. (2011). "Effects of diesel particulate filter retrofits and accelerated fleet turnover on drayage truck emissions at the Port of Oakland." *Environ. Sci. Technol.* **In press**.

Eiguren-Fernandez, A. and A. H. Miguel (2012). "Size-Resolved Polycyclic Aromatic Hydrocarbon Emission Factors from On-Road Gasoline and Diesel Vehicles: Temperature Effect on the Nuclei-Mode." *Environ. Sci. Technol.* **46**(5): 2607-2615.

Fine, P. M., B. Chakrabarti, et al. (2004). "Diurnal variations of individual organic compound constituents of ultrafine and accumulation mode particulate matter in the Los Angeles basin." *Environ. Sci. Technol.* **38**(5): 1296-1304.

Fruin, S. A., A. M. Winer, et al. (2004). "Black carbon concentrations in California vehicles and estimation of in-vehicle diesel exhaust particulate matter exposures." *Atmos. Environ.* **38**(25): 4123-4133.

Fujita, E. M., B. Zielinska, et al. (2007). "Variations in speciated emissions from spark-ignition and compression-ignition motor vehicles in California's south coast air basin." *J. Air Waste Manag. Assoc.* **57**(6): 705-720.

Furuya, K., Y. Kudo, et al. (2001). "Seasonal variation and their characterization of suspended particulate matter in the air of subway stations." *J. Trace Microprobe Tech.* **19**(4): 469-485.

Garg, B. D., S. H. Cadle, et al. (2000). "Brake wear particulate matter emissions." *Environ. Sci. Technol.* **34**(21): 4463-4469.

Geller, V. D., S. B. Sardar, et al. (2005). "Measurements of particle number and mass concentrations and size distributions in a tunnel environment." *Environ. Sci. Technol.* **39**(22): 8653-8663.

Gorner, P., D. Bemer, et al. (1995). "Photometer measurement of polydisperse aerosols." *J. Aerosol Sci.* **26**(8): 1281-1302.

Gouriou, F., J. P. Morin, et al. (2004). "On-road measurements of particle number concentrations and size distributions in urban and tunnel environments." *Atmos. Environ.* **38**(18): 2831-2840.

Grieshop, A. P., E. M. Lipsky, et al. (2006). "Fine particle emission factors from vehicles in a highway tunnel: Effects of fleet composition and season." *Atmos. Environ.* **40**: S287-S298.

Harrison, R. M., R. Tilling, et al. (2003). "A study of trace metals and polycyclic aromatic hydrocarbons in the roadside environment." *Atmos. Environ.* **37**(17): 2391-2402.

Heal, M. R., I. J. Beverland, et al. (2000). "Intercomparison of five PM10 monitoring devices and the implications for exposure measurement in epidemiological research." *Journal of Environmental Monitoring* **2**(5): 455-461.

Hesterberg, T. W., C. A. Lapin, et al. (2008). "A comparison of emissions from vehicles fueled with diesel or compressed natural gas." *Environ. Sci. Technol.* **42**(17): 6437-6445.

Hinds, W. C. (1999). Aerosol Technology: Properties, Behavior, and Measurement of Airborne Particles. New York, NY, Wiley-Interscience.

Hu, S., A. Polidori, et al. (2008). "Redox activity and chemical speciation of size fractioned PM in the communities of the Los Angeles-Long Beach harbor." *Atmospheric Chemistry and Physics* **8**(21): 6439-6451.

Hueglin, C., R. Gehrig, et al. (2005). "Chemical characterisation of PM2.5, PM10 and coarse particles at urban, near-city and rural sites in Switzerland." *Atmos. Environ.* **39**(4): 637-651.

Hughes, L. S., J. O. Allen, et al. (2000). "Evolution of atmospheric particles along trajectories crossing the Los Angeles basin." *Environ. Sci. Technol.* **34**(15): 3058-3068.

Hughes, L. S., G. R. Cass, et al. (1998). "Physical and chemical characterization of atmospheric ultrafine particles in the Los Angeles area." *Environ. Sci. Technol.* **32**(9): 1153-1161.

Johansson, C. and P. A. Johansson (2003). "Particulate matter in the underground of Stockholm." *Atmos. Environ.* **37**(1): 3-9.

Kang, S., H. Hwang, et al. (2008). "Chemical Compositions of Subway Particles in Seoul, Korea Determined by a Quantitative Single Particle Analysis." *Environ. Sci. Technol.* **42**(24): 9051-9057.

Karlsson, H. L., A. G. Ljungman, et al. (2006). "Comparison of genotoxic and inflammatory effects of particles generated by wood combustion, a road simulator and collected from street and subway." *Toxicol. Lett.* **165**(3): 203-211.

Karlsson, H. L., L. Nilsson, et al. (2005). "Subway particles are more genotoxic than street particles and induce oxidative stress in cultured human lung cells." *Chem. Res. Toxicol.* **18**(1): 19-23.

Kerr, S. C., J. J. Schauer, et al. (2004). "Regional haze in Wisconsin: sources and the spatial distribution." *J. Environ. Eng. Sci.* **3**(3): 213-222.

Kim, B. M., J. Cassmassi, et al. (2001). "Positive organic carbon artifacts on filter medium during PM2.5 sampling in the South Coast Air Basin." *Aerosol Sci. Technol.* **34**(1): 35-41.

Kim, J. Y., S. R. Magari, et al. (2004). "Comparison of fine particle measurements from a direct-reading instrument and a gravimetric sampling method." *Journal of Occupational and Environmental Hygiene* **1**(11): 707-715.

Kim, K. Y., Y. S. Kim, et al. (2008). "Spatial distribution of particulate matter (PM10 and PM2.5) in Seoul Metropolitan Subway stations." *J. Hazard. Mater.* **154**(1-3): 440-443.

Kim, S., S. Shen, et al. (2002). "Size distribution and diurnal and seasonal trends of ultrafine particles in source and receptor sites of the Los Angeles basin." *J. Air Waste Manag. Assoc.* **52**(3): 297-307.

Kingham, S., M. Durand, et al. (2006). "Winter comparison of TEOM, MiniVol and DustTrak PM10 monitors in a woodsmoke environment." *Atmos. Environ.* **40**(2): 338-347.

Kirchstetter, T. W., R. A. Harley, et al. (1999). "On-road measurement of fine particle and nitrogen oxide emissions from light- and heavy-duty motor vehicles." *Atmos. Environ.* **33**(18): 2955-2968.

Krudysz, M. A., J. R. Froines, et al. (2008). "Intra-community spatial variation of size-fractionated PM mass, OC, EC, and trace elements in the Long Beach, CA area." *Atmos. Environ.* **42**(21): 5374-5389.

Kuhn, T., S. Biswas, et al. (2005b). "Physical and chemical characteristics and volatility of PM in the proximity of a light-duty vehicle freeway." *Aerosol Sci. Technol.* **39**(4): 347-357.

Kuhn, T., S. Biswas, et al. (2005a). "Diurnal and seasonal characteristics of particle volatility and chemical composition in the vicinity of a light-duty vehicle freeway." *Atmos. Environ.* **39**(37): 7154-7166.

Landreman, A. P., M. M. Shafer, et al. (2008). "A macrophage-based method for the assessment of the reactive oxygen species (ROS) activity of atmospheric particulate matter (PM) and application to routine (daily-24 h) aerosol monitoring studies." *Aerosol Sci. Technol.* **42**(11): 946-957.

Lee, G., S. You, et al. (2012). "Assessing air quality and health benefits of the Clean Truck Program in the Alameda corridor, CA." *Transportation Research Part a-Policy and Practice* **46**(8): 1177-1193.

Li, N., M. Y. Wang, et al. (2009). "The Adjuvant Effect of Ambient Particulate Matter Is Closely Reflected by the Particulate Oxidant Potential." *Environ. Health Perspect.* **117**(7): 1116-1123.

Liao, D. P., J. Creason, et al. (1999). "Daily variation of particulate air pollution and poor cardiac autonomic control in the elderly." *Environ. Health Perspect.* **107**(7): 521-525.

Lin, C. C., S. J. Chen, et al. (2005). "Characteristics of metals in nano/ultrafine/fine/coarse particles collected beside a heavily trafficked road." *Environ. Sci. Technol.* **39**(21): 8113-8122.

Loft, S., C. Stevns-Hansen, et al. (2005). "Oxidative stress and inflammation as mediators of health effects or air pollution." *Free Radical Res.* **39**: S26-S26.

Lough, G. C., J. J. Schauer, et al. (2005). "Emissions of metals associated with motor vehicle roadways." *Environ. Sci. Technol.* **39**(3): 826-836.

Lowenthal, D. H., C. F. Rodgers, et al. (1995). "Sensitivity of Estimated Light Extinction Coefficients to Model Assumptions and Measurement Errors." *Atmos. Environ.* **29**(7): 751-766.

Lowenthal, D. H., B. Zielinska, et al. (1994). "Characterization of Heavy-Duty Diesel Vehicle Emissions." *Atmos. Environ.* **28**(4): 731-743.

Mar, T. F., G. A. Norris, et al. (2000). "Associations between air pollution and mortality in Phoenix, 1995-1997." *Environ. Health Perspect.* **108**(4): 347-353.

Marcazzan, G. M., S. Vaccaro, et al. (2001). "Characterisation of PM10 and PM2.5 particulate matter in the ambient air of Milan (Italy)." *Atmos. Environ.* **35**(27): 4639-4650.

Marder, A. R. (2000). "The metallurgy of zinc-coated steel." *Prog. Mater Sci.* **45**(3): 191-271.

Metzger, K. B., P. E. Tolbert, et al. (2004). "Ambient air pollution and cardiovascular emergency department visits." *Epidemiology* **15**(1): 46-56.

Miguel, A. H., T. W. Kirchstetter, et al. (1998). "On-road emissions of particulate polycyclic aromatic hydrocarbons and black carbon from gasoline and diesel vehicles." *Environ. Sci. Technol.* **32**(4): 450-455.

Minguillon, M. C., M. Arhami, et al. (2008). "Seasonal and spatial variations of sources of fine and quasi-ultrafine particulate matter in neighborhoods near the Los Angeles-Long Beach harbor." *Atmos. Environ.* **42**(32): 7317-7328.

Misra, C., M. Singh, et al. (2002). "Development and evaluation of a personal cascade impactor sampler (PCIS)." *J. Aerosol Sci.* **33**(7): 1027-1047.

Moore, K. F., Z. Ning, et al. (2007). "Daily variation in the properties of urban ultrafine aerosol - Part I: Physical characterization and volatility." *Atmos. Environ.* **41**(38): 8633-8646.

Morgan, T. E., D. A. Davis, et al. (2011). "Glutamatergic Neurons in Rodent Models Respond to Nanoscale Particulate Urban Air Pollutants in Vivo and in Vitro." *Environ. Health Perspect.* **119**(7): 1003-1009.

Murruni, L. G., V. Solanes, et al. (2009). "Concentrations and elemental composition of particulate matter in the Buenos Aires underground system." *Atmos. Environ.* **43**(30): 4577-4583.

Naumova, Y. Y., J. H. Offenberg, et al. (2003). "Gas/particle distribution of polycyclic aromatic hydrocarbons in coupled outdoor/indoor atmospheres." *Atmos. Environ.* **37**(5): 703-719.

Nieuwenhuijsen, M. J., J. E. Gomez-Perales, et al. (2007). "Levels of particulate air pollution, its elemental composition, determinants and health effects in metro systems." *Atmos. Environ.* **41**(37): 7995-8006.

Ning, Z. and T. L. Chan (2007). "On-road remote sensing of liquefied petroleum gas (LPG) vehicle emissions measurement and emission factors estimation." *Atmos. Environ.* **41**(39): 9099-9110.

Ning, Z., M. D. Geller, et al. (2007). "Daily variation in chemical characteristics of urban ultrafine aerosols and inference of their sources." *Environ. Sci. Technol.* **41**(17): 6000-6006.

Ning, Z., N. Hudda, et al. (2010). "Impact of roadside noise barriers on particle size distributions and pollutants concentrations near freeways." *Atmos. Environ.* **44**(26): 3118-3127.

Ning, Z., A. Polidori, et al. (2008). "Emission factors of PM species based on freeway measurements and comparison with tunnel and dynamometer studies." *Atmos. Environ.* **42**(13): 3099-3114.

Ntziachristos, L., Z. Ning, et al. (2007). "Fine, ultrafine and nanoparticle trace element compositions near a major freeway with a high heavy-duty diesel fraction." *Atmos. Environ.* **41**(27): 5684-5696.

Oberdorster, G., E. Oberdorster, et al. (2005). "Nanotoxicology: An emerging discipline evolving from studies of ultrafine particles." *Environ. Health Perspect.* **113**(7): 823-839.

Ostro, B. D., W. Y. Feng, et al. (2008). "The impact of components of fine particulate matter on cardiovascular mortality in susceptible subpopulations." *Occup. Environ. Med.* **65**(11): 750-756.

Pakbin, P., Z. Ning, et al. (2011). "Seasonal and Spatial Coarse Particle Elemental Concentrations in the Los Angeles Area." *Aerosol Sci. Technol.* **45**(8): 949-U156.

Park, D. U. and K. C. Ha (2008). "Characteristics of PM10, PM2.5, CO2 and CO monitored in interiors and platforms of subway train in Seoul, Korea." *Environment International* **34**(5): 629-634.

Peters, T. M. and D. Leith (2004). "Particle deposition in industrial duct bends." *Ann. Occup. Hyg.* **48**(5): 483-490.

Pfeifer, G. D., R. M. Harrison, et al. (1999). "Personal exposures to airborne metals in London taxi drivers and office workers in 1995 and 1996." *Sci. Total Environ.* **235**(1-3): 253-260.

Phuleria, H. C., M. D. Geller, et al. (2006). "Size-resolved emissions of organic tracers from light-and heavy-duty vehicles measured in a California roadway tunnel." *Environ. Sci. Technol.* **40**(13): 4109-4118.

Phuleria, H. C., R. J. Sheesley, et al. (2007). "Roadside measurements of size-segregated particulate organic compounds near gasoline and diesel-dominated freeways in Los Angeles, CA." *Atmos. Environ.* **41**(22): 4653-4671.

Polidori, A., S. Hu, et al. (2008). "Real-time characterization of particle-bound polycyclic aromatic hydrocarbons in ambient aerosols and from motor-vehicle exhaust." *Atmos. Chem. Phys.* **8**(5): 1277-1291.

Pope, C. A. and D. W. Dockery (2006). "Health effects of fine particulate air pollution: Lines that connect." *J. Air Waste Manag. Assoc.* **56**(6): 709-742.

Prichard, H. M. and P. C. Fisher (2012). "Identification of Platinum and Palladium Particles Emitted from Vehicles and Dispersed into the Surface Environment." *Environ. Sci. Technol.* **46**(6): 3149-3154.

Querol, X., A. Alastuey, et al. (2001). "PM 10 and PM2.5 source apportionment in the Barcelona Metropolitan area, Catalonia, Spain." *Atmos. Environ.* **35**(36): 6407-6419.

Raut, J. C., P. Chazette, et al. (2009). "Link between aerosol optical, microphysical and chemical measurements in an underground railway station in Paris." *Atmos. Environ.* **43**(4): 860-868.

Rogge, W. F., L. M. Hildemann, et al. (1993a). "Sources of Fine Organic Aerosol .2. Noncatalyst and Catalyst-Equipped Automobiles and Heavy-Duty Diesel Trucks." *Environ. Sci. Technol.* **27**(4): 636-651.

Rogge, W. F., L. M. Hildemann, et al. (1993b). "Sources of Fine Organic Aerosol .3. Road Dust, Tire Debris, and Organometallic Brake Lining Dust - Roads as Sources and Sinks." *Environ. Sci. Technol.* **27**(9): 1892-1904.

Saldiva, P. H. N., R. W. Clarke, et al. (2002). "Lung inflammation induced by concentrated ambient air particles is related to particle composition." *Am. J. Respir. Crit. Care Med.* **165**(12): 1610-1617.

Salma, I., R. Ocskay, et al. (2007). "Sampling artefacts, concentration and chemical composition of fine water-soluble organic carbon and humic-like substances in a continental urban atmospheric environment." *Atmos. Environ.* **41**(19): 4106-4118.

Salma, I., T. Weidinger, et al. (2007). "Time-resolved mass concentration, composition and sources of aerosol particles in a metropolitan underground railway station." *Atmos. Environ.* **41**(37): 8391-8405.

Samet, J. M., F. Dominici, et al. (2000). "Fine particulate air pollution and mortality in 20 US Cities, 1987-1994." *N. Engl. J. Med.* **343**(24): 1742-1749.

Sanders, P. G., N. Xu, et al. (2003). "Airborne brake wear debris: Size distributions, composition, and a comparison of dynamometer and vehicle tests." *Environ. Sci. Technol.* **37**(18): 4060-4069.

Sardar, S. B., P. M. Fine, et al. (2005). "Seasonal and spatial variability of the size-resolved chemical composition of particulate matter (PM10) in the Los Angeles Basin." *Journal of Geophysical Research-Atmospheres* **110**(D7).

Sauvain, J. J., T. V. Duc, et al. (2003). "Exposure to carcinogenic polycyclic aromatic compounds and health risk assessment for diesel-exhaust exposed workers." *Int. Arch. Occ. Env. Hea.* **76**(6): 443-455.

Schauer, J. J. (2003). "Evaluation of elemental carbon as a marker for diesel particulate matter." *J. Expo. Anal. Environ. Epidemiol.* **13**(6): 443-453.

Schauer, J. J., M. J. Kleeman, et al. (1999). "Measurement of emissions from air pollution sources. 1. C-1 through C-29 organic compounds from meat charbroiling." *Environ. Sci. Technol.* **33**(10): 1566-1577.

Schauer, J. J., M. J. Kleeman, et al. (1999). "Measurement of emissions from air pollution sources. 2. C-1 through C-30 organic compounds from medium duty diesel trucks." *Environ. Sci. Technol.* **33**(10): 1578-1587.

Schauer, J. J., M. J. Kleeman, et al. (2002). "Measurement of emissions from air pollution sources. 5. C-1-C-32 organic compounds from gasoline-powered motor vehicles." *Environ. Sci. Technol.* **36**(6): 1169-1180.

Schauer, J. J., G. C. Lough, et al. (2006). Characterization of Metals Emitted from Motor Vehicles, Health Effects Institute. Report number 133.

Schauer, J. J., W. F. Rogge, et al. (1996). "Source apportionment of airborne particulate matter using organic compounds as tracers." *Atmos. Environ.* **30**(22): 3837-3855.

Schwartz, J., F. Laden, et al. (2002). "The concentration-response relation between PM2.5 and daily deaths." *Environ. Health Perspect.* **110**(10): 1025-1029.

Seaton, A., J. Cherrie, et al. (2005). "The London Underground: dust and hazards to health." *Occup. Environ. Med.* **62**(6): 355-362.

Seinfeld, J. H. and S. N. Pandis (2006). Atmospheric Chemistry and Physics: From Air Pollution to Climate Change. Hoboken, N.J., John Wiley & Sons, Inc.

Simoneit, B. R. T. (1989). "Organic-Matter of the Troposphere .5. Application of Molecular Marker Analysis to Biogenic Emissions into the Troposphere for Source Reconciliations." *Journal of Atmospheric Chemistry* **8**(3): 251-275.

Singh, M., C. Misra, et al. (2003). "Field evaluation of a personal cascade impactor sampler (PCIS)." *Atmos. Environ.* **37**(34): 4781-4793.

Sioutas, C., S. Kim, et al. (2000). "Field evaluation of a modified DataRAM MIE scattering monitor for real-time PM2.5 mass concentration measurements." *Atmos. Environ.* **34**(28): 4829-4838.

Sitzmann, B., M. Kendall, et al. (1999). "Characterisation of airborne particles in London by computer-controlled scanning electron microscopy." *Sci. Total Environ.* **241**(1-3): 63-73.

Sternbeck, J., A. Sjodin, et al. (2002). "Metal emissions from road traffic and the influence of resuspension - results from two tunnel studies." *Atmos. Environ.* **36**(30): 4735-4744.

Tao, F., B. Gonzalez-Flecha, et al. (2003). "Reactive oxygen species in pulmonary inflammation by ambient particulates." *Free Radic. Biol. Med.* **35**(4): 327-340.

Taylor, S. R. and S. M. McLennan (1985). The Continental Crust: Its Composition and Evolution. Oxford, Boston, Palo Alto, Victoria, Blackwell Scientific Publications.

Tonne, C., S. Melly, et al. (2007). "A case-control analysis of exposure to traffic and acute myocardial infarction." *Environ. Health Perspect.* **115**(1): 53-57.

Turpin, B. J. and H. J. Lim (2001). "Species contributions to PM2.5 mass concentrations: Revisiting common assumptions for estimating organic mass." *Aerosol Sci. Technol.* **35**(1): 602-610.

Turpin, B. J., P. Saxena, et al. (2000). "Measuring and simulating particulate organics in the atmosphere: problems and prospects." *Atmos. Environ.* **34**(18): 2983-3013.

Verma, V., M. M. Shafer, et al. (2010). "Contribution of transition metals in the reactive oxygen species activity of PM emissions from retrofitted heavy-duty vehicles." *Atmos. Environ.* **44**(39): 5165-5173.

Weimer, S., C. Mohr, et al. (2009). "Mobile measurements of aerosol number and volume size distributions in an Alpine valley: Influence of traffic versus wood burning." *Atmos. Environ.* **43**(3): 624-630.

Weiss, M., P. Bonnel, et al. (2011). "On-Road Emissions of Light-Duty Vehicles in Europe." *Environ. Sci. Technol.* **45**(19): 8575-8581.

Westerdahl, D., S. Fruin, et al. (2005). "Mobile platform measurements of ultrafine particles and associated pollutant concentrations on freeways and residential streets in Los Angeles." *Atmos. Environ.* **39**(20): 3597-3610.

Xia, T., P. Korge, et al. (2004). "Quinones and aromatic chemical compounds in particulate matter induce mitochondrial dysfunction: Implications for ultrafine particle toxicity." *Environ. Health Perspect.* **112**(14): 1347-1358.

Yanosky, J. D., P. L. Williams, et al. (2002). "A comparison of two direct-reading aerosol monitors with the federal reference method for PM2.5 in indoor air." *Atmos. Environ.* **36**(1): 107-113.

Yanowitz, J., M. S. Graboski, et al. (1999). "Chassis dynamometer study of emissions from 21 in-use heavy duty diesel vehicles." *Environ. Sci. Technol.* **33**(2): 209-216.

Yli-Tuomi, T., P. Aarnio, et al. (2005). "Emissions of fine particles, NOx, and CO from on-road vehicles in Finland." *Atmos. Environ.* **39**(35): 6696-6706.

Zhang, X. Q. and P. H. McMurry (1987). "Theoretical-Analysis of Evaporative Losses from Impactor and Filter Deposits." *Atmos. Environ.* **21**(8): 1779-1789.

Zhang, Y. X., J. J. Schauer, et al. (2008). "Source apportionment of in vitro reactive oxygen species bioassay activity from atmospheric particulate matter." *Environ. Sci. Technol.* **42**(19): 7502-7509.

Zhu, Y. F., W. C. Hinds, et al. (2002). "Concentration and size distribution of ultrafine particles near a major highway." *J. Air Waste Manag. Assoc.* **52**(9): 1032-1042.

Zielinska, B., J. Sagebiel, et al. (2004). "Emission rates and comparative chemical composition from selected in-use diesel and gasoline-fueled vehicles." *J. Air Waste Manag. Assoc.* **54**(9): 1138-1150.